

This volume is the property of the University of Oklahoma, but the literary rights of the author are a separate property and must be respected. Passages must not be copied or closely paraphrased without the previous written consent of the author. If the reader obtains any assistance from this volume, he must give proper credit in his own work.

I grant the University of Oklahoma Libraries permission to make a copy of my thesis upon the request of individuals or libraries. This permission is granted with the understanding that a copy will be provided for research purposes only, and that requestors will be informed of these restrictions.

NAME [REDACTED]

DATE July 28 2008

A library which borrows this thesis for use by its patrons is expected to secure the signature of each user.

This thesis by FAIYAZ M. ALI has been used by the following persons, whose signatures attest their acceptance of the above restrictions.

---

---

NAME AND ADDRESS

DATE

UNIVERSITY OF OKLAHOMA

GRADUATE COLLEGE

A SUBSURFACE STUDY OF THE LOWER RED FORK SANDSTONE IN THE  
DEEPER PART OF THE ANADARKO BASIN IN CADDO AND WASHITA  
COUNTIES, OKLAHOMA.

A THESIS APPROVED FOR THE  
CONOCO PHILLIPS SCHOOL OF GEOLOGY AND GEOPHYSICS

A THESIS

SUBMITTED TO THE GRADUATE COLLEGE

in partial fulfillment of the requirements for the

Degree of

BY  
MASTER OF SCIENCE

Richard A. Clark  
Richard A. Clark

Richard Andrews  
Richard Andrews

BY  
James Ferguson  
James Ferguson

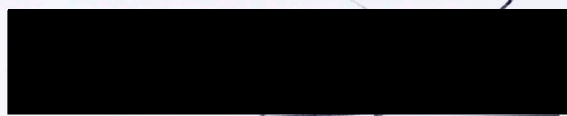
FAIYAZ M. ALI  
Norman, Oklahoma  
2008

00  
THESIS  
ALI  
cop. 2

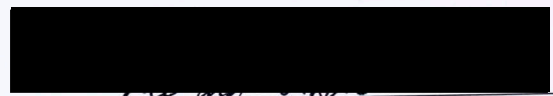
A SUBSURFACE STUDY OF THE LOWER RED FORK SANDSTONE IN THE  
DEEPER PART OF THE ANADARKO BASIN IN CADDO AND WASHITA  
COUNTIES, OKLAHOMA.

A THESIS APPROVED FOR THE  
CONOCO PHILLIPS SCHOOL OF GEOLOGY AND GEOPHYSICS

BY



Roger Slatt, Chair



Richard Andrews



James Forgotson

## ACKNOWLEDGMENTS

The following thesis has been completed due to support from many people. First and foremost I would like to thank Richard R. Denning, an Oklahoma Oilman, President and CEO of Indian Exploration Company LLC based in Oklahoma City, Oklahoma, for funding my master's degree and providing priceless recommendations.

I would also like to thank my thesis committee. Dr. Roger M. Slatt, my thesis advisor, thank you for providing me with invaluable advice and a sense of direction throughout my entire stay at the university. Dr. James M. Forgoon and Richard D. Andrews also provided tremendous insight that led to the completion of this thesis. Thank you.

I would also like to extend my appreciation to the geoscientists and the team at Indian Exploration Company LLC. Gene K. Behrens, William C. Mantey, Richard B. Opalka, Jan M. Dodson, EdSo Miller, and John T. Hall provided me with excellent insight, knowledge, and sense of direction. Without the support from the Indian Team and thesis committee this thesis simply would not have been possible. Thank you very much. Last but not least, I would like to thank my wife Sana for her patience and support throughout my master's.

© Copyright FAIYAZ MOHAMMED ALI 2008

ALL RIGHTS RESERVED.

## ACKNOWLEDGMENTS

The following thesis has been completed due to support from many people. First and foremost I would like to thank Richard R. Dunning, an Oklahoma Oilman, President and CEO of Indian Exploration Company LLC based in Oklahoma City, Oklahoma, for funding my master's degree and providing priceless recommendations.

I would also like to thank my thesis committee. Dr. Roger M. Slatt, my thesis advisor, thank you for providing me with invaluable advice and a sense of direction throughout my entire stay at the university. Dr. James M. Forgotson and Richard D. Andrews also provided tremendous insight that led to the completion of this thesis. Thank you.

I would also like to extend my appreciation to the geoscientists and the team at Indian Exploration Company LLC. Gene K. Behrens, William C. Manthey, Richard B. Opalka, Jan M. Dodson, Eddie Miller, and John T. Hull provided me with excellent insight, knowledge, and sense of direction. Without the support from the Indian Team and thesis committee this thesis simply would not have been possible. Thank you very much. Last but not least, I would like to thank my wife Sana for her patience and support throughout my master's.

Regional Stratigraphy	20
1. CORE ANALYSIS	22
a. Core Description	22
b. Core Plug Analysis	44
c. Thin Sections Analysis	47
d. Depositional Environment Interpretation	66

Acknowledgements.....	iv
Table of Contents.....	v
List of Tables.....	vii
List of Figures.....	viii
List of Plates.....	xii
Abstract.....	xiv
<b>CHAPTERS</b> .....	<b>19</b>
<b>1. INTRODUCTION.....</b>	<b>1</b>
a. General.....	1
b. Location.....	4
c. Objective and Significance.....	5
d. Previous Studies.....	5
e. Fundamental Data.....	15
<b>2. REGIONAL GEOLOGY.....</b>	<b>17</b>
a. Basin History.....	17
b. Regional Structure.....	20
c. Regional Stratigraphy.....	20
<b>3. CORE ANALYSIS.....</b>	<b>22</b>
a. Core Description.....	22
b. Core Plug Analysis.....	44
c. Thin Sections Analysis.....	47
d. Depositional Environment Interpretation.....	66

4. WELL LOGS.....	67
a. General.....	67
b. Gamma Ray.....	67
c. Resistivity.....	68
d. Porosity.....	68
e. Log Signatures for Depositional Environment.....	73
5. SEQUENCE STRATIGRAPHY AND WELL LOG CROSS SECTION.....	79
a. General.....	79
b. Sequence Stratigraphy.....	81
6. GEOLOGICAL MAPS.....	89
a. General.....	89
b. Structure.....	89
c. Interval Isopach.....	90
7. DISCUSSION.....	93
a. General.....	93
b. Uncertainties in Interpretation.....	93
c. Future Studies.....	93
8. CONCLUSIONS.....	95
REFERENCES.....	97

## LIST OF TABLES

<b>Chapter 1: Introduction</b>	
1.1: Whiting's (1982) list of five core wells.....	9
1.2: Pennsylvanian stratigraphic section of the Anadarko Basin.....	12
1.3: Johnson's (1984) list of Lower Red Fork cores.....	14
1.4: List of cores incorporated into this thesis.....	16
<b>Chapter 3: Core Analysis</b>	
3.1: Hunt Gillingham #1 core plug analysis.....	45
3.2: Amoco Smith Unit 1 core plug analysis.....	46
3.3: Hunt Gillingham #1 thin section analysis.....	47
3.4: Amoco Smith Unit 1 core plug analysis.....	58
<b>Chapter 4: Well Logs</b>	
4.1: Hunt Gillingham #1 grain density measurements.....	70
4.2: Amoco Smith #1 grain density measurements.....	70
3.3: Amoco Smith Unit 1 cored and perforated interval.....	25
3.4: Siltstone with siderite stains (depth: 14,148.5' Hunt Gillingham #1).....	26
3.5: Very thin layers of alternating siltstone and dark gray shale (depth: 14,146' Hunt Gillingham #1).....	27
3.6: Thinner and more subtle layers of alternating siltstone and dark gray shale (depth: 14,135' Hunt Gillingham #1).....	27
3.7: Planar dark gray shale and siltstone beds with bioturbation (depth: 14,128' Hunt Gillingham #1).....	28
3.8: Alternating siltstone and shale layers being eroded by a sandstone layer (depth: 14,117' Hunt Gillingham #1).....	29
3.9: Alternating siltstone and shale layers being eroded - detailed (depth: 14,117' Hunt Gillingham #1).....	30



## LIST OF FIGURES

### Chapter 1: Introduction

- 1.1: Small scale type log showing individual Red Fork Members.....3
- 1.2: General county map southwestern Oklahoma highlighting the study area.....4
- 1.3: Map of the area of interest in relation to the Clinton-Weatherford Trend, Strong City District, and SW Leedy Field.....6
- 1.4: Map of the area of interest in relation to the Clinton-Weatherford Trend, Strong City District, and SW Leedy Field with well control.....8
- 1.5: Whiting's (1982) five study wells relative to the thesis location.....10
- 1.6: Johnson's (1984) study area in comparison to the area of interest.....14

### Chapter 2: Regional Geology

- 2.1: Geologic provinces of Oklahoma (Northcutt et. al. 1995).....18

### Chapter 3: Core Analysis

- 3.1: Location of the cored wells incorporated into the thesis.....23
- 3.2: Hunt Gillingham #1 cored and perforated interval.....24
- 3.3: Amoco Smith Unit 1 cored and perforated interval.....25
- 3.4: Siltstone with siderite stains (depth: 14,148.5' Hunt Gillingham #1).....26
- 3.5: Very thin layers of alternating siltstone and dark gray shale (depth: 14,146' Hunt Gillingham #1).....27
- 3.6: Thinner and more subtle layers of alternating siltstone and dark gray shale (depth: 14,135' Hunt Gillingham #1).....27
- 3.7: Planar dark gray shale and siltstone beds with bioturbation (depth: 14,128' Hunt Gillingham #1).....28
- 3.8: Alternating siltstone and shale layers being eroded by a sandstone layer (depth: 14,117' Hunt Gillingham #1).....29
- 3.9: Alternating siltstone and shale layers being eroded – detailed (depth: 14,117' Hunt Gillingham #1).....30

3.10: Fine grained sandstone with bioturbation (depth: 14,115.5' Hunt Gillingham #1).....	30
3.11: Fine grained sandstone with planar and cross bedded dark gray shale, with presence of micro-faulting (depth: 14,115' Hunt Gillingham #1).....	31
3.12: Fine grained sandstone with mud clasts, ripples, and bioturbation (depth: 14,111.5' Hunt Gillingham #1).....	31
3.13: Dark gray shale and siltstone lenticular interbeds (depth: 14,091.5' Hunt Gillingham #1).....	32
3.14: Erosional feature overlying the alternating beds (depth: 14,091' Hunt Gillingham #1) .....	33
3.15: Wavy and lenticular siltstone with shale interbeds (depth: 14,089.5' Hunt Gillingham #1).....	33
3.16: Lenticular siltstone and shale interbeds (depth: 14,089' Hunt Gillingham #1).....	34
3.17: Shale and siltstone interbeds that are planar, wavy, and lenticular (depth: 14,085' Hunt Gillingham #1).....	34
3.18: Shaly sandstone with bioturbation (depth: 13,321' Smith Amoco Unit 1).....	35
3.19: Seven feet of core displaying coarsening upward sequences (depth: 13,315' to 13,308' Smith Amoco Unit 1).....	36
3.20: Siltstone and shale interbeds with siderite stains (depth: 13,310' Smith Amoco Unit 1).....	37
3.21: Fine grained sandstone (depth: 13,298' Smith Amoco Unit 1).....	37
3.22: Fine grained sandstone with bioturbation (depth: 13,286' Smith Amoco Unit 1).....	38
3.23: Coarsening upward sequence with extensive bioturbation (depth: 13,284' to 13,277' Smith Amoco Unit 1) .....	39
3.24: Shaly sandstone with trace fossil (depth: 13,283' Smith Amoco Unit 1).....	40
3.25: Shaly sandstone with bioturbation (depth: 13,283' Smith Amoco Unit 1).....	40
3.26: Dark shale between two sandstone bodies (depth: 13,277' to 13,270' Smith Amoco Unit 1).....	41

3.27: Fine grained wavy and lenticular sandstone with dark gray shale beds (depth: 13,275.5' Smith Amoco Unit 1).....	42
3.28: Fine grained sandstone with sharp angular contact (depth: 13,272' Smith Amoco Unit 1).....	42
3.29: Fine grained sandstone with shale clasts (depth: 13,271' Smith Amoco Unit 1)...	43
3.30: Thin section Hunt Gillingham #1 depth: 14,146.90' .....	50
3.31: Thin section Hunt Gillingham #1 depth: 14,117.00' .....	51
3.32: Thin section Hunt Gillingham #1 depth: 14,115.40' .....	52
3.33: Thin section Hunt Gillingham #1 depth: 14,114.40' .....	53
3.34: Thin section Hunt Gillingham #1 depth: 14,112.20' .....	54
3.35: Thin section Hunt Gillingham #1 depth: 14,103.50' .....	55
3.36: Thin section Hunt Gillingham #1 depth: 14,096.15' .....	56
3.37: Thin section Hunt Gillingham #1 depth: 14,089.65' .....	57
3.38: Thin section Amoco Smith Unit 1 depth: 13,309.00' .....	59
3.39: Thin section Amoco Smith Unit 1 depth: 13,307.45' .....	60
3.40: Thin section Amoco Smith Unit 1 depth: 13,305.60' .....	61
3.41: Thin section Amoco Smith Unit 1 depth: 13,299.25' .....	62
3.42: Thin section Amoco Smith Unit 1 depth: 13,295.70' .....	63
3.43: Thin section Amoco Smith Unit 1 depth: 13,280.35' .....	64
3.44: Thin section Amoco Smith Unit 1 depth: 13,266.30' .....	65

#### Chapter 4: Well Logs

4.1: Hunt Gillingham #1 entire Red Fork interval.....	74
4.2: Hunt Gillingham #1 Lower Red Fork Sandstone.....	75
4.3: Amoco Smith Unit 1 entire Red Fork interval.....	76

4.4: Amoco Smith Unit 1 Lower Red Fork Sandstone.....	77
-------------------------------------------------------	----

### Chapter 5: Cross Sections

5.1: Small scale sequence stratigraphic type log.....	80
5.2: Type log of two wells with different depositional environments and their sequence stratigraphic markers.....	84
5.3: Relative location of two wells with different depositional environments in relation to the shelf break.....	85
5.4: Generalized sequence stratigraphic model for the Lower Red Fork Sandstone.....	88
VII. Base cross section map.	
VIII. Sequence stratigraphic type log II.	
IX. Large scale logs with sequence stratigraphic markers.	
X. Generalized sequence stratigraphic model of the Lower Red Fork Sandstone	
XI. Generalized sequence stratigraphic model with cross section, and Type Log locations.	
XII. Cross section A - A'.	
XIII. Cross section B - B'.	
XIV. Cross section C - C'.	
XV. Cross section X - X'.	
XVI. Cross section Y - Y'.	
XVII. Cross section Z - Z'.	
XVIII. Structure at base of Lower Red Fork Sandstone.	
XIX. Structure at top of Lower Red Fork Sandstone.	
XX. Lower Red Fork Sandstone interval isopach.	

LIST OF PLATES

- I. Lithologic type log.
- II. Detailed cored and perforated intervals – Hunt Gillingham #1.
- III. Detailed cored and perforated intervals – Amoco Smith Unit #1.
- IV. Core description – Hunt Gillingham #1.
- V. Core description – Amoco Smith Unit #1.
- VI. Porosity comparison.
- VII. Base cross section map.
- VIII. Sequence stratigraphic type log II.
- IX. Large scale logs with sequence stratigraphic markers.
- X. Generalized sequence stratigraphic model of the Lower Red Fork Sandstone
- XI. Generalized sequence stratigraphic model with cross section, and Type Log locations.
- XII. Cross section A – A'.
- XIII. Cross section B – B'.
- XIV. Cross section C – C'.
- XV. Cross section X – X'.
- XVI. Cross section Y – Y'.
- XVII. Cross section Z – Z'.
- XVIII. Structure at base of Lower Red Fork Sandstone.
- XIX. Structure at top of Lower Red Fork Sandstone.
- XX. Lower Red Fork Sandstone interval isopach.

- XXI. Lower Red Fork Sandstone net sandstone map.
- XXII. HST-2 gross sandstone map – submarine fans.
- XXIII. HST-2 net sandstone map – submarine fans.
- XXIV. HST-3 gross sandstone map – older shallow marine shoreface bars.
- XXV. HST-3 net sandstone map – older shallow marine shoreface bars.
- XXVI. HST-3 porosity sandstone map – older shallow marine shoreface bars.
- XXVII. LST-4 gross sandstone map – older incised channels.
- XXVIII. LST-4 net sandstone map – older incised channels.
- XXIX. LST-4 porosity sandstone map – older incised channels.
- XXX. HST-4 gross sand map – younger shallow marine shoreface bars.
- XXXI. LST-5 gross sand map – younger incised channels.

## ABSTRACT

The Lower Red Fork Sandstone in the Anadarko Basin is of Pennsylvanian age (Desmoinesian Series), within the Cherokee Group. This subsurface analysis of the Lower Red Fork Sandstone in Caddo and Washita Counties, Oklahoma incorporated three hundred and forty eight wells, two cores, including core plug porosity and permeability measurements, and thin section petrography.

The Lower Red Fork Sandstone was split into four sequence stratigraphic packages, three of which contain complete lowstand to highstand cycles. Each sequence stratigraphic package was based on gamma ray, resistivity, and conductivity log characters. Three distinct log characters define systems tracts and their bounding surfaces. A blocky log character represents a Lowstand Systems Tract, a bell shape log represents a Transgressive Systems Tract, and a funnel shaped log character represents a Highstand Systems Tract. Changes in log characteristics over the entire study area are directly related to the distribution of marine and non-marine depositional facies and environments.

Structure maps were constructed for the base and the top of the Lower Red Fork Sandstone. The base structure map revealed the paleo-shoreline and paleo-shelf break at the onset of Lower Red Fork Sandstone deposition. Gross sandstone, net sandstone, porosity sandstone maps were constructed for each sequence stratigraphic package. The maps display three distinct trends. First, Highstand Systems Tract deposits of submarine fans were identified and mapped in the northwestern portion of the study. Second, northwest-southeast trending linear shallow marine shoreface bars were identified and mapped to the northeast, landward of the paleo-shoreline. Third, northeast-southwest

trending incised channel sandstones comprising parts of fluvial-deltaic complexes were identified and mapped farther southwest, towards the deeper part of the basin.

Successive episodes of progradational shoreface bars/distributary channels were deposited progressively southwestward, towards the deeper parts of the basin as the paleo-shelf edges and paleo-shore lines migrated. Detailed subdivision of shallow marine sands revealed two distinct sandstone trends with lowstand distributary channels crosscutting shallow marine shoreface bars. Deep water deposits may occur farther basinward and warrant further exploration.



## CHAPTER 1

### INTRODUCTION

#### a) General

The subject of this thesis is the Lower Red Fork sandstone in the Anadarko Basin of southwestern Oklahoma. The Red Fork sandstone is of Pennsylvanian age (Desmoinesian Series) and is confined within the Cherokee Group. The Red Fork sandstone is one of the main contributors of oil and gas production in the state of Oklahoma. Approximately 187 million barrels of oil and more than 3 trillion cubic feet of gas have been produced from 1979 through 1995 (Andrews, 1997). To date, oil and gas production from the Red Fork is even far greater. In order to explore for Red Fork sandstones, it is crucial to understand the geologic processes that trap hydrocarbons in these prolific reservoirs.

Successful hydrocarbon exploration must be based upon the assumption that hydrocarbons form and trap as a result of geological processes. If all oil and gas fields were due to chance with a random distribution of chance, then there would be little reason to believe that geology contributes to successful oil and gas exploration (Swanson, 1967). Under this premise, a detailed study of the Red Fork sandstone in this area will assist in exploring for hydrocarbons. In this study, the Red Fork sandstone is informally divided into Upper, Middle, and Lower units. Throughout the thesis, Red Fork sandstone overlies the Inola Limestone. The small scale lithologic type log in Figure 1.1 displays the individual Red Fork sandstones. The Upper Red Fork sandstone is typically overlain by the Pink limestone in most of the Anadarko Basin. However in

the area of study the Pink limestone is not very well developed and the Upper Red Fork sandstone is overlain by the Skinner sandstone.

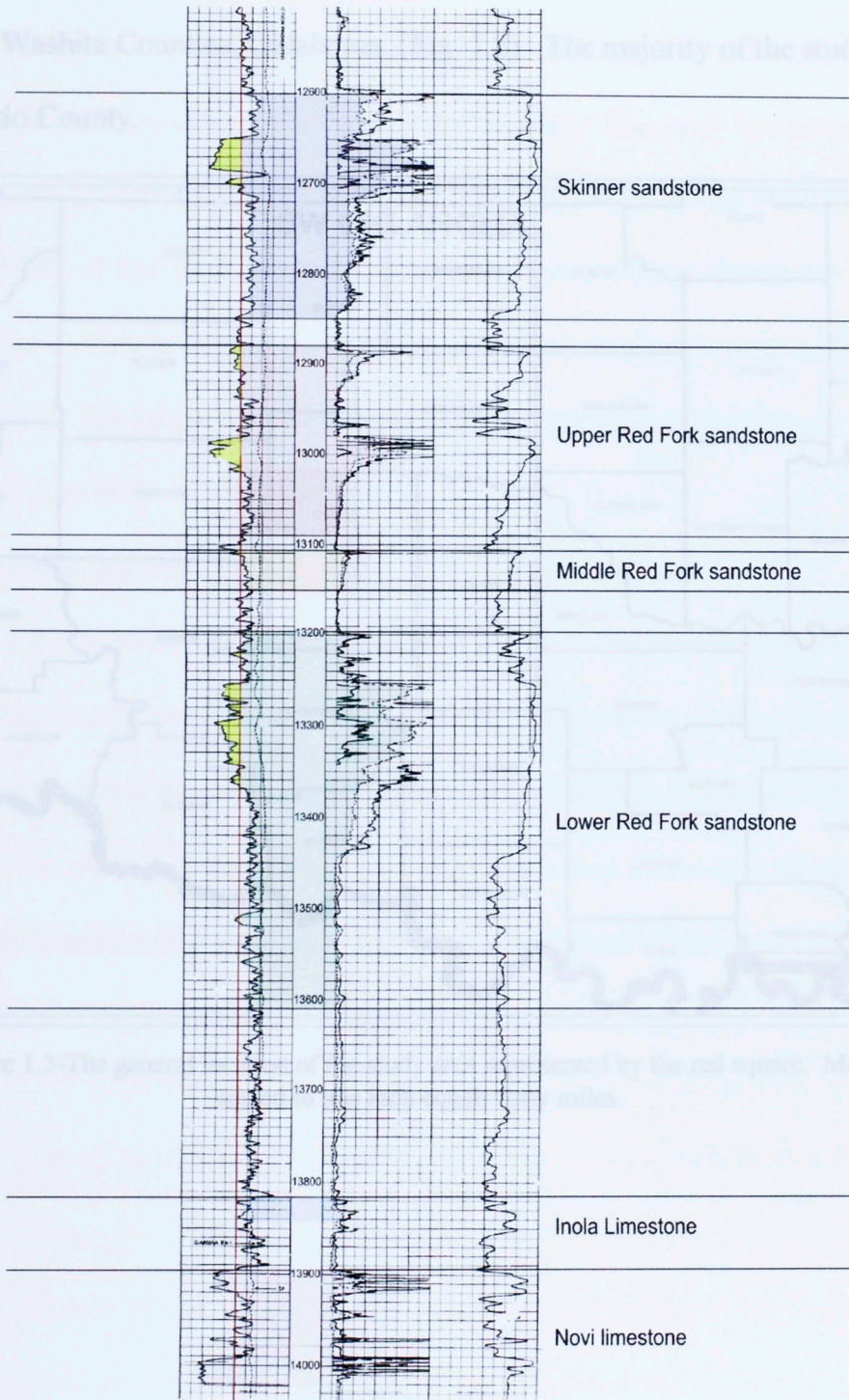
The top of the Lower Red Fork sandstone in the study area is around 13,000 feet deep and deepens southwestward, towards the basin axis. It contains relatively tight sandstone and shale intervals with thicknesses ranging from 300-800 feet. In the thesis area, the Lower Red Fork sandstone is predominantly a gas producing formation.



Figure L.1-The type log showing the individual Red Fork sandstone members confined by adjacent stratigraphic zones. Starting with the oldest to youngest stratigraphic formations are Novi limestone in violet, Inola Limestone in blue, Lower Red Fork sandstone in green, Middle Red Fork sandstone in yellow, and Upper Red Fork sandstone in red. The large scale type log is in the back pocket, (Plate I).

## TYPE LOG

Amoco Production  
J. E. Smith Unit # 1  
C W/2 Sec.26 - 10N - 12W  
KB 1565'



**Figure 1.1-The type log showing the individual Red Fork sandstone members confined by adjacent stratigraphic zones. Starting with the oldest to youngest stratigraphic formations are Novi limestone in violet, Inola Limestone in blue, Lower Red Fork sandstone in green, Middle Red Fork sandstone in yellow, and Upper Red Fork sandstone in red. The large scale type log is in the back pocket, (Plate I).**

## b) Location

The study area is located in the deeper part of the Anadarko Basin. It is enclosed within the following Townships and Ranges: 7N through 10N and 11W through 14W of Caddo and Washita Counties, Oklahoma, (Fig. 1.2). The majority of the study area lies within Caddo County.

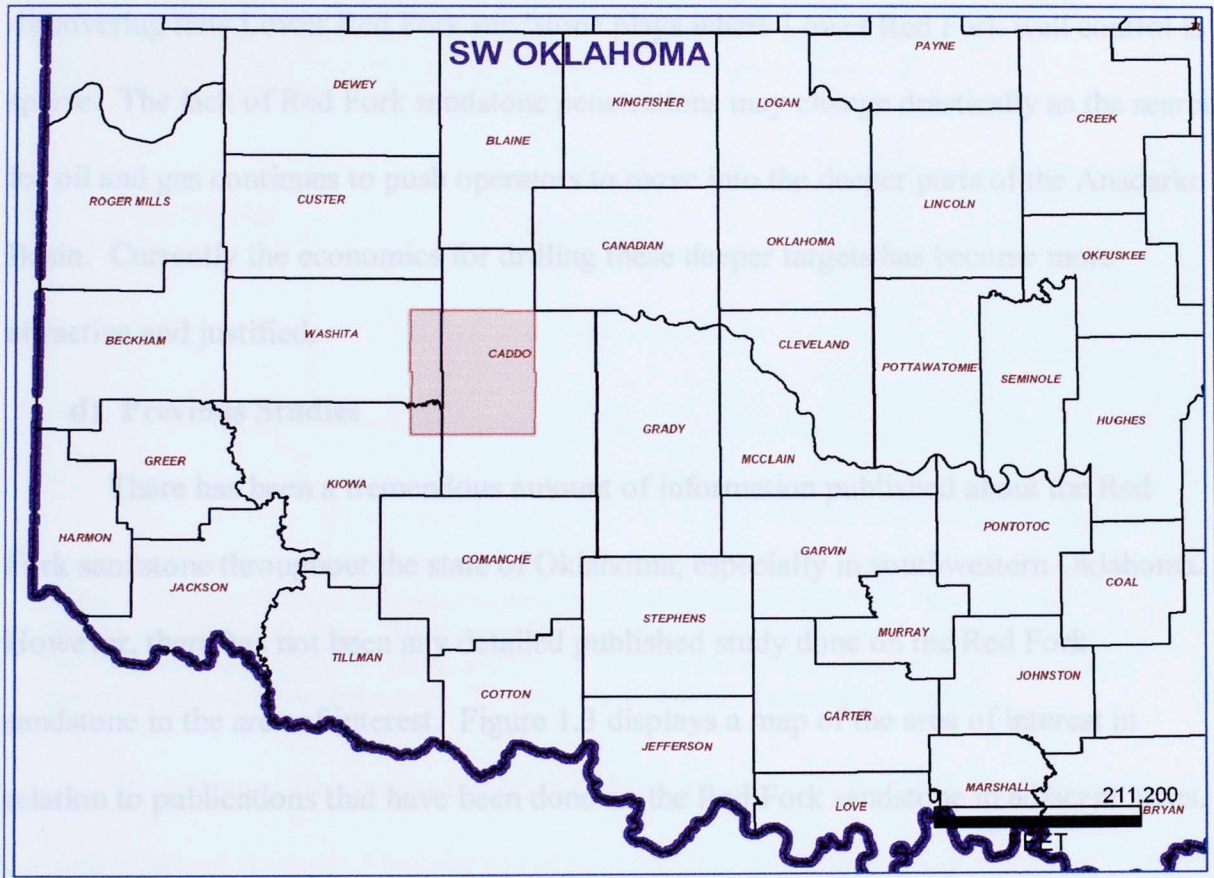


Figure 1.2-The general location of the study area represented by the red square. Map is scaled to one inch equals forty miles.

### **c) Objective and Significance**

The purpose of the thesis is to determine the depositional history and sequence stratigraphy of the Lower Red Fork sandstone. This analysis will assist in identifying potential exploration areas for the Lower Red Fork sandstone in Caddo and Washita Counties. This thesis is significant for multiple reasons. The study has potential for discovering new Lower Red Fork sandstone plays where Lower Red Fork well control is sparse. The lack of Red Fork sandstone penetrations may change drastically as the search for oil and gas continues to push operators to move into the deeper parts of the Anadarko Basin. Currently the economics for drilling these deeper targets has become more attractive and justified.

### **d) Previous Studies**

There has been a tremendous amount of information published about the Red Fork sandstone throughout the state of Oklahoma, especially in southwestern Oklahoma. However, there has not been any detailed published study done on the Red Fork sandstone in the area of interest. Figure 1.3 displays a map of the area of interest in relation to publications that have been done on the Red Fork sandstone in adjacent areas.

documented and studied. Clement (1991) published a detailed account of East Clinton Field which is included in the Clinton-Weatherford trend. The trend goes through three counties, starting at the southern boundaries of Blaine County, then proceeding westward from 12N-12W to 12N-19W to the northwestern portions of Caddo, and then straight west through the southern parts of Custer County. The depositional environment described by Clement (1991) is an Incised Valley Fill composed of three different stages of deposition which combine to form a major deltaic complex. Deep water deposits occur farther west. Clement (1991) described the three stages of valley fill in great detail in his

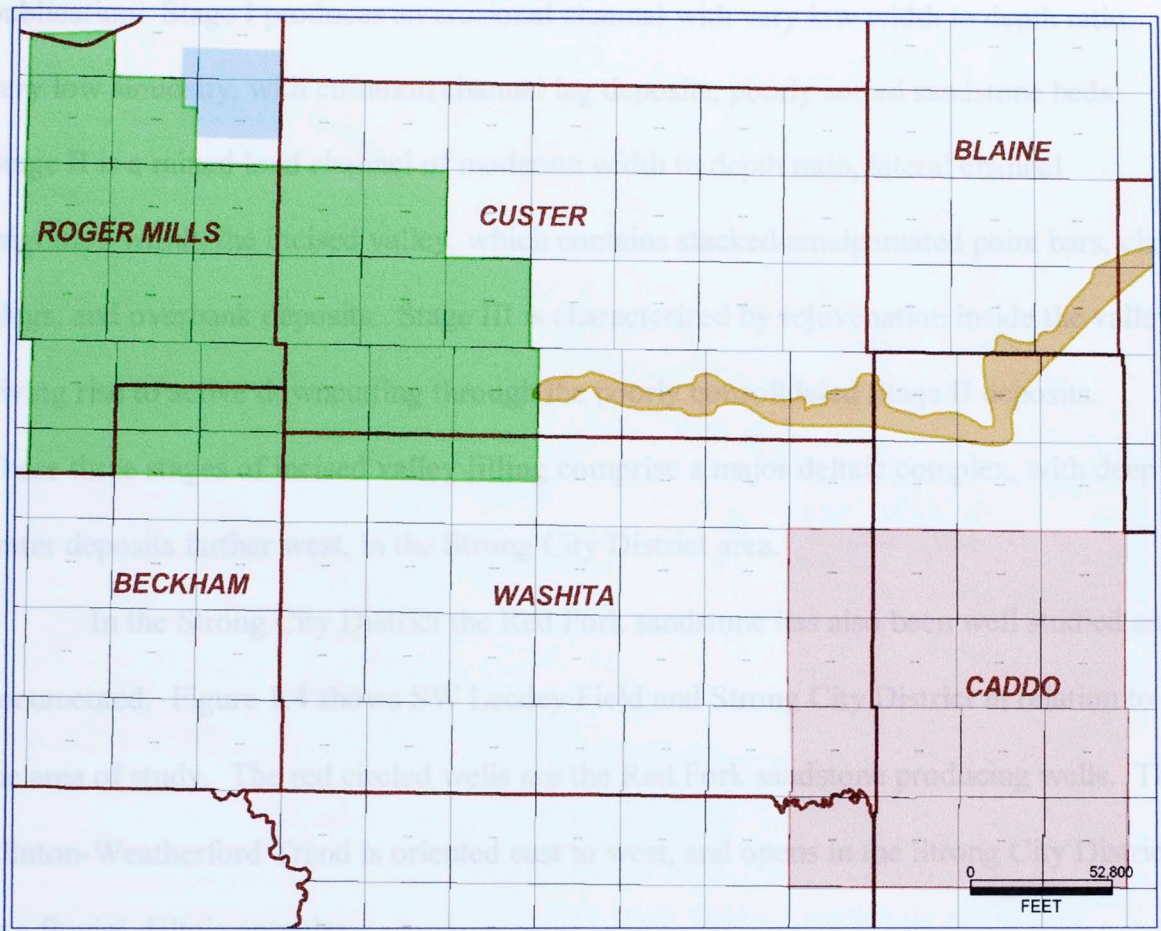


Figure 1.3-Map of the area of interest in relation to the Clinton-Weatherford Trend, Strong City District and SW Leedy Field. The Clinton-Weatherford Trend is highlighted in brown. Strong City District is highlighted by green, and the SW Leedy Field is highlighted by blue. The area of interest is denoted by the red square. The map is scaled to one inch equals 10 miles.

The Clinton-Weatherford trend is an Upper Red Fork play that has been well documented and studied. Clement (1991) published a detailed account of East Clinton Field which is included in the Clinton-Weatherford trend. The trend goes through three counties, starting at the southern boundaries of Blaine County, then proceeding westward from 12N-12W to 12N-19W to the northwestern portions of Caddo, and then straight west through the southern parts of Custer County. The depositional environment described by Clement (1991) is an Incised Valley Fill composed of three different stages of deposition which combine to form a major deltaic complex. Deep water deposits occur farther west. Clement (1991) described the three stages of valley fill in great detail in his

publication. Stage I produces an erosional channel with very low width to depth ratio, very low sinuosity, with common channel lag deposits, poorly sorted sandstone beds. Stage II is a mixed load channel of moderate width to depth ratio, lateral channel migration within the incised valley, which contains stacked/amalgamated point bars, clay plugs, and overbank deposits. Stage III is characterized by rejuvenation inside the valley giving rise to active downcutting through the poorly consolidated Stage II deposits. These three stages of incised valley filling comprise a major deltaic complex, with deep water deposits farther west, in the Strong City District area.

In the Strong City District the Red Fork sandstone has also been well studied and documented. Figure 1.4 shows SW Leedey Field and Strong City District in relation to the area of study. The red circled wells are the Red Fork sandstone producing wells. The Clinton-Weatherford Trend is oriented east to west, and opens in the Strong City District as a fluvial-deltaic complex.

In 2002 Puckette and Al-Shaieb conducted a study on the Red Fork sandstone in the Strong City District and SW Leedey Field. They split the Red Fork sandstone into the Upper and Lower Red Fork. Only the Upper Red Fork sandstone was studied in both of the fields. In the Strong City District, Puckette, et al. (2002) determined that a large fluvial-deltaic complex formed as the sands prograded toward the Anadarko Basin. As sea level dropped, lowstand system tract sands were transported beyond the shelf break and deposited onto the slope and basin floor as submarine fan complexes. In the SW Leedey Field sands were deposited as shallow marine shelf bars (Puckette, et al., 2002).

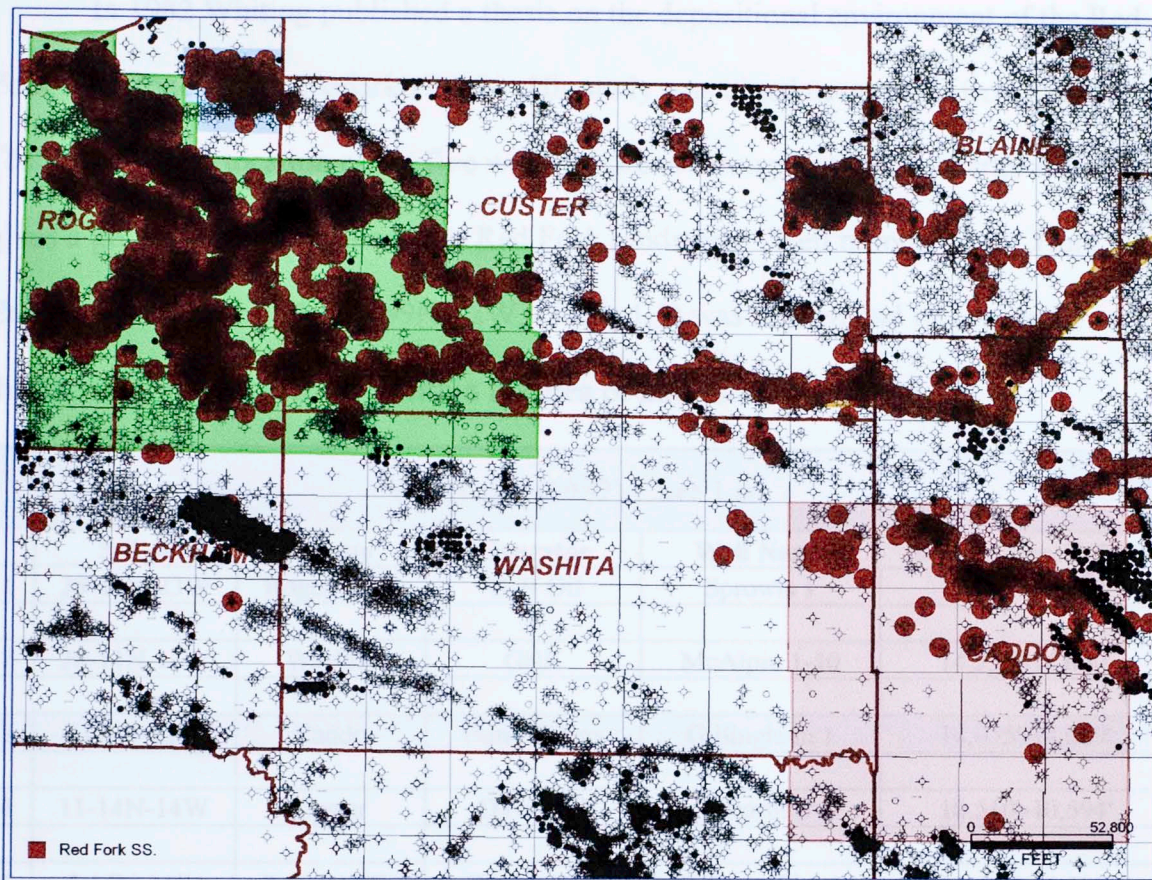


Figure 1.4-Map showing Strong City District and SW Leedy Field in relation to the area of study. Wells colored in red are Red Fork sandstone producers. The Strong City District is highlighted by the green shaded area, and the SW Leedy Field is highlighted by the light blue shaded area north of the Strong City District area. The area of interest is enclosed by the red shaded square at the southeast corner of the map. The map is scaled to one inch equals 10 miles.

In 2002 Puckette and Al-Shaieb conducted a study on the Red Fork sandstone in the Strong City District and SW Leedy Field. They split the Red Fork sandstone into the Upper and Lower Red Fork. Only the Upper Red Fork sandstone was studied in both of the fields. In the Strong City District, Puckette, et al. (2002) determined that a large fluvial-deltaic complex formed as the sands prograded toward the Anadarko Basin. As sea level dropped, lowstand system tract sands were transported beyond the shelf break and deposited onto the slope and basin floor as submarine fan complexes. In the SW Leedy Field sands were deposited as shallow marine shelf bars (Puckette, et. al., 2002).



In 1982 Whiting published a thesis on the depositional environment of the Red Fork sandstone in the Anadarko Basin. His study was based upon cores from five wells, (Table 1.1). The location of the five wells is spread throughout the Anadarko Basin, and gives a good general analysis of the Red Fork sandstone. Well number three, Hunt Energy's Gillingham #1 in 21-9N-12W, (Table 1.1) was studied and incorporated into this thesis as it is located well within the area of interest.

<b>Whiting's (1982) Core List</b>					
	<b>S-T-R</b>	<b>County</b>	<b>Operator</b>	<b>Well Name</b>	<b>Interval Depth (feet)</b>
1	38-13N-23W	Roger Mills	Gulf Oil	Sprowls 1	12,692'-12,751'
2	28-11N-16W	Washita	GHK	McAlpin 1-10	14,555'-14,600'
3	21-9N-12W	Caddo	Hunt Energy	Gillingham 1	14,055'-14,069'
4	11-14N-14W	Custer	Davis Oil	Stearns 3	10,510'-10,594'
5	5-15N-21W	Roger Mills	Woods Pet.	Switzer 'C' 5-1	11,443'-11,503'

Table 1.1 Whiting's list of five core wells. Core from well number 3 was studied and incorporated into this thesis.

Figure 1.5 shows Whiting's (1982) five study wells relative to the thesis area.

Whiting did not split the Red Fork sandstone into any units and concluded that it was deposited in a deep marine environment, by turbidity currents, and exhibits ordered sequences of sedimentary structures characteristics of turbidite deposition (Whiting, 1982).

the Tonkawa sandstone is of Pennsylvanian age, similar to the Red Fork. However the Tonkawa is younger in geological time compared to the Red Fork. Table 1.2 shows the Pennsylvanian stratigraphic section of the Anadarko Basin. The table displays the Tonkawa sandstone in comparison to the Red Fork sandstone on the stratigraphic column. Kumar and Slatt (1984) concluded that the Lower Tonkawa was deposited as a submarine fan complex, the Middle Tonkawa was deposited on a

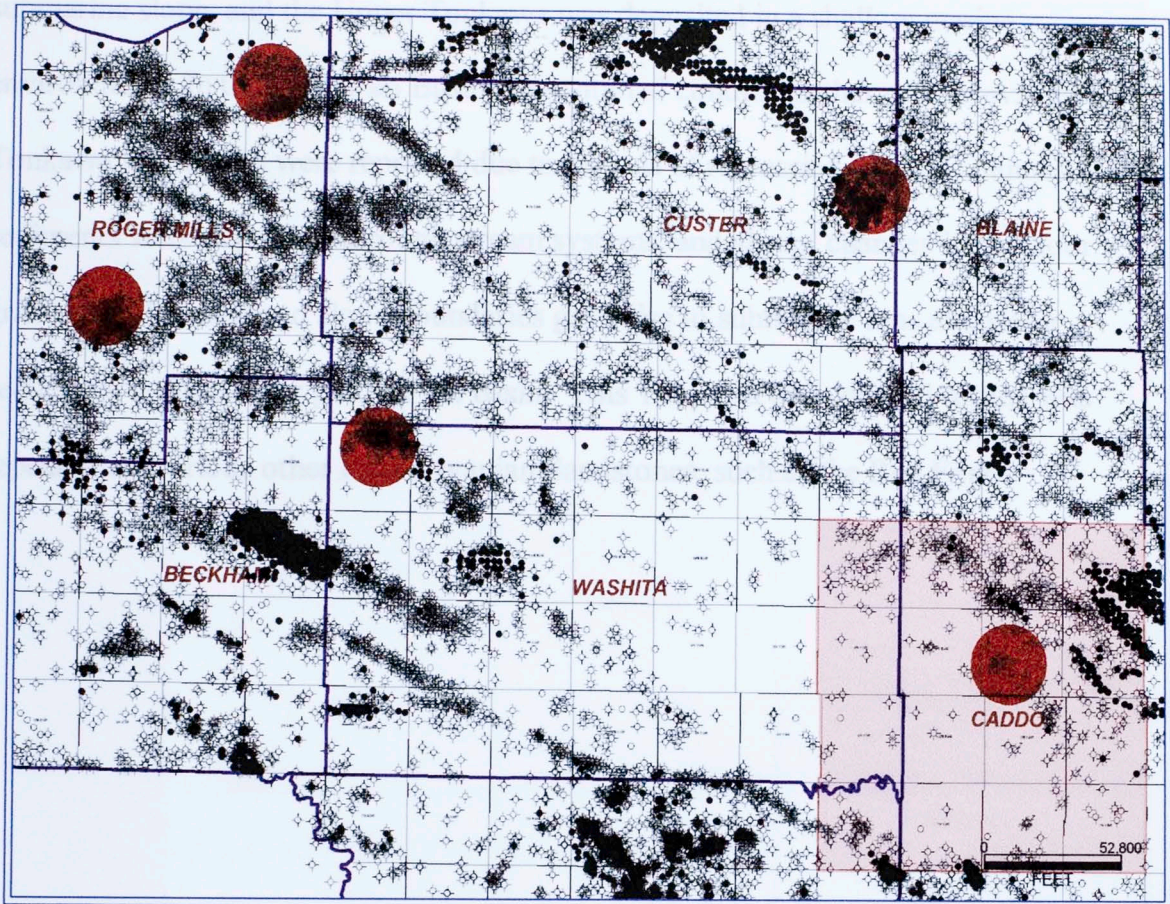


Figure 1.5-Map showing Whiting's (1982) five study wells relative to the thesis area. One inch equals ten miles.

In 1984 Kumar and Slatt conducted a study on the Missourian-Virgilian Tonkawa sandstone in the deeper part of the Anadarko Basin. The study area included parts of: Dewey, Custer, Blaine, Caddo, and Canadian Counties. The Tonkawa sandstone was split into Upper, Middle, and Lower Tonkawa. This study is relevant to this thesis because the Tonkawa sandstone is of Pennsylvanian age, similar to the Red Fork. However the Tonkawa is younger in geological time compared to the Red Fork. Table 1.2 shows the Pennsylvanian stratigraphic section of the Anadarko Basin. The table displays the Tonkawa sandstone in comparison to the Red Fork sandstone on the stratigraphic column. Kumar and Slatt (1984) concluded that the Lower Tonkawa was deposited as a submarine fan complex, the Middle Tonkawa was deposited on a

submarine slope, and the Upper Tonkawa was deposited in a shallow marine environment. In the Anadarko Basin, depositional conditions that were prevalent for Tonkawa sandstones were repeated due to periods of regression. Large volumes of sediments were deposited through stream systems, and abrupt changes in sea floor gradient at the shelf and slope boundaries gave rise to submarine fans and slope sequences in the deeper parts of the basin. This Tonkawa depositional setting was repeated for various other Pennsylvanian Sandstones, such as the Red Fork.

System	Series	Group	Formation	
Pennsylvanian	Missourian	Douglas	Endicott	
			Hoover Sandstone	
			Toronto	
	Missourian	Lansing	Haskell Limestone	
			Upper Tonkawa	
			Middle Tonkawa	
	Desmoinesian	Kansas City	Wade	
			Avant	
		Desmoinesian	Marmaton	Medrano
				Cottage Grove
Hogshooter				
Atokan	Cherokee	Marchand		
		Checkerboard		
	Atokan	Cherokee	Cleveland	
			Big Lime	
			Oswego	
Morrowan		Prue		
		Verdigris		
		Skinner		
Morrowan		Pink Lime		
		Red Fork		
		Inola		
Morrowan		13 Finger (Nov)		
		Purveyer		
		Squaw Belly		
Morrowan		Primrose		

Table 1.2 shows the Pennsylvanian stratigraphic section of the Anadarko Basin.

Pennsylvanian Geologic Section of the Anadarko Basin			
System	Series	Group	Formation
PENNSYLVANIAN	Virgillian		Brownville Limestone Wabaunese Edwards Lecompton Hoover Sandstone Elgin Oread Limestone Heebner
		Douglas	Endicott Lovell Toronto Haskell Limestone Upper Tonkawa
			Middle Tonkawa Lower Tonkawa
	Missourian	Lansing	Wade Avant Medrano
		Kansas City	Cottage Grove Hogshooter
			Marchand Checkerboard Cleveland
	Desmoinesian	Marmaton	Big Lime Oswego
		Cherokee	Prue Verdigris Skinner Pink Lime Red Fork Inola
		Atokan	13 Finger (Novi)
	Morrowan		Puryear Squaw Belly Primrose

Table 1.2 shows the Pennsylvanian stratigraphic section of the Anadarko Basin.

In 1984 Johnson published a thesis on the depositional environment, reservoir trend, and diagenetic history of the Red Fork sandstone while at Oklahoma State University. The study area covered parts of Blaine, Caddo, and Custer Counties, Oklahoma, (Fig. 1.6). The Red Fork sandstone was split into Upper and Lower intervals. Johnson (1984) examined two cores from the Lower Red Fork sandstone, (Table 1.3). Locations of the two cored wells are highlighted by red circles in Figure 1.6. Johnson also examined 51 thin sections from the two cores he studied.

By contrast, deposition of the Upper Red Fork sandstone was determined to be a result of maximal progradation of a deltaic sequence. The Lower Red Fork sandstone was strongly influenced by a shelf-slope break. Deposition of the Lower Red Fork sandstone was determined to be in submarine canyons and as submarine fans. According to the study, primary porosity had been destroyed by compaction and cementation. However secondary porosity had developed due to dissolution of siliceous mud fragments and possibly calcite cements, (Johnson, 1984).

Figure 1.6-Map displaying Johnson's study area and two cored wells in comparison to the area of interest. One inch equals ten miles. Johnson's study is highlighted by a blue rectangle and the area of interest is highlighted by the red square.

Johnson's (1984) Lower Red Fork Cores					
	S-T-R	County	Operator	Well Name	Interval Depth (feet)
1	18-14N-13W	Blaine	Southport	Switzer 2	12,602-12,751
2	17-14N-14W	Custer	Davis Oil	Herring 1	10,857-10,917

Table 1.3 displays the two cores Johnson studied for the Lower Red Fork sandstone.

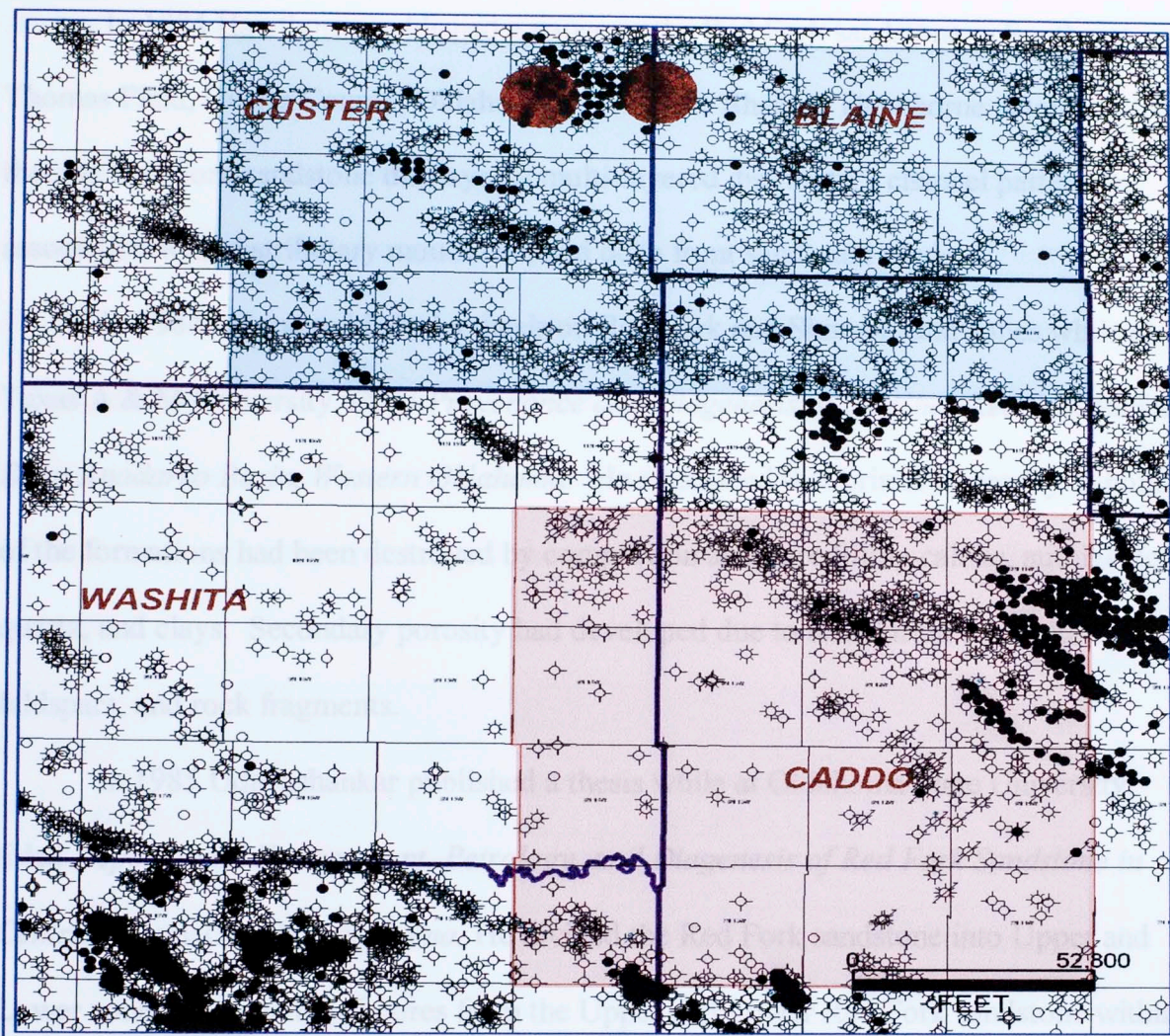


Figure 1.6-Map displaying Johnson's study area and two cored wells in comparison to the area of interest. One inch equals ten miles. Johnson's study is highlighted by a blue rectangle and the area of interest is highlighted by the red square.

Johnson's (1984) Lower Red Fork Cores					
	S-T-R	County	Operator	Well Name	Interval Depth (feet)
1	18-14N-13W	Blaine	Southport	Switzer 2	12,692'-12,751'
2	17-14N-14W	Custer	Davis Oil	Herring 1	10,857'-10,917'

Table 1.3 displays the two cores Johnson studied for the Lower Red Fork sandstone.

In 1984 Hawthorne published a paper on the Red Fork sandstone in Southeast Thomas Field, Custer County, Oklahoma in the Shale Shaker. Hawthorne determined that the Red Fork sandstone displayed a multi-layered distributary channel pattern, in association with distributary mouth bars and delta front sands and muds.

In 1984 Levine published a thesis on Red Fork and Skinner sandstones while at Texas A & M University, titled *Provenance and Diagenesis of the Cherokee Sandstones, Deep Anadarko Basin, Western Oklahoma*. He concluded that primary porosity in both of the formations had been destroyed by compaction and pore filling calcite, authigenic quartz, and clays. Secondary porosity had developed due to dissolution of calcite cement, feldspars, and rock fragments.

In 1985 Udayashankar published a thesis while at Oklahoma State University, titled *Depositional Environment, Petrology, and Diagenesis of Red Fork Sandstone in Central Dewey County, Oklahoma*. He divided the Red Fork sandstone into Upper and Lower zones. He examined cores from the Upper and Lower Red Fork sandstone within Putnam Field in Township 17N and Ranges 17W and 18W. Study of 140 thin sections indicated that the primary porosity in both the upper and lower zones was destroyed by diagenetic processes, and secondary porosity was generated by dissolution of shale clasts, feldspars, and quartz. Also, the depositional environment of the study area was found to be at the paleoshelf near deltaic distributary channels.

#### **e) Fundamental Data**

The basic data that was utilized for this study includes well logs, core descriptions, core plug analysis, and thin section petrographic descriptions. Well logs include the following: gamma ray, resistivity, neutron porosity, and density porosity. The

majority of the logs were available at the Oklahoma City Geological Library in Oklahoma City, Oklahoma. There are seven wells in the study area that have Lower Red Fork sandstone core. However only two cores were studied due to their optimum location in comparison to the reservoir quality sands (Table 1.4). Cores were rented from the Oklahoma Petroleum Information Center (OPIC). Core plugs were made by the OGS in Norman, and then sent to Core Lab in Houston to be analyzed for porosity and permeability under reservoir pressure. Thin sections were cut from the core plugs to describe the petrography of the cores. All of the mapping was done using GeoPlus Petra software.

<b>Core List</b>					
	<b>S-T-R</b>	<b>County</b>	<b>Operator</b>	<b>Well Name</b>	<b>Interval Depth</b>
1	21-9N-12W	Caddo	Hunt	Gillingham 1	14,085'-14,099'
					14,101'-14,149'
2	26-10N-12W	Caddo	Amoco	Smith 1	13,262'-13,322'

Table 1.4 shows two cores that were incorporated into this thesis.



## CHAPTER 2

### REGIONAL GEOLOGY

#### a) Basin History

The Anadarko Basin is located in parts of southwest Oklahoma and the Texas Panhandle. The Basin is an asymmetric basin bounded on the north by the Anadarko Shelf, on the east by the Nemaha Ridge, and on the south and southwest by the Amarillo-Wichita Uplift. Figure 2.1 shows the geologic provinces of Oklahoma. The location of Anadarko Basin and its surrounding features are highlighted.

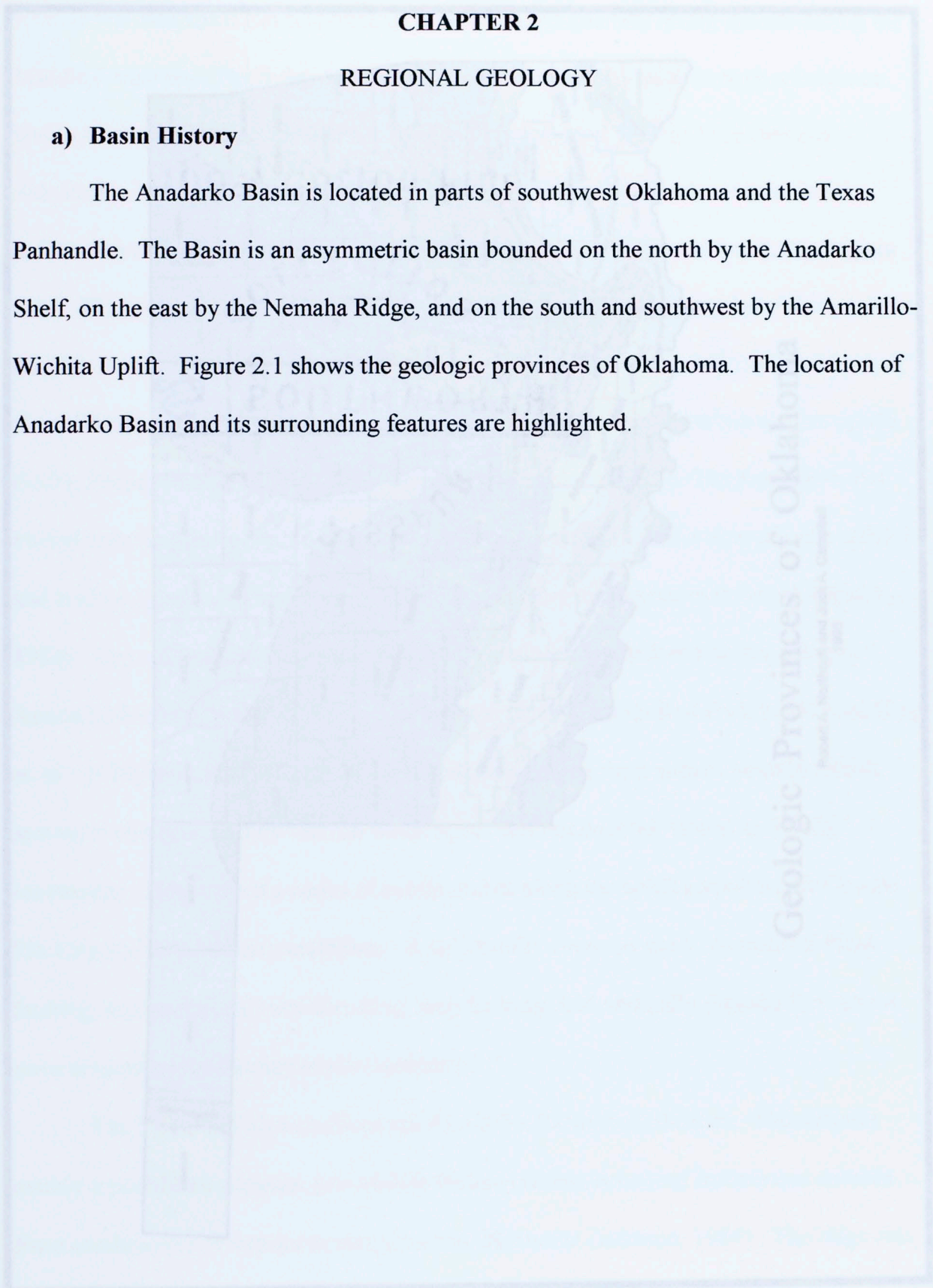


Figure 2.1-Map highlighting the Geologic Provinces of Oklahoma (Northcutt et al. 1995)

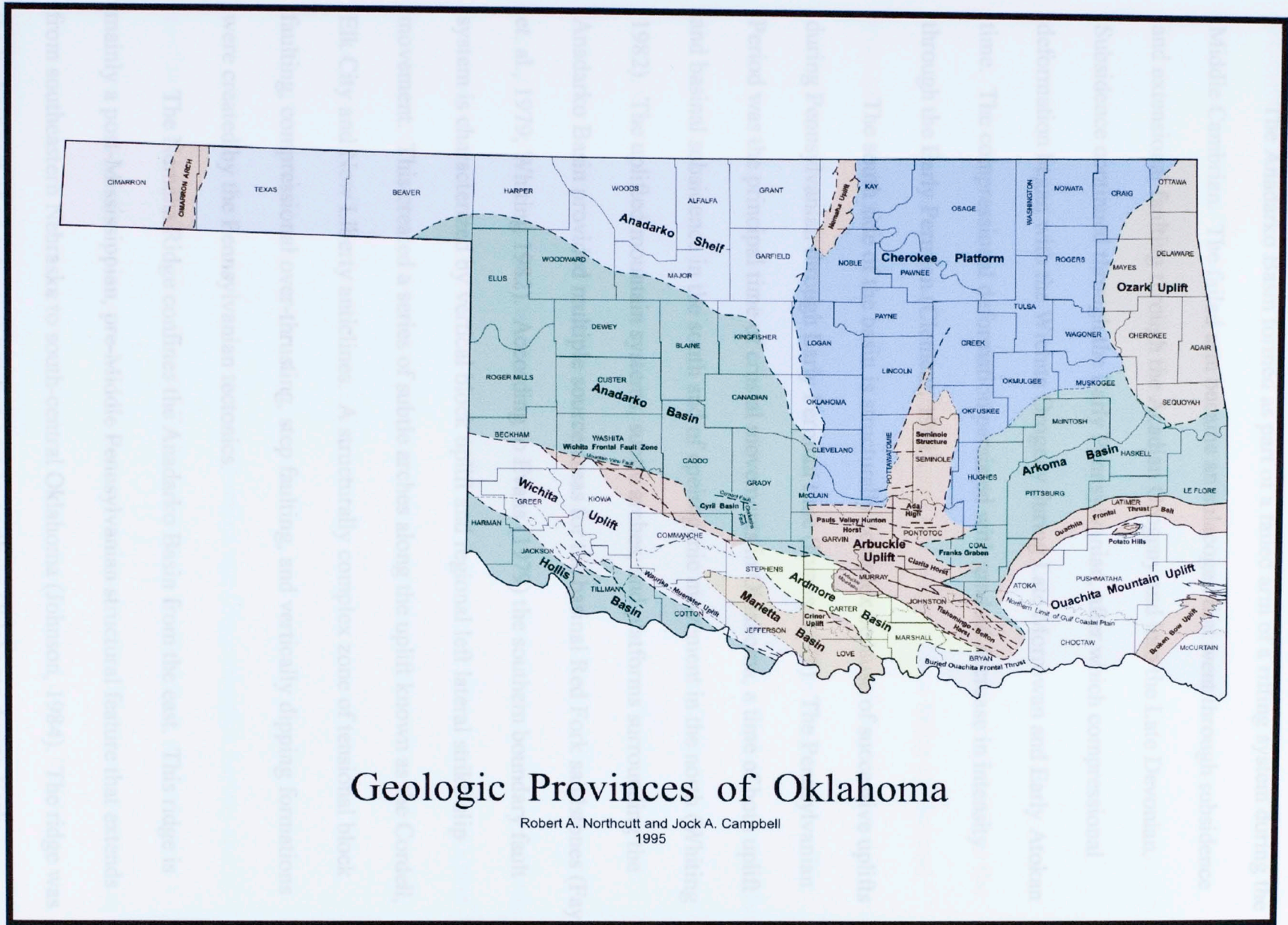


Figure 2.1-Map highlighting the Geologic Provinces of Oklahoma (Northcutt et. al. 1995).

The Anadarko Basin formed as part of a failed arm of a rifting system during the Middle Cambrian. The failed arm became an aulacogen that went through subsidence and extensional faulting through the Acadian Orogeny and into the Late Devonian. Subsidence continued through the Early Pennsylvanian, after which compressional deformation began with the Wichita Orogeny during Late Morrowan and Early Atokan time. The compressional deformation persisted with gradual decrease in intensity through the Early Permian (Clement, 1991).

The south side of the basin is structurally complex because of successive uplifts during Pennsylvanian through Early Permian time (Evans, 1979). The Pennsylvanian Period was the principal time of crustal movements in Oklahoma, a time of both uplift and basinal subsidence in the south and of epeirogenic movement in the north (Whiting 1982). The uplifted mountain systems, subtle arches, and platforms surrounding the Anadarko Basin provided multiple source areas for the basinal Red Fork sandstones (Fay et. al., 1979; Whiting 1982). According to Evans (1979) the southern boundary fault system is characterized by vertical block uplift and regional left lateral strike-slip movement. This created a series of subtle arches along the uplift known as the Cordell, Elk City and New Liberty anticlines. A structurally complex zone of tensional block faulting, compressional over-thrusting, step faulting, and vertically dipping formations were created by the Pennsylvanian tectonics.

The Nemaha Ridge confines the Anadarko Basin from the east. This ridge is mainly a post-Mississippian, pre-Middle Pennsylvanian structural feature that extends from southeastern Nebraska to south-central Oklahoma (Johnson, 1984). The ridge was the highest part of an extensive positive area in northern Oklahoma during Early

Pennsylvanian time (Whiting, 1982). Rapid erosion and numerous episodes of subsidence resulted in partial submergence of the Nemaha highlands during Desmoinesian time (Cole 1969). The gently dipping Anadarko Shelf confines the basin from the north and northwest.

### **b) Regional Structure**

The regional structure within the area of interest is relatively simple. Up to the Late Mississippian time the basin was subsiding and sediment was being transported from the north and northeast. This caused basement-involved tension that created a subtle hinge known as the Corn Eakly – Fort Cobb Anticline. The hinge separated the deeper basinal environment from the shallower shelf environment. With the onset of the Wichita Orogeny during the Early Pennsylvanian (Late Morrowan-Early Atokan) the hinge became more prominent with local highs and lows. This set the paleostructure before the Lower Red Fork sandstone was deposited from the north and northeast. From the Early Pennsylvanian to the Permian, the Corn Eakly – Fort Cobb Anticline gradually became pronounced with continued compressional deformation. The Amarillo-Wichita Uplift system created subtle arches and platforms in the south and southwest that could have provided additional sediment source areas.

### **c) Regional Stratigraphy**

The Red Fork sandstone is of Pennsylvanian age (Desmoinesian Series) and is confined within the Cherokee Group. Table 1.2 displays the Red Fork sandstone in relation to other adjacent formations of the Anadarko Basin. The Red Fork sandstone is partitioned into three units in the study area: Upper, Middle, and Lower Red Fork.

Hawthorne (1985) also divided the Red Fork sandstone into three distinct units: A, B, and

C. Figure 1.1 shows a type log of the Red Fork sandstone. The Inola Limestone confines the Red Fork sandstone on the bottom and Pink limestone caps the Red Fork sandstone. However, in the study area, Pink limestone is not very well developed and the Skinner sandstone caps the Red Fork sandstone.

The Cherokee Group in the subsurface contains the following informal stratigraphic intervals, from the oldest to the youngest: Inola Limestone, Red Fork sandstone, Pink limestone, Skinner sandstone, and Verdigris Limestone. The Inola Limestone overlies the Atokan Group, and comprises the basal Cherokee Group. The limestone is from 5 to 30 feet thick, and thickens and thins irregularly in the study area. The Red Fork sandstone overlies the Inola Limestone. The Lower Red Fork sandstone's thickness ranges from 250 to 850 feet, and thickens towards the west and southwest. The Middle Red Fork sandstone's thickness ranges from 5 to 50 feet. It thickens towards the middle of the study area and then thins further west and southwest. The thickness of the Upper Red Fork sandstone ranges from 30 to 250 feet, and thickens towards the west and southwest. The thicknesses of the Skinner sandstone and the Verdigris Limestone remain relatively constant with minor thickening toward the west and southwest. The Verdigris Limestone defines the top of the Cherokee Group.

## CHAPTER 3

### CORE ANALYSIS

#### a) Core Description

Two cores in the thesis area were examined. They are from the following wells, (Fig. 3.1).

	<u>Operator</u>	<u>Well Name</u>	<u>Location</u>	<u>Cored Interval</u>
1)	Hunt Energy	Gillingham #1	21-9N-12W	14,085'-14,149'
2)	Amoco	J.E. Smith Unit 1	26-10N-12W	13,262'-13,322'

Figures 3.2 and 3.3 show the depth of cored and perforated interval for Hunt Energy Gillingham #1 and for the Amoco Smith Unit 1 well, respectively. Plates II and III display the two wells at a larger scale. A 75 API cut off is used to denote sandstone, and an 8% cross-plot porosity cut off is used to denote porous sandstone. A detailed core description was completed for both of the cores (Plates IV and V).

Figure 3.1-Map showing the location of the cored wells within the study area. The green circles denote wells that are Lower Red Fork sandstone gas producers. The location of the Hunt Energy Gillingham #1 is centered in the thesis area, highlighted by a blue arrow. The Amoco Smith Unit 1 well is highlighted by a red arrow, within a heavily developed Lower Red Fork sandstone producing area. One inch equals three and half miles.

There was a core-to-log correction for both of the wells. Thirty feet was added to the cored depth of the Hunt Energy Gillingham #1 well. Three feet were added to the cored depth of the Amoco Smith Unit 1 well. This was based on the observation that the core descriptions complement the log curve signature better with the correction. Usually core-to-log corrections are done with a core gamma scan record, if available, however this information was never located for these wells.

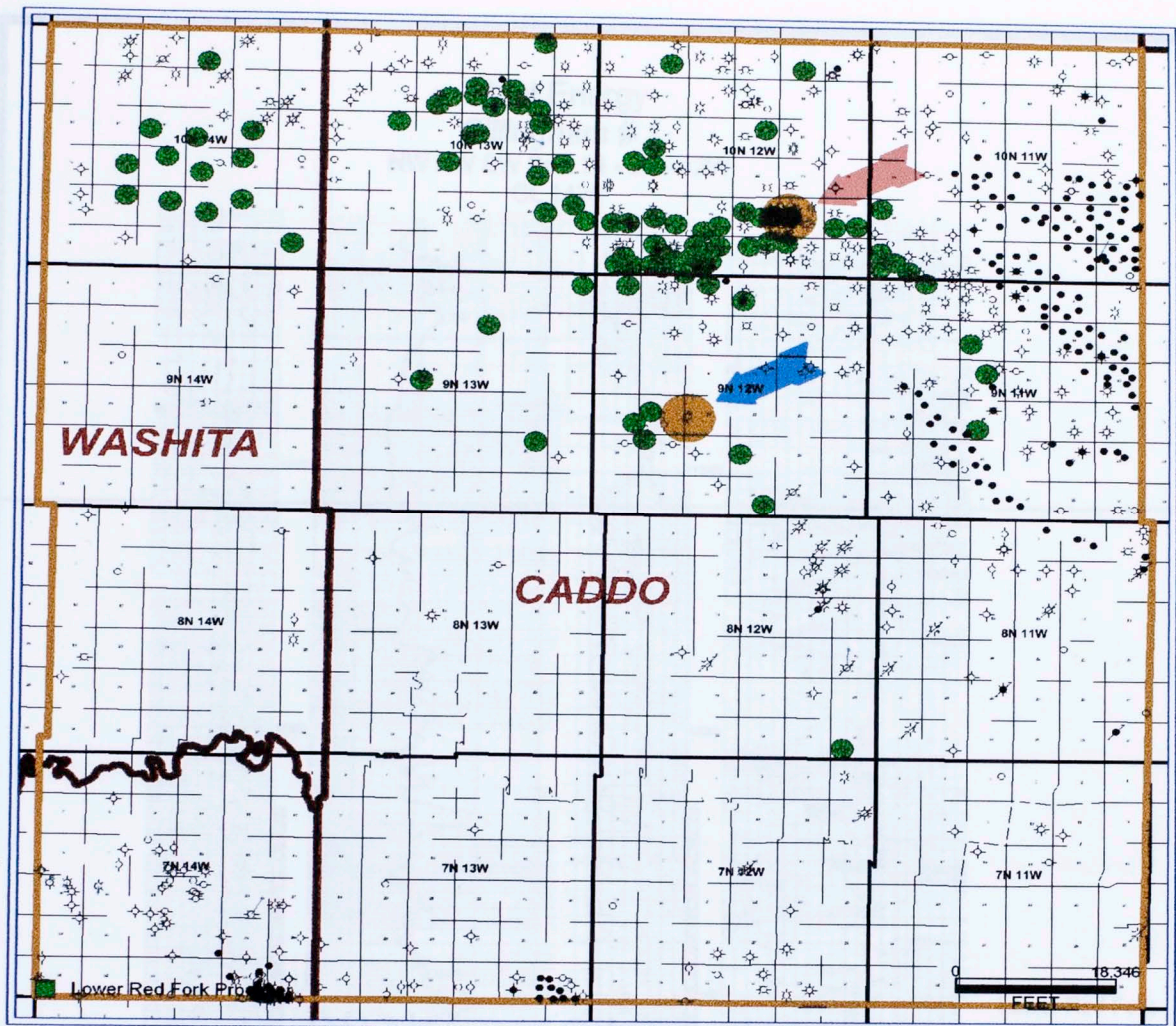


Figure 3.1-Map showing the location of the cored wells within the study area. The green circles denote wells that are Lower Red Fork sandstone gas producers. The location of the Hunt Energy Gillingham #1 is centered in the thesis area, highlighted by a blue arrow. The Amoco Smith Unit 1 well is highlighted by a red arrow, within a heavily developed Lower Red Fork sandstone producing area. One inch equals three and half miles.

There was a core-to-log correction for both of the wells. Thirty feet was added to the cored depth of the Hunt Energy Gillingham #1 well. Three feet were added to the cored depth of the Amoco Smith Unit 1 well. This was based on the observation that the core descriptions complement the log curve signature better with the correction. Usually core-to-log corrections are done with a core gamma scan record, if available, however this information was never located for these wells.

Hunt Energy  
 Gillingham # 1  
 NW NW SW Sec. 21 - 9N - 12W  
 GL 1424'

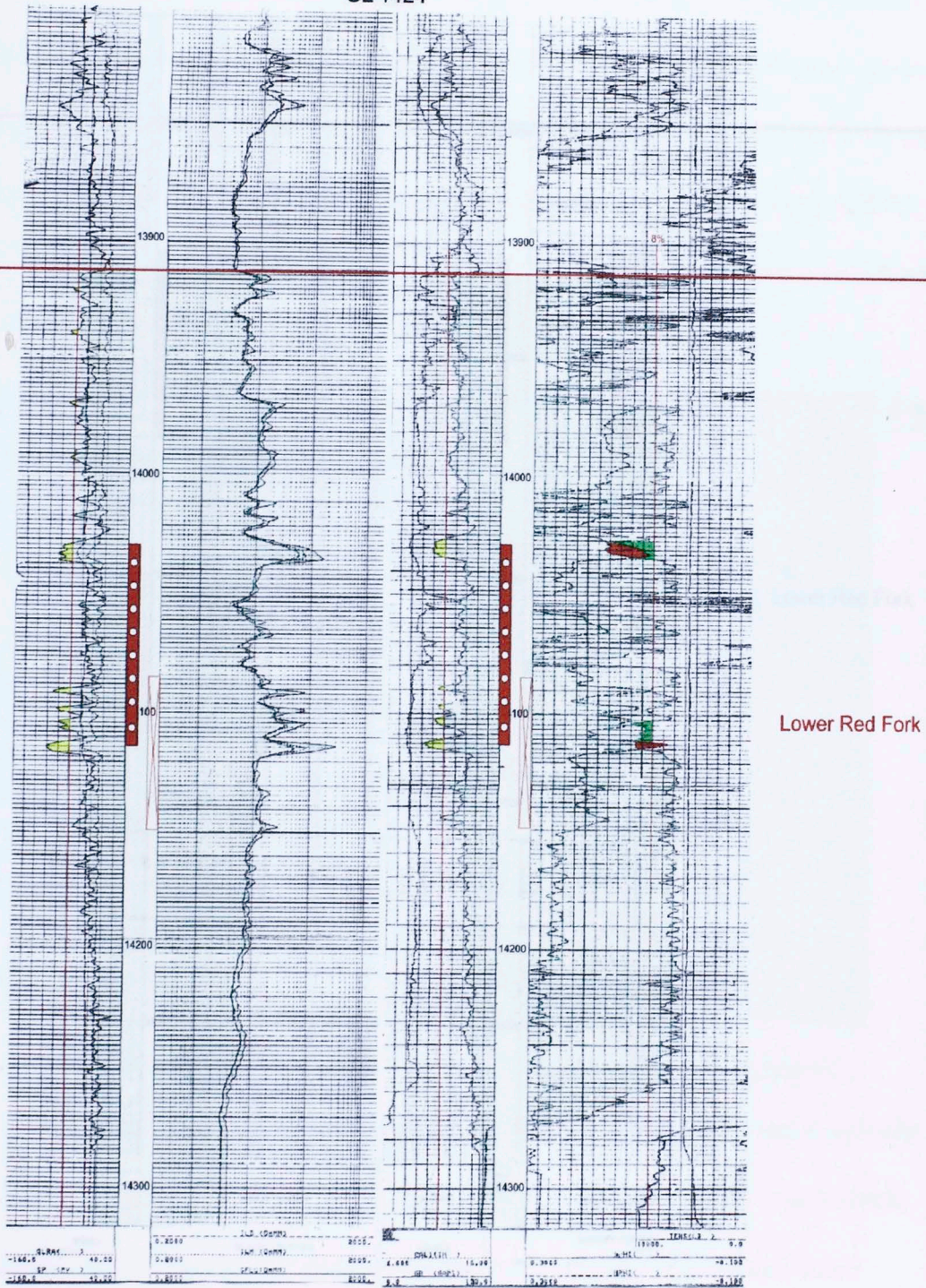


Figure 3.2-The location of Hunt Energy Gillingham #1 cored interval on the dual induction, and neutron/density logs. Plate II displays more detail.



Amoco Production  
 J.E. Smith Unit Well # 1  
 C SW Sec. 26 10N 12W  
 KB 1565'

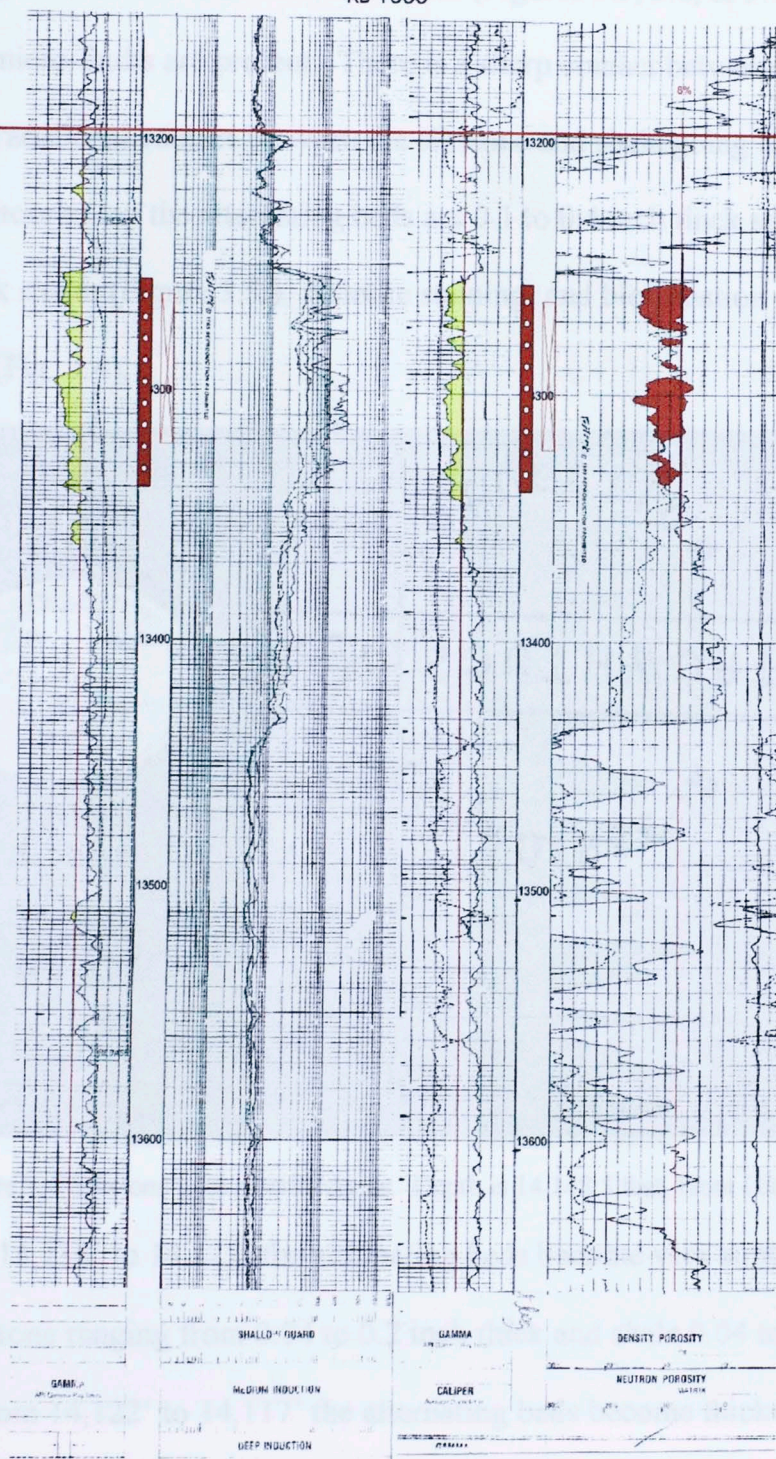


Figure 3.3-The location of Amoco Smith Unit 1 cored interval on the dual induction, and neutron/density logs. Plate III displays more detail.

The Hunt Gillingham #1 core is 62 feet of continuous core except for 2 feet missing near the middle. The lowermost 32 feet (14,149' to 14,117') comprises a series of alternating thin-bedded siltstones and shales (Figures 3.5, 3.6, & 3.7). Bioturbation, and normal micro-faults are present. There is a sharp contact between shale and siltstone beds and a gradational contact between the siltstone and shale going from bottom to top. From the bottom to top the alternating beds are 0.1 to 0.4 inch thick siltstones, and 0.1 to 0.3 inch thick shales (Figure 3.5). Siderite staining, and bioturbation occur throughout this interval (Fig. 3.4).



Figure 3.4-Siltstone with siderite stains. Depth is 14,148.5 feet, Hunt Gillingham #1.

From 14,136' to 14,122' the alternating beds become very subtle and relatively thin with siltstone ranging from 0.04 to 0.2 inch thick and shale 0.04 to 0.1 inch thick, (Fig. 3.6). From 14,122' to 14,117' the alternating beds become thicker and more prominent with a significant presence of bioturbation (Fig. 3.7).

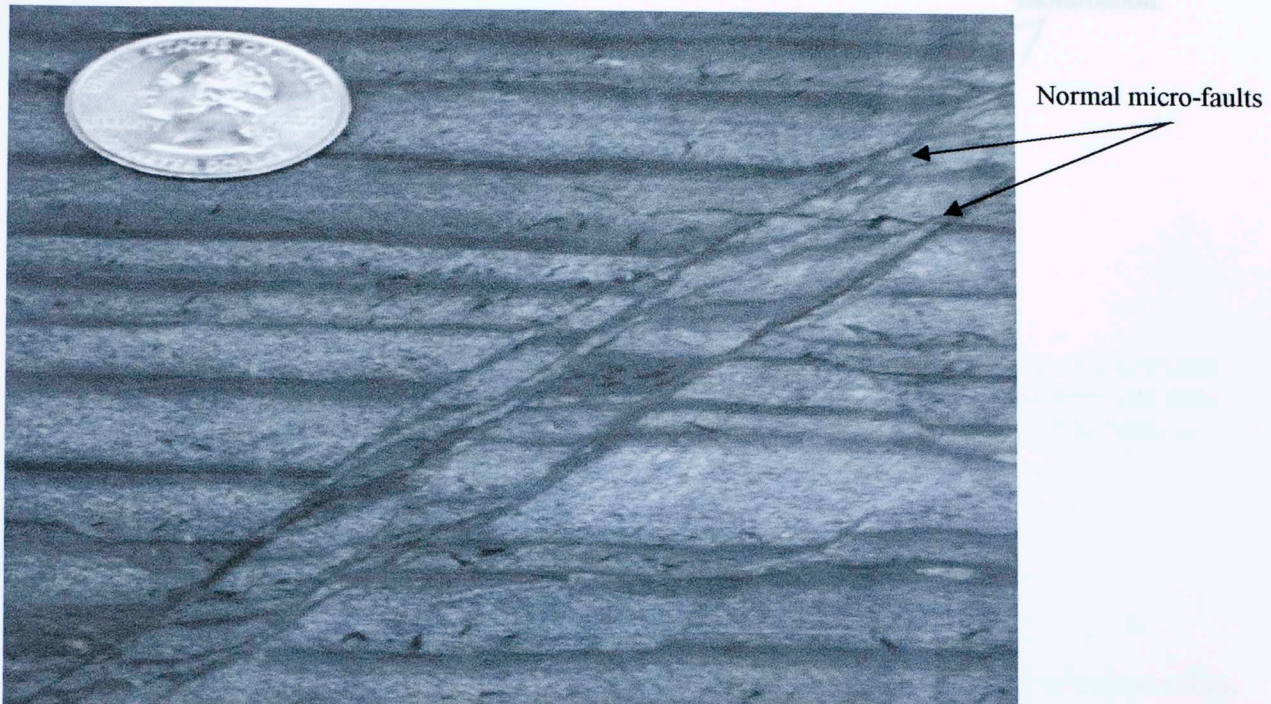


Figure 3.5-Very thin layers of alternating siltstone and dark gray shale. Siltstone is around 0.1 to 0.4 inch thick, and the dark gray shale is around 0.1 to 0.3 inch thick. Small faults are present. Depth is 14,146 feet, Hunt Gillingham #1.

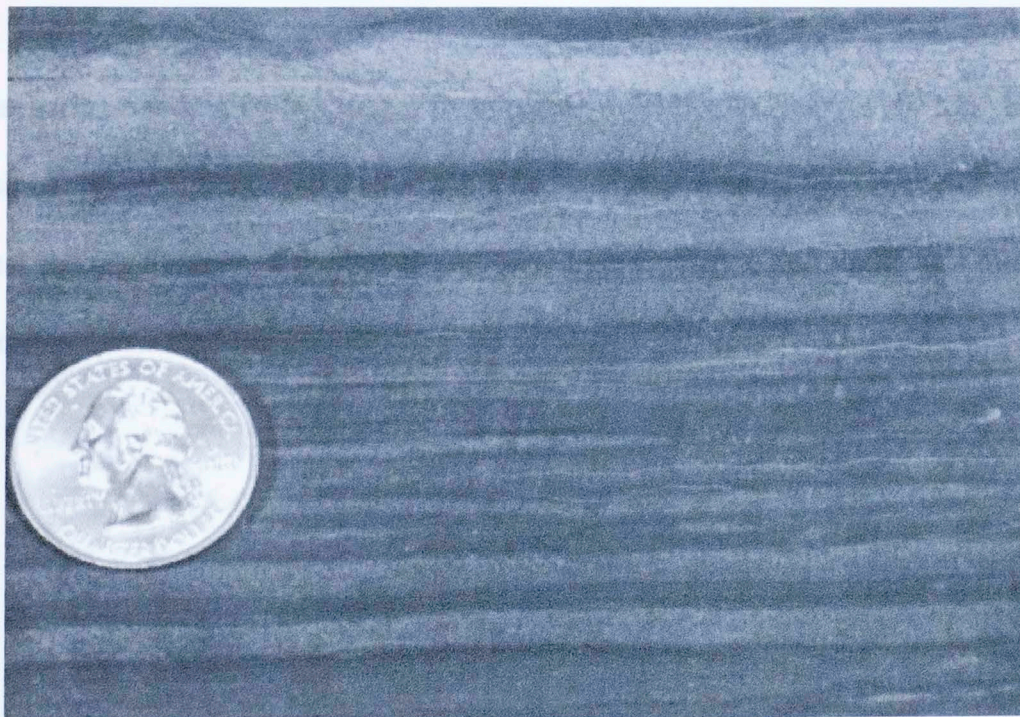


Figure 3.6-Relatively thinner and subtle layers of alternating siltstone and shale. Depth is 14,135 feet, Hunt Gillingham #1.

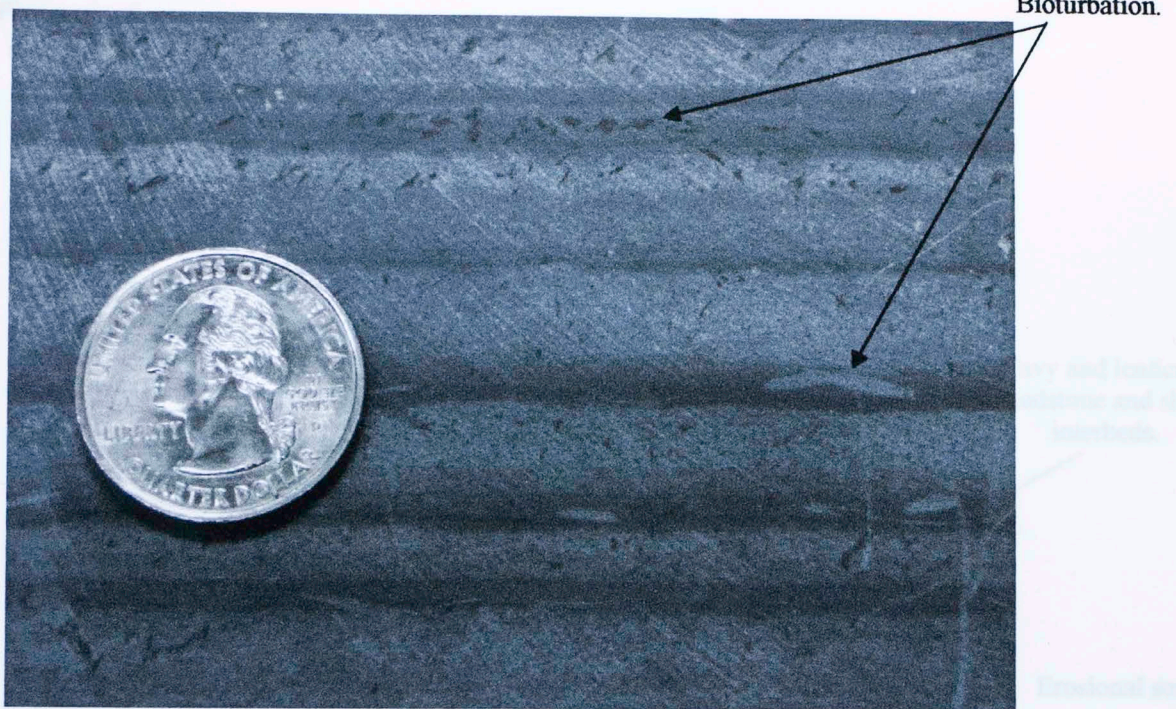
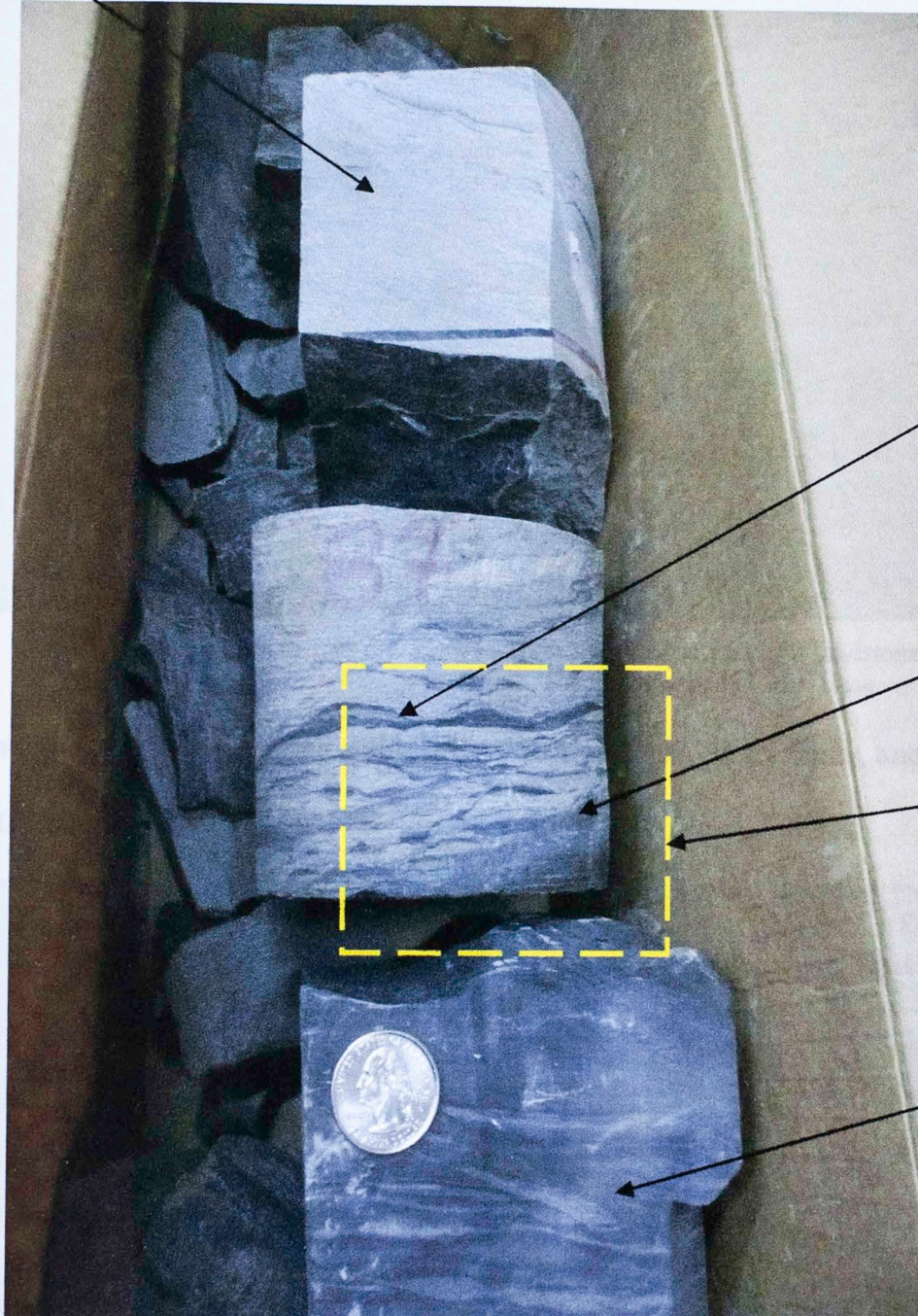


Figure 3.7-Dark gray shale with 0.04 to 0.2 inch thick layers and siltstone with 0.1 to 0.4 inch thick bioturbated planar beds. Depth is 14,128 feet, Hunt Gillingham #1.

The bottom 32 feet core was filled with these alternating shale and siltstone beds. The alternating bedding style changes from planar to lenticular towards the top. However an erosional feature cuts into the alternating beds (Figs. 3.8 and 3.9). On top of the erosional feature there are a few wavy and lenticular sandstone and shale beds overlain by relatively clean sandstone.

Fine grained sandstone.



Wavy and lenticular sandstone and shale interbeds.

Erosional surface.

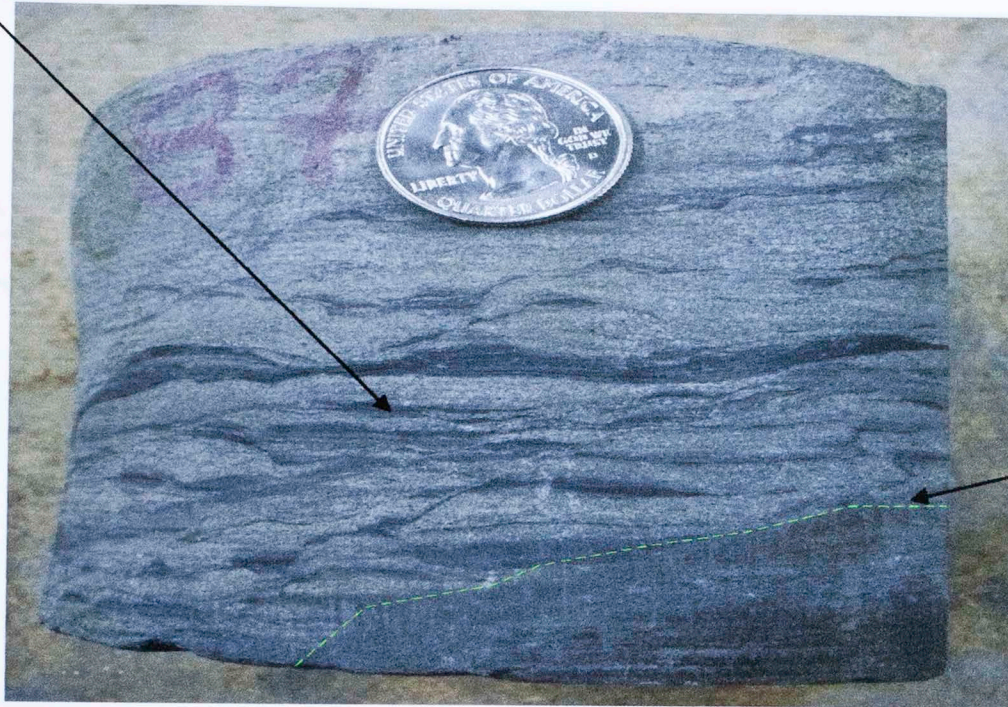
Figure 3.9

Alternating lenticular siltstone and shale layers.

Figure 3.8-Alternating siltstone and shale beds which are overlain by a sandstone bed that has an erosional base. The depth is 14,117 feet, Hunt Gillingham #1.

Figure 3.10-Fine grained sandstone with Nucleation. Depth is 14,115.5 feet, Hunt Gillingham #1.

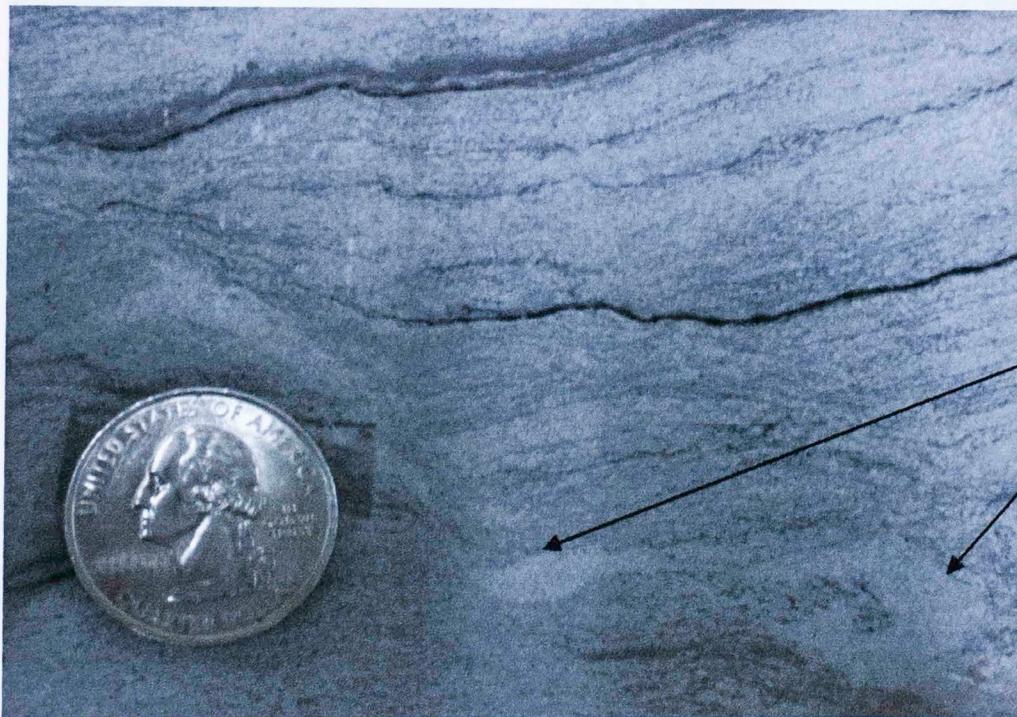
Wavy and lenticular sandstone and shale interbeds.



Erosional surface.

Figure 3.9-Alternating siltstone and shale layers which are overlain by a sandstone layer highlighted by the green dashed line. The depth is 14,117 feet, Hunt

The fine grained sandstone exhibits bioturbation, mud clasts, faults, and ripples, (Figs. 3.10 through 3.12).



Bioturbation.

Figure 3.10-Fine grained sandstone with bioturbation. Depth is 14,115.5 feet, Hunt Gillingham #1.

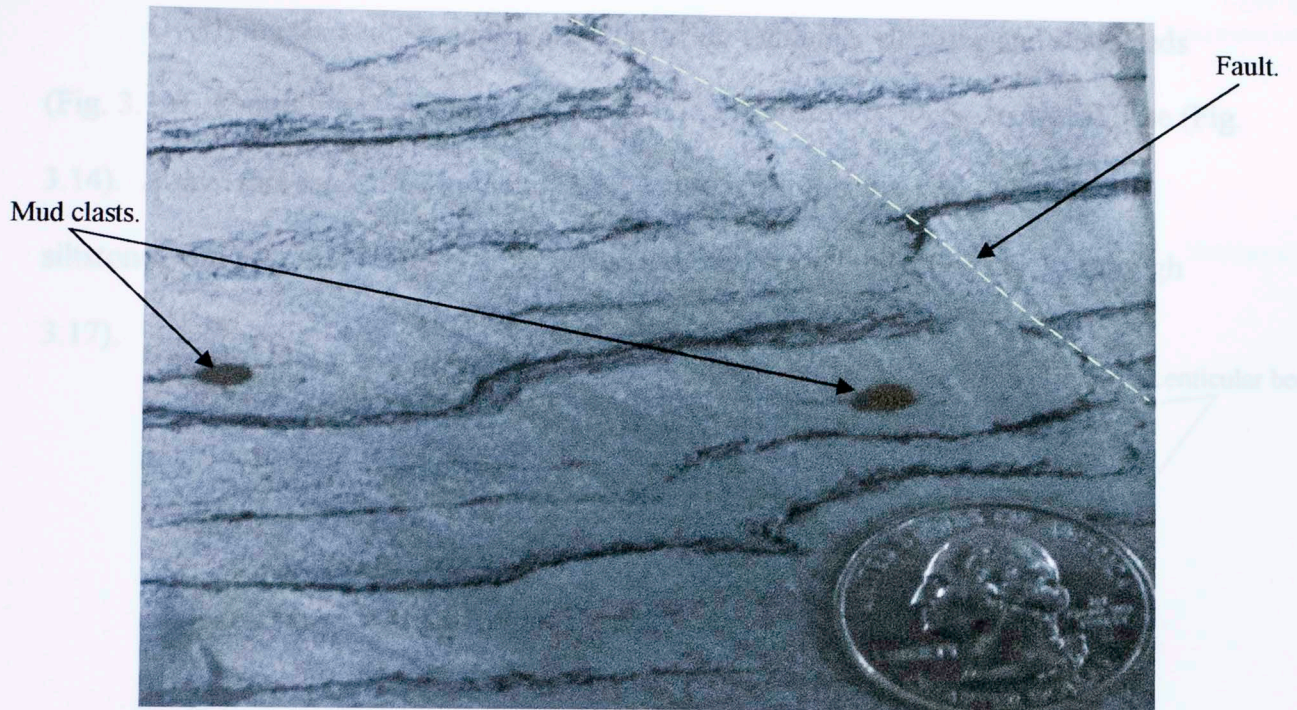


Figure 3.11-Fine grained sandstone with dark gray shale 0.04 to 0.1 inch thick. There is a presence of micro faulting and mud clasts 0.1 to 0.2 inch in diameter. Depth is 14,115 feet, Hunt Gillingham #1.

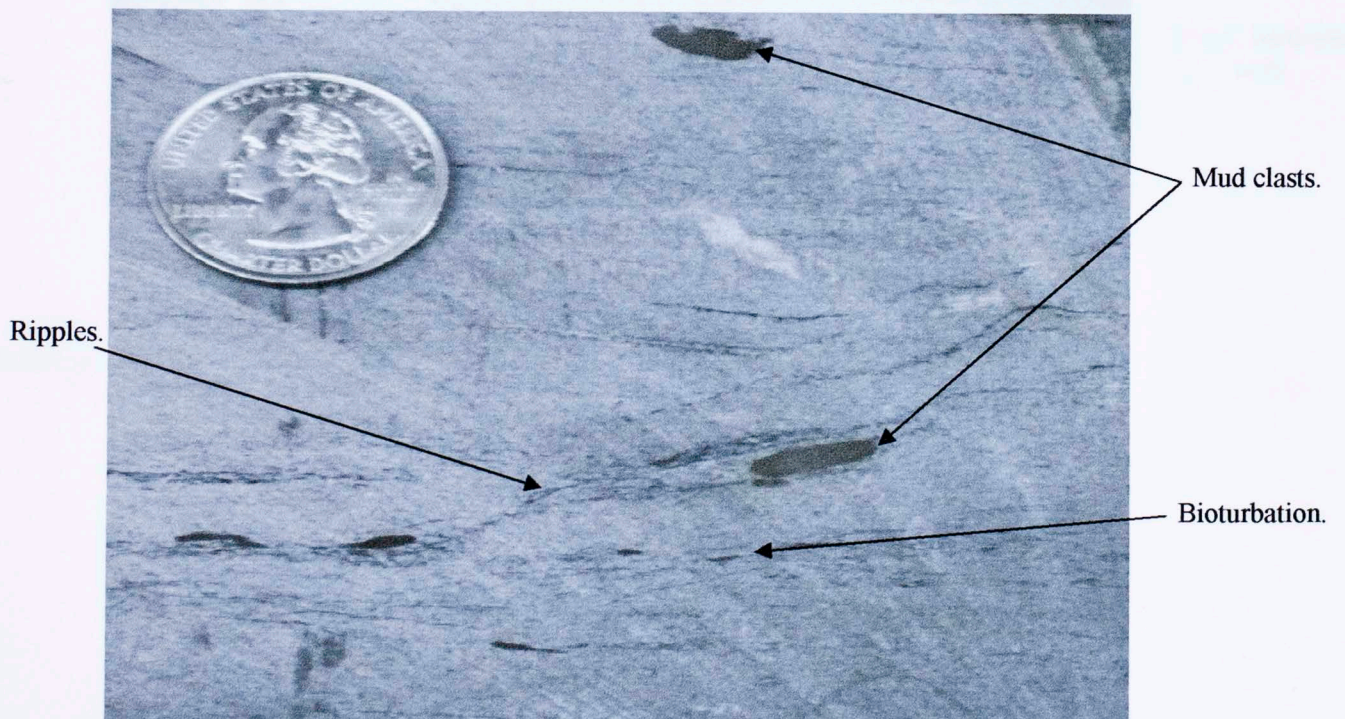


Figure 3.12-Fine grained sandstone with mud clasts around 0.1 inch in diameter. Ripples and bioturbation are present. Dark gray shale layers are 0.04 inch thick. Depth is 14,111.5 feet, Hunt Gillingham #1.

Overlying the sandstone bed are alternating lenticular siltstone and shale beds (Fig. 3.13). Overlying this alternating interval is a sandstone with an erosional base (Fig. 3.14). Above this sandstone to the top of the core is another interval of alternating siltstones and shales containing a variety of sedimentary features (Figs. 3.15 through 3.17).

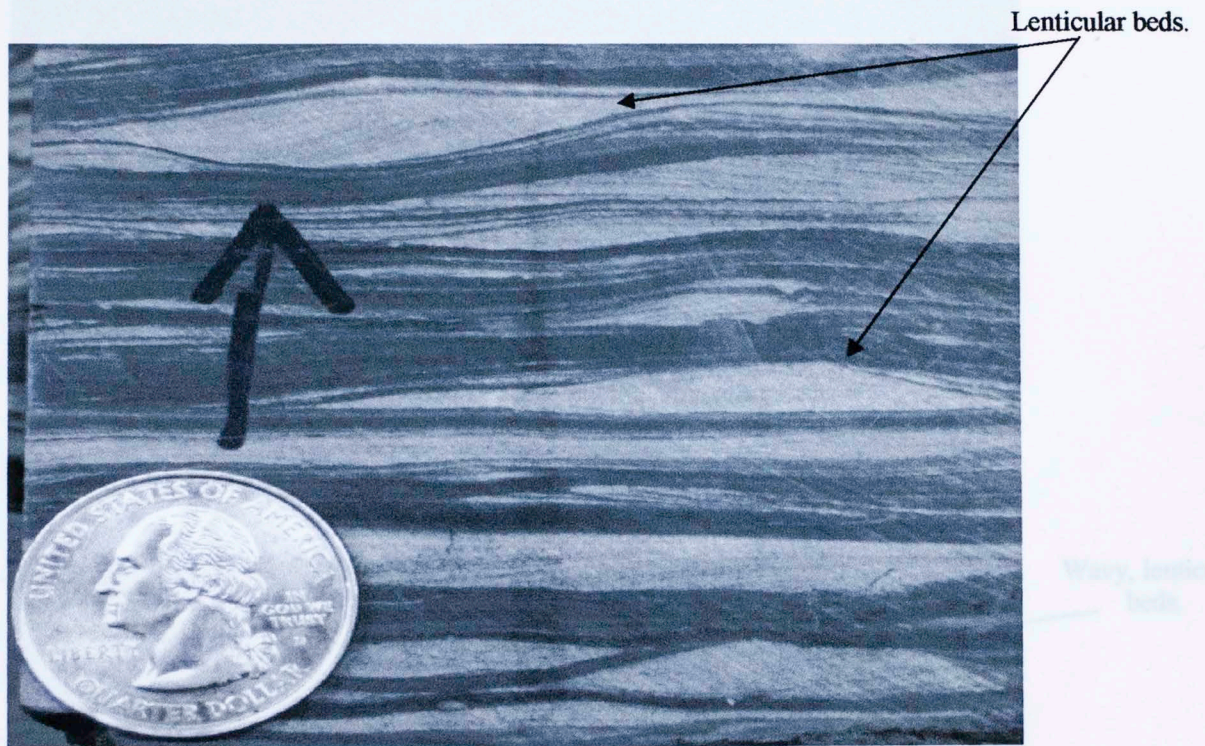


Figure 3.13-Dark gray shale and lenticular siltstone interbeds that are up to 0.6 inch thick. Depth is 14,091.5 feet, Hunt Gillingham #1.





Figure 3.14-Erosional feature overlying the alternating beds.  
Depth is 14,091 feet, Hunt Gillingham #1.

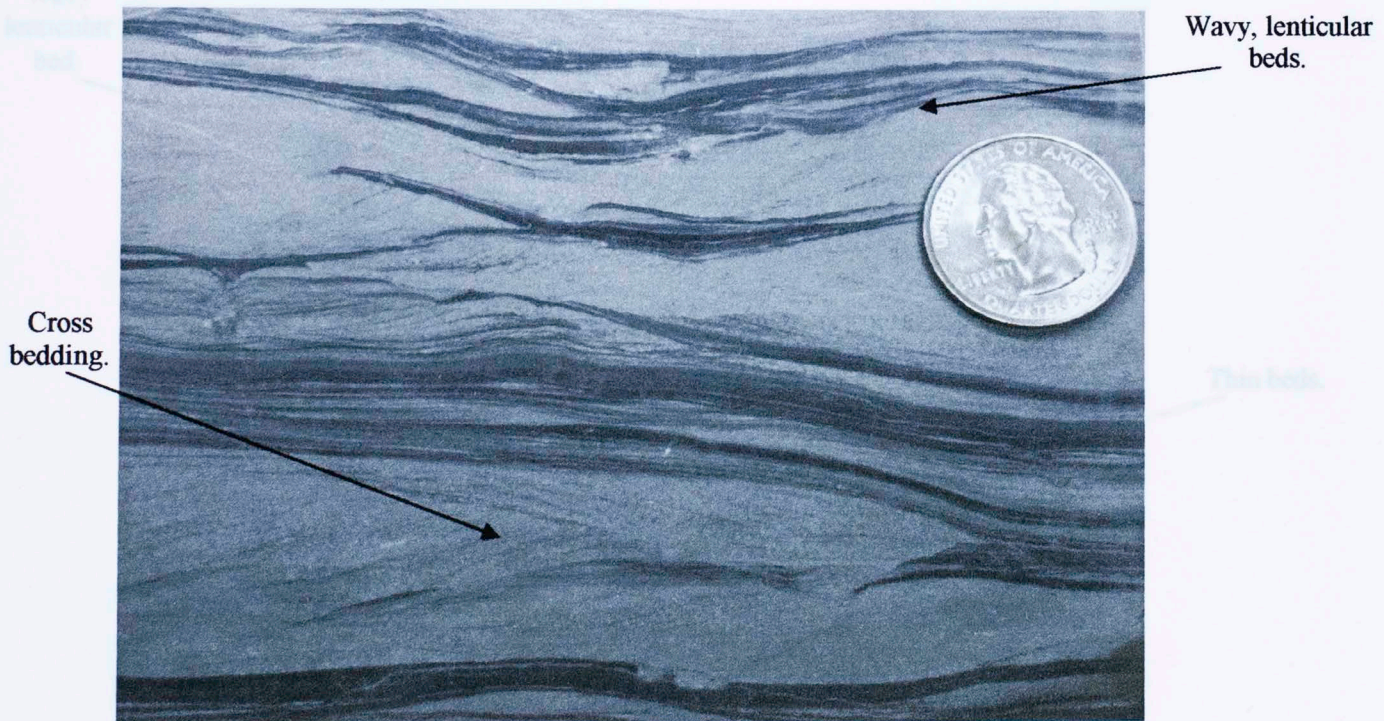


Figure-3.15 Wavy and lenticular siltstone with shale interbeds that are 0.04 to 0.2 inch thick. Cross bedding is present. Depth is 14,089.5 feet, Hunt Gillingham #1.

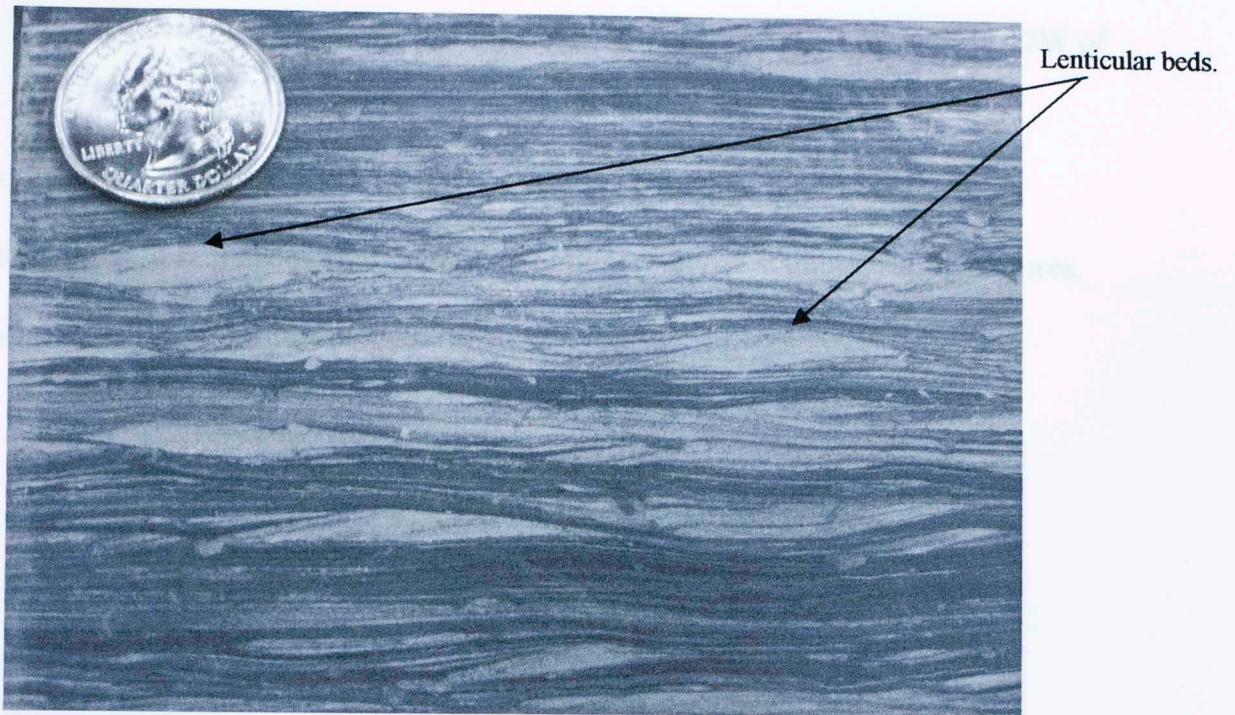


Figure 3.16-Lenticular siltstone and shale interbeds that are 0.04 to 0.2 inch thick. Depth is 14,089 feet, Hunt Gillingham #1.



Figure 3.17-Shale with 0.2 to 0.4 inch thick, interbedded siltstone lenses that contain planar, wavy, and lenticular features. Depth is 14,085 feet, Hunt

The second core examined was from the Amoco Smith Unit 1 in 26-10N-12W of Caddo Co., Oklahoma. This well had 60 feet of continuous core with six missing sections, each less than a foot thick. From the bottom, upward there is a series of coarsening upward sequences containing laminations, siderite staining, slump features, and trace fossils (Figs. 3.18 through 3.25).

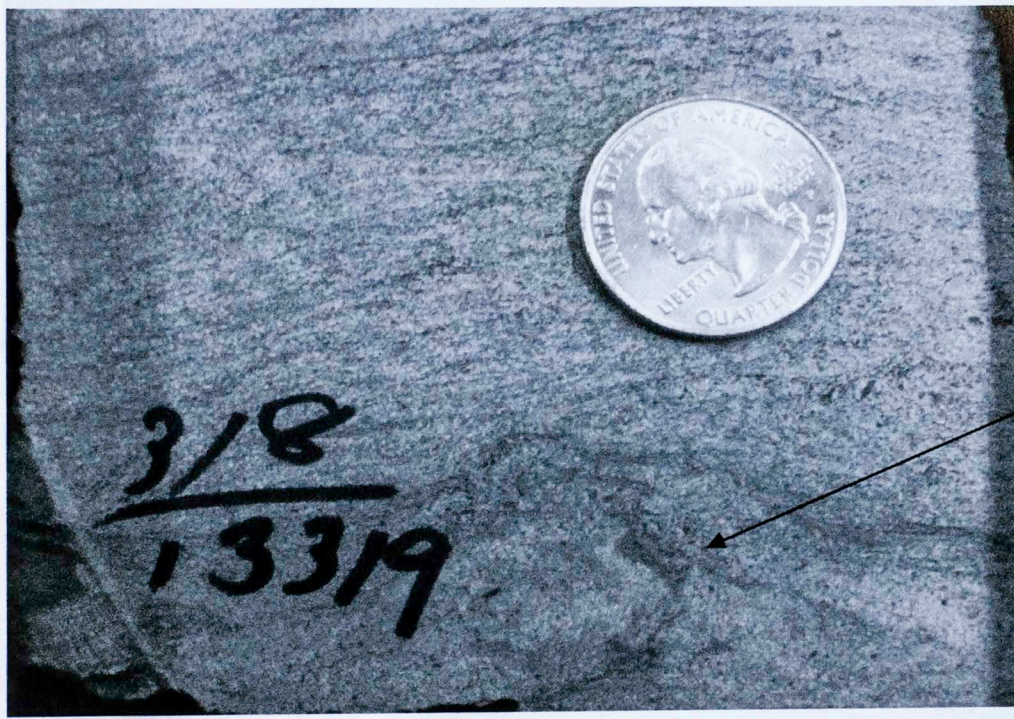


Figure 3.18-Shaly sandstone with trace fossil. Depth is 13,321 feet, Amoco Smith Unit 1.

Figure 3.20

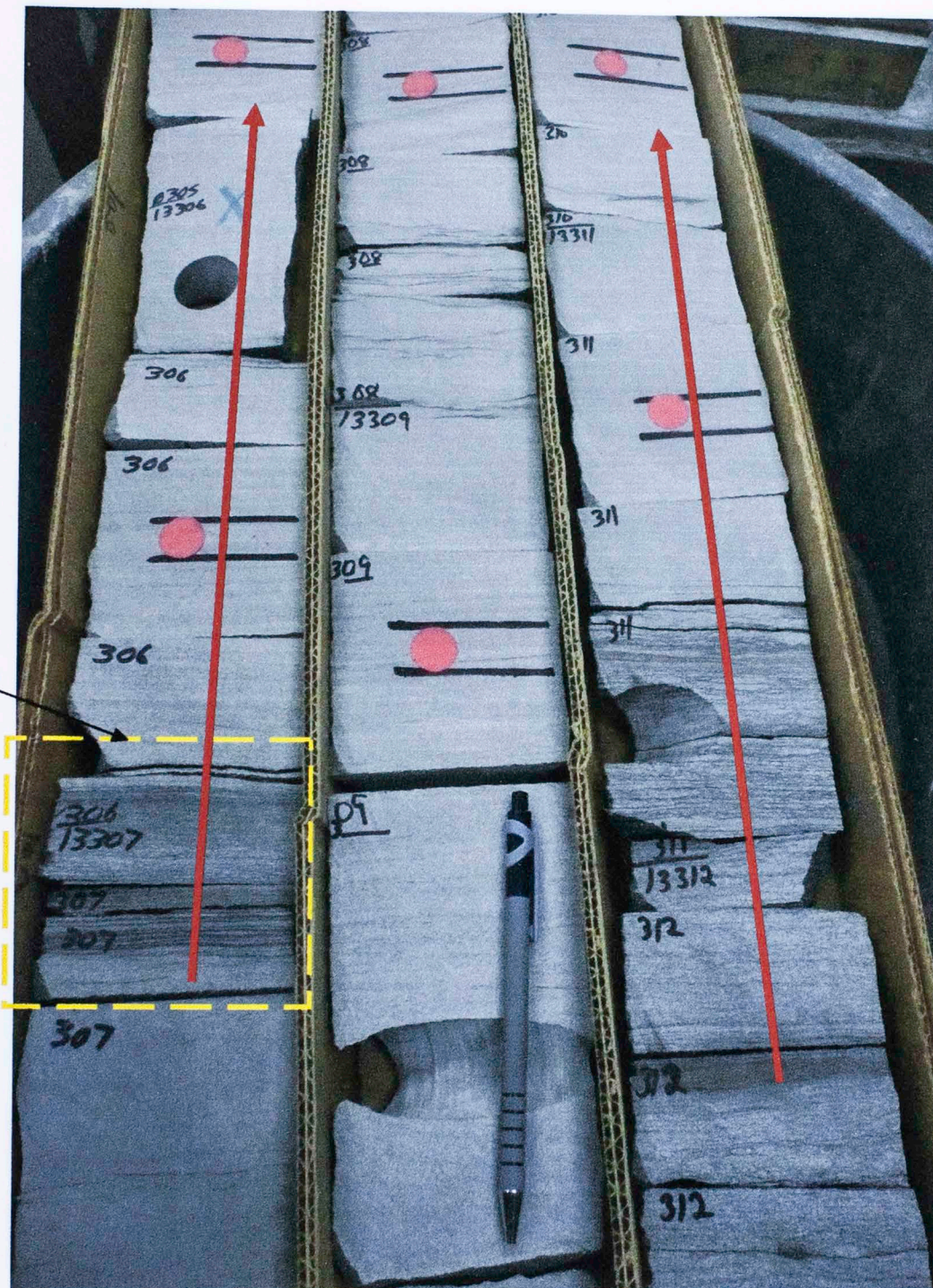


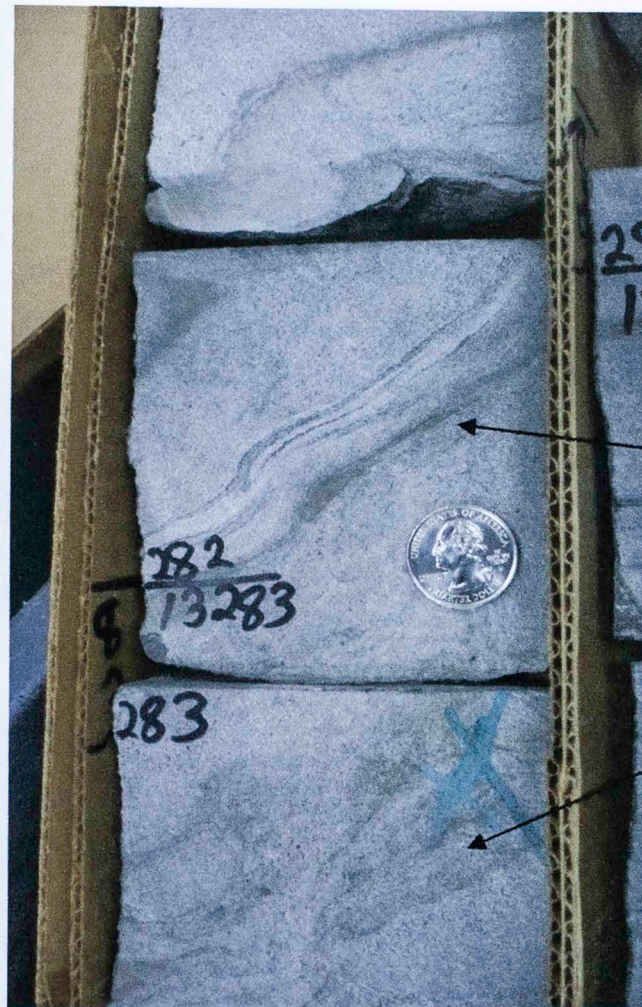
Figure 3.19-Seven feet of core displaying two coarsening upward sequences by red arrow, going from silty shale to fine grained sandstone. Red dots highlight core plugs that were utilized for prior testing. Depth is from 13,315 to 13,308 feet, Amoco Smith Unit 1.



Figure 3.20-Siltstone and shale interbeds with siderite stains. Depth is 13,310 feet, Amoco Smith Unit 1.



Figure 3.21-Fine grained, laminated sandstone. Depth is 13,298 feet, Amoco Smith Unit 1.



Slump Feature.

Bioturbation.

Figure 3.22-Fine grained sandstone with slump feature and bioturbation. Depth is 13,286 feet, Amoco Smith Unit 1.



Figure 3.25

Figure 3.24

Figure 3.23-Several coarsening upward sequences, highlighted by red arrows, with extensive bioturbation. Depth is from 13,284 to 13,277 feet, Amoco Smith Unit 1.



Figure 3.24-Shaly sandstone with bioturbation. Depth is 13,283 feet, Amoco Smith Unit 1.

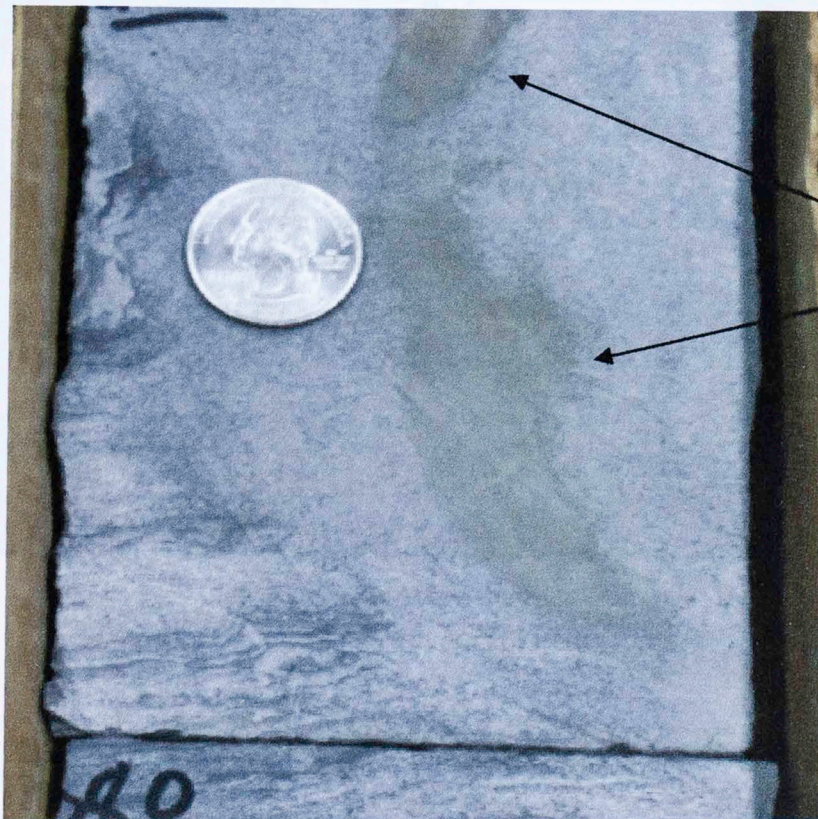


Figure 3.25-Shaly sandstone with bioturbation. Depth is 13,283 feet, Amoco Smith Unit 1.



Figure 3.29

Figure 3.28

Figure 3.27



Figure 3.26-Dark shale between two sandstone intervals. Depth is 13,277 to 13,270 feet, Amoco Smith Unit 1.

Figure 3.27-Fine grained sandstone with regular structural contact with dark grey shale. Depth is 13,272 feet, Amoco Smith Unit 1.

Rip up clasts



Shale laminations.

Figure 3.27-Fine grained wavy and lenticular sandstone with dark gray shale interbeds that are 0.2 to 0.3 inch thick, and shale ripup clasts. Depth is 13,275.5 feet, Amoco Smith Unit 1.



Erosional surface.

Figure 3.28-Fine grained sandstone with angular erosional contact with dark gray shale. Depth is 13,272 feet, Amoco Smith Unit 1.

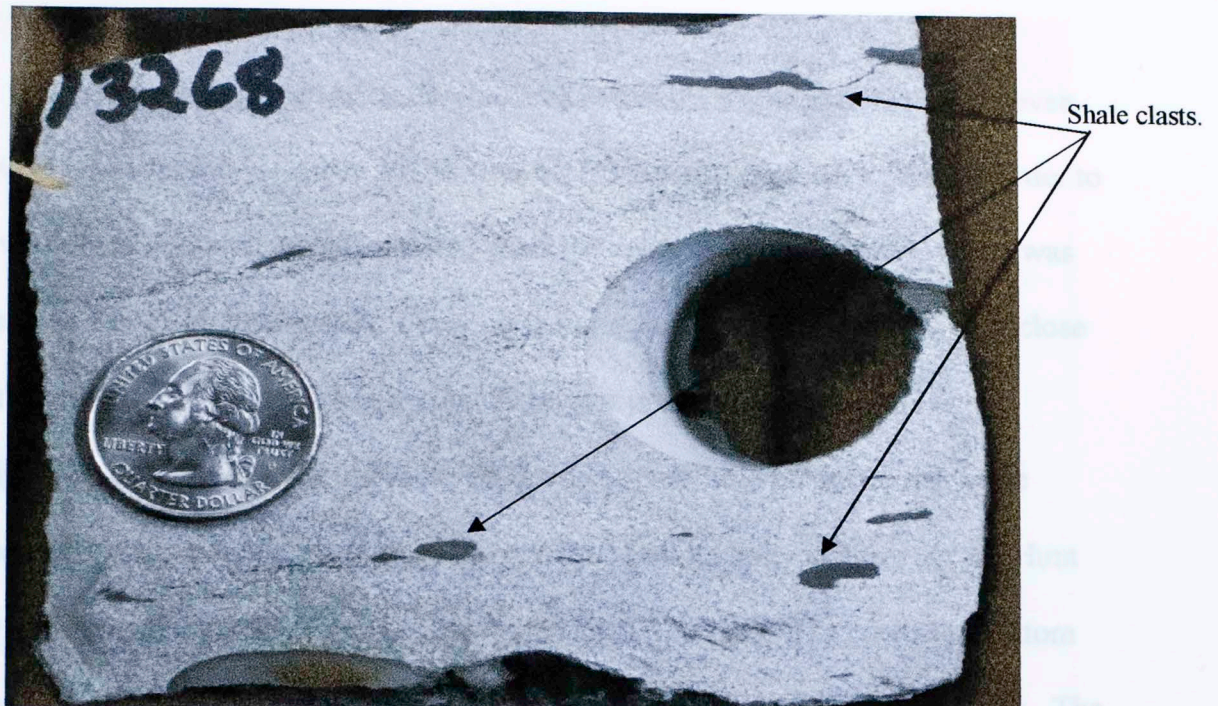


Figure 3.29-Fine grained sandstone with oriented shale clasts that are 0.1 to 0.2 inch in diameter. Depth is 13,271 feet, Amoco Smith Unit 1.

## **b) Core Plug Analysis**

Fifteen core plugs were taken from the Hunt Energy Gillingham #1, and eleven plugs were taken from the Amoco Smith Unit 1. Horizontal plugs were taken in order to obtain maximum reservoir quality values. Basic porosity and permeability testing was performed at Core Lab in Houston, Texas on the plugs under conditions that were close to reservoir pressure (Tables 3.1 and 3.2). Reservoir pressure was obtained from IP/Dwights IHS Data. The pressures are corrected bottom hole pressures that were reported from initial production tests. The corrected bottom hole pressure for the Hunt Energy Gillingham #1 is 5825 psi, and it was tested at 4700 psi. The corrected bottom hole pressure for the Amoco Smith Unit 1 is 6950 psi, and it was tested at 3600 psi. The plugs were tested at lower pressures as stated above due to lack of pore pressure. The pore pressure or the net hydrostatic confining pressure is typically less than the reservoir pressure. This value was estimated in the lab quantitatively, which yielded the above values for the net hydrostatic confining pressure.

Table 3.1 and 3.2 list porosity and permeability results for Hunt Gillingham #1 and Amoco Smith #1, respectively. The porosity measurements were done using helium, and the permeability measurements were done using nitrogen. There are two reported values for the permeability data. The first value is the air permeability of the core plug, and the second value is air permeability, corrected for the Klinkenberg effect, which accounts for the expansion of gas as it traverses through the core plug. The gas expands due to pressure decrease as a function of the length of the core. The Klinkenberg permeability values are always lower than air permeability values due to the gas expansion correction.

<b>Hunt Gillingham #1 Core Plugs</b>				
<b>Depth</b>	<b>Confining</b>	<b>Porosity</b>	<b>Permeability</b>	
<b>(feet)</b>	<b>Pressure</b>	<b>(%)</b>	<b>Kair</b>	<b>Klinkenberg</b>
	<b>(psi)</b>		<b>(mD)</b>	<b>(mD)</b>
14089.65	4700	1.72	0.0004	0.0001
14090.55	Ambient			
14091.65	4700	3.69	0.0015	0.0005
14096.15	4700	4.33	0.0126	0.0058
14103.50	4700	3.58	0.0006	0.0002
14108.40	4700	4.39	0.0008	0.0003
14108.55	4700	4.32	0.0044	0.0018
14112.20	4700	5.48	0.0012	0.0004
14114.40	4700	4.42	NA	NA
14115.40	4700	3.96	0.0004	0.0001
14117.00	4700	3.47	0.0004	0.0001
14132.75	4700	2.74	NA	NA
14133.15	4700	2.68	NA	NA
14143.45	4700	3.10	0.0007	0.0002
14146.90	4700	2.63	NA	NA

Table 3.1 Hunt Gillingham #1 core plug analysis.

A total of fourteen core plugs from the Hunt Gillingham #1 were tested. Four core plugs reported permeability values below the measurement range and are shown in the table as not available (NA). Another sample was deemed unsuitable for testing. The porosity and permeability values are very low, and below reservoir quality for this formation. The reasons for the porosity and permeability being low were investigated by thin section analysis, discussed in the next section.

Amoco Smith #1 Core Plugs				
Depth (feet)	Confining Pressure (psi)	Porosity (%)	Permeability	
			Kair (mD)	Klinkenberg (mD)
13262.40	3600	9.42	0.0100	0.0050
13266.30	3600	9.20	0.0100	0.0050
13275.10	3600	4.74	0.0010	0.0003
13280.35	3600	6.29	0.0020	0.0010
13286.15	3600	6.45	0.0020	0.0010
13295.70	3600	8.73	0.0150	0.0110
13299.25	3600	10.98	0.0330	0.0250
13305.60	3600	6.96	0.0030	0.0010
13306.10	3600	8.16	0.0060	0.0020
13307.45	3600	8.12	0.0030	0.0010
13309.00	3600	6.91	0.0020	0.0010

Table 3.2 Amoco Smith #1 core plug analysis.

The porosity values from the Amoco Smith Unit 1 display good reservoir quality for the Lower Red Fork sandstone. The permeability values are very low and beneath reservoir quality. The reasons for permeability values being so low were investigated by thin section analysis, which is also discussed in the next section.

Depth (feet)	Grain (%)	Clay (%)	Porosity (%)	Hydrocarbons (%)	Grain Density (g/cc)
14089.65	84.07	12.38	1.72	1.00	2.71
14096.15	85.00	9.17	4.33	1.30	2.68
14101.30	84.50	10.67	3.58	1.25	2.68
14112.20	82.00	8.52	5.46	4.00	2.69
14114.40	78.38	9.08	4.42	20.00	2.69
14115.40	82.50	10.24	3.96	2.00	2.68
14117.00	79.00	9.55	3.47	2.00	2.69
14146.50	84.00	12.37	2.40	1.00	2.7

Table 3.3 Depth of thin sections, compositional percentages, and grain densities for the Hunt Offshoot #1.

### c) Thin Section Analysis

Thin sections were cut from the core to describe their petrography. A total of fifteen thin sections from clean sandstones were made; depths in cores are highlighted in (Plates IV and V). Eight were from the Hunt Energy Gillingham #1, and seven were from Amoco's Smith Unit 1. The thin sections were injected with blue epoxy for porosity discrimination.

Table 3.3 displays data from the Hunt Gillingham #1 well. Porosity and grain density measurements were provided by Core Lab. Thin sections were described using Folk's (1980) classification scheme. Grain, cement, and hydrocarbon percentages were determined by point counts. Grain size varies from very fine sand to silt, sorting ranges from well to moderate, and the grains are subangular. Going from bottom to top of the core, the thin section photomicrographs are shown in figures 3.29 to 3.36. The thin sections will be referred to throughout the chapter.

Hunt Gillingham #1 Thin Sections					
Depth (feet)	Grain (%)	Cement (%)	Porosity (%)	Hydrocarbons (%)	Grain Density (g/cc)
14089.65	84.00	13.28	1.72	1.00	2.71
14096.15	85.00	9.17	4.33	1.50	2.68
14103.50	84.50	10.67	3.58	1.25	2.68
14112.20	82.00	8.52	5.48	4.00	2.69
14114.40	58.58	9.00	4.42	28.00	2.69
14115.40	83.50	10.54	3.96	2.00	2.68
14117.00	78.00	9.53	3.47	9.00	2.69
14146.90	84.00	12.37	2.63	1.00	2.7

Table 3.3 Depth of thin sections, compositional percentages, and grain densities for the Hunt Gillingham #1.

The purpose of petrographic analysis was to determine mineralogical composition and diagenetic features that would elucidate the nature of these tight Lower Red Fork sandstone reservoirs. Core plug porosity values from Hunt Gillingham #1 are lower than those of the Amoco Smith #1. Both of the cores have very low permeability values. The eight samples from Hunt Gillingham #1 are classified as sub-arkosic arenites. Levine (1984) classified the entire Red Fork sandstone as feldspathic litharenites. Johnson (1984) classified the Lower Red Fork sandstone as lithic to sublithic arenites. The thin sections examined in this thesis did not have high rock fragment content. Clement (1991) reported subarkosic arenites based on samples along the trend.

The Hunt Gillingham #1 thin sections consist of quartz grains, feldspars, micas, clays, rock fragments, and pyrobitumen. The thin sections exhibit a large amount of clay which is due to alteration of feldspar minerals. This feature is highlighted in most of the thin sections by dirty brownish appearing minerals, (Fig 3.30 through 3.37). The clays seem to plug up the reservoir, reducing the porosity and permeability. Clement (1991) concluded that the high percentage of clays was responsible for plugging the rock and leading to lower production.

Another factor reducing the reservoir quality is compaction (Figures 3.34 and 3.36). The Lower Red sandstone is relatively deep, typically penetrated in the study area around 13,000 feet or deeper. Johnson (1984) concluded the Lower Red Fork sandstone experienced extensive diagenesis by compaction, precipitation of cements, and authigenic mineralization. Levine (1984) documented how porosity and permeability was destroyed by compaction and pore filling cements.



Secondary porosity features were observed in the thin sections. Figures 3.32 and 3.35 highlight migratory pathways created by dissolution. Johnson (1984) reported that secondary porosity was created by dissolution of siliceous mud fragments, and calcite cements. Levine (1984) concluded secondary porosity was developed by dissolution following increased burial.



Figure 3.35 Thin Section Collection of  
Sample 141403  
Major Element Analysis  
Major element analysis of  
Thin section 141403  
Sample 141403

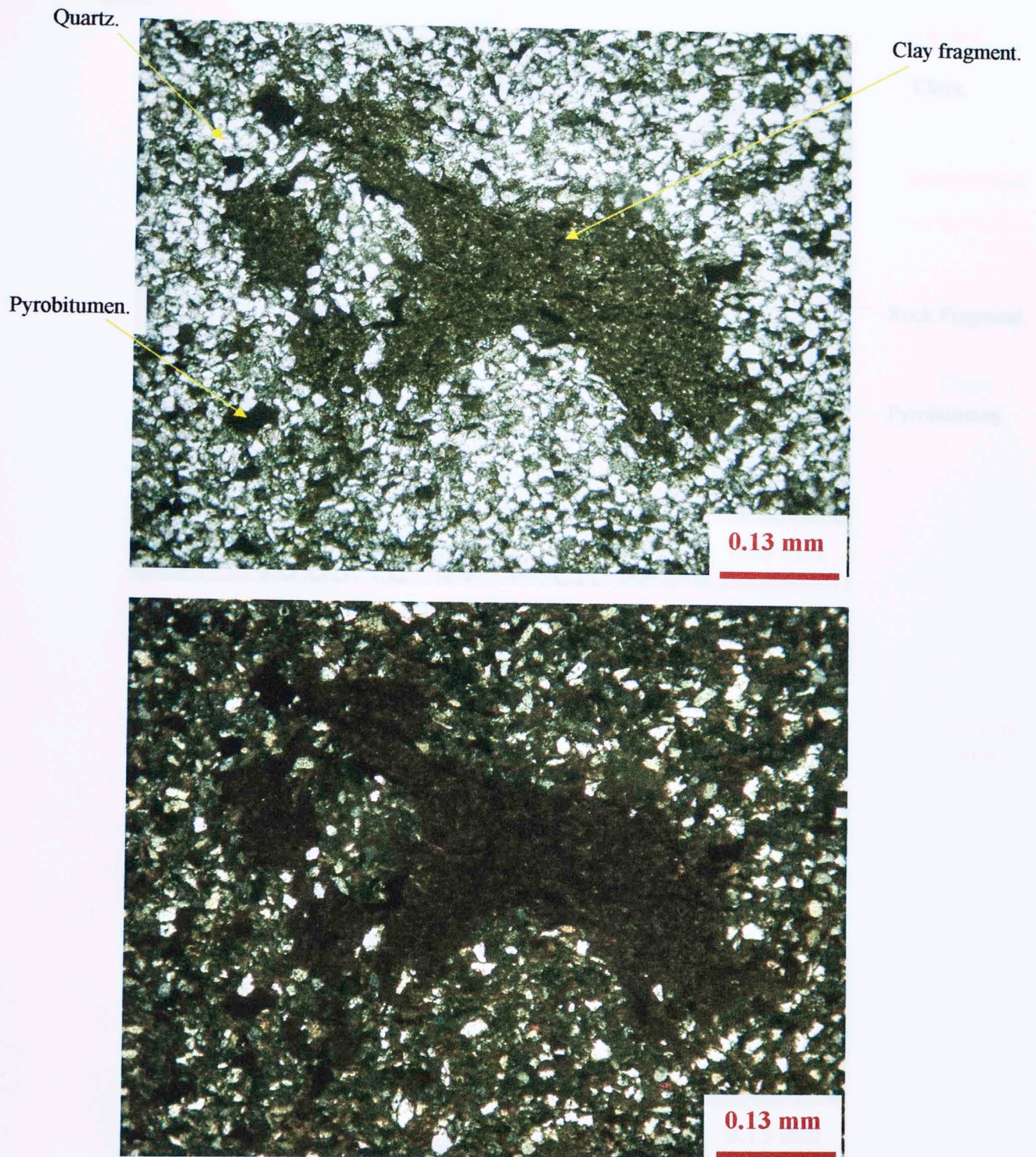
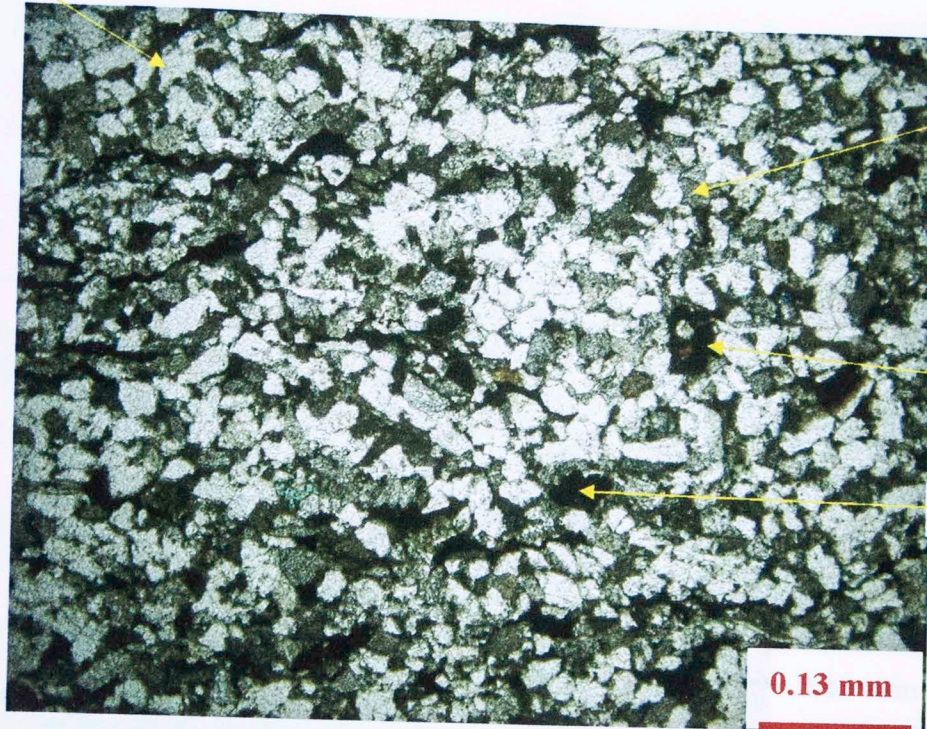


Figure-3.30 Hunt Gillingham #1  
 Depth: 14,146.90'  
 Magnification: 40x  
 Plane polarized light (above)  
 Cross polarized light (below)  
 Siltstone with large compacted clay fragment.

Quartz.

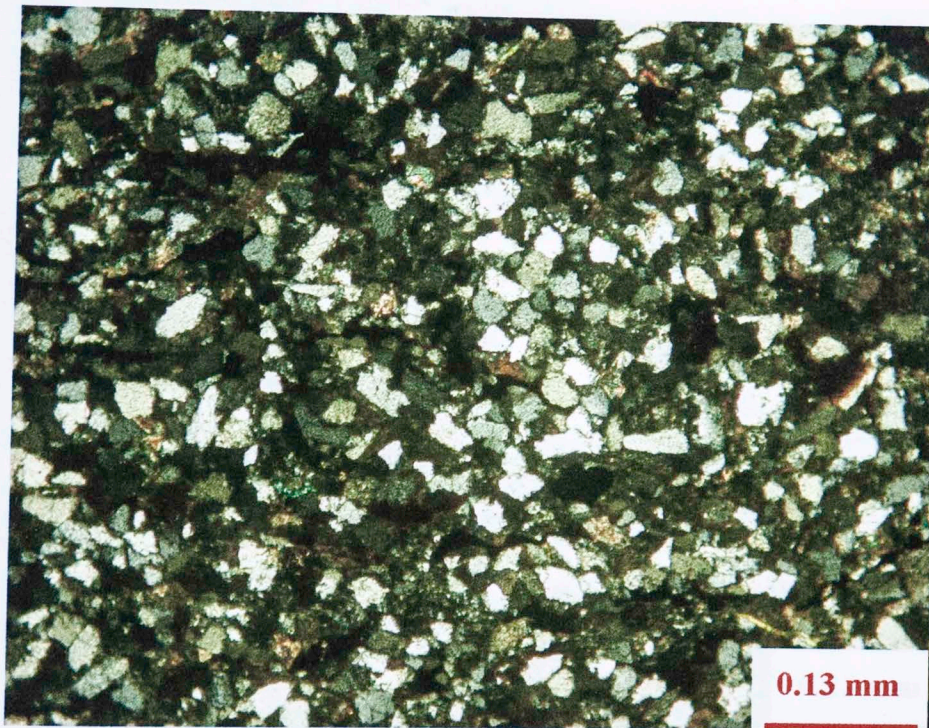


Clays.

Rock Fragment.

Pyrobitumen.

0.13 mm



0.13 mm

Figure-3.31 Hunt Gillingham #1

*Depth: 14,117.00'*

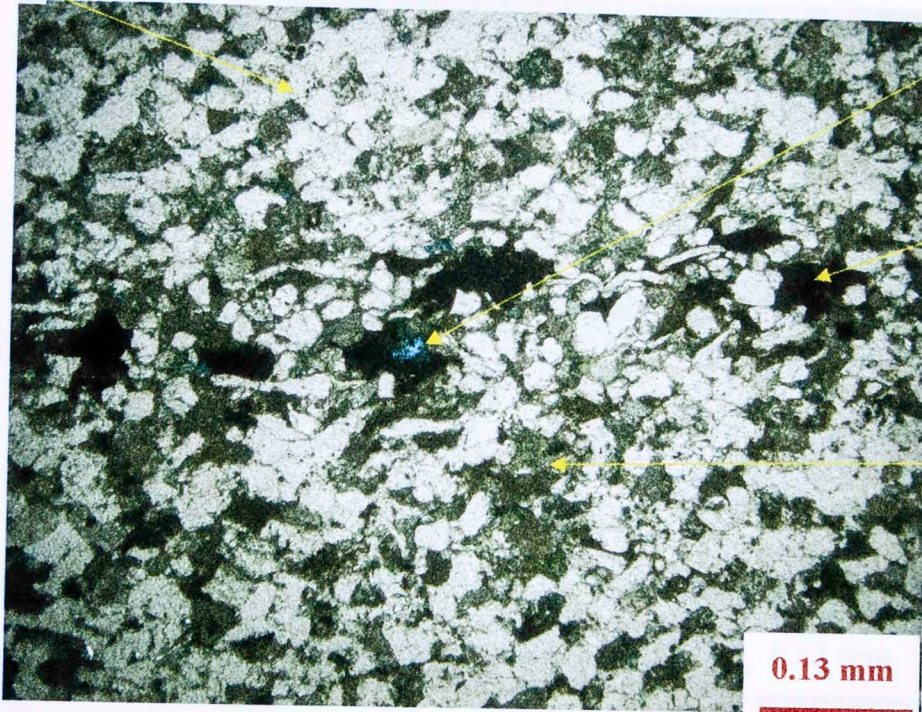
*Magnification: 40x*

*Plane polarized light (above)*

*Cross polarized light (below)*

Very fine sandstone with significant amount of pyrobitumen.

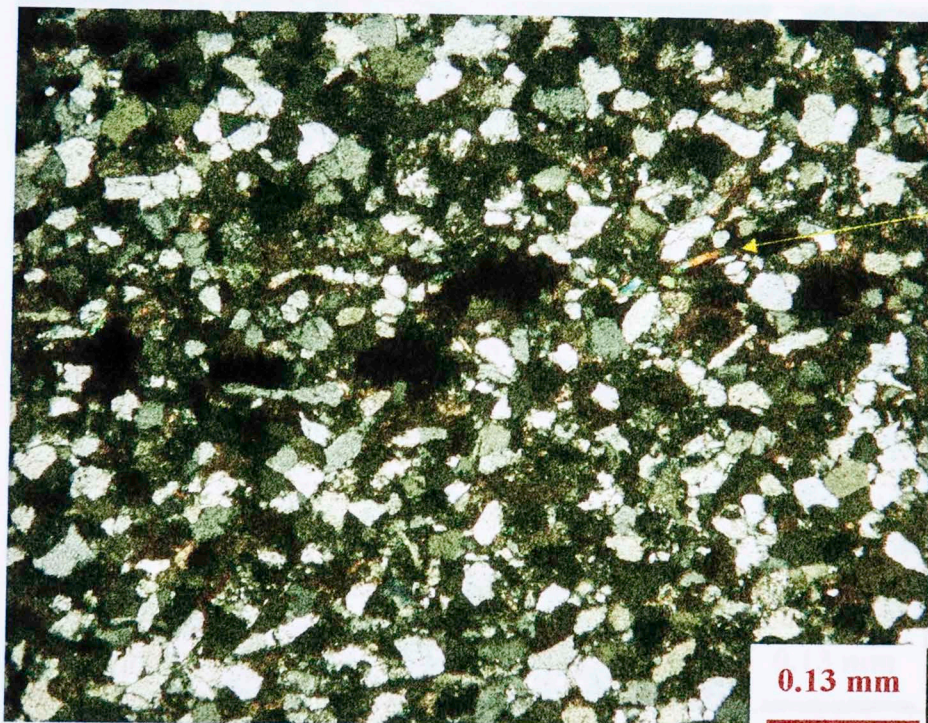
Quartz.



Porosity.

Pyrobitumen.

Clays.



Muscovite  
Mica.

Figure-3.32 Hunt Gillingham #1  
Depth: 14,115.40'  
Magnification: 40x  
Plane polarized light (above)  
Cross polarized light (below)  
Very fine sandstone with significant amount of  
pyrobitumen.

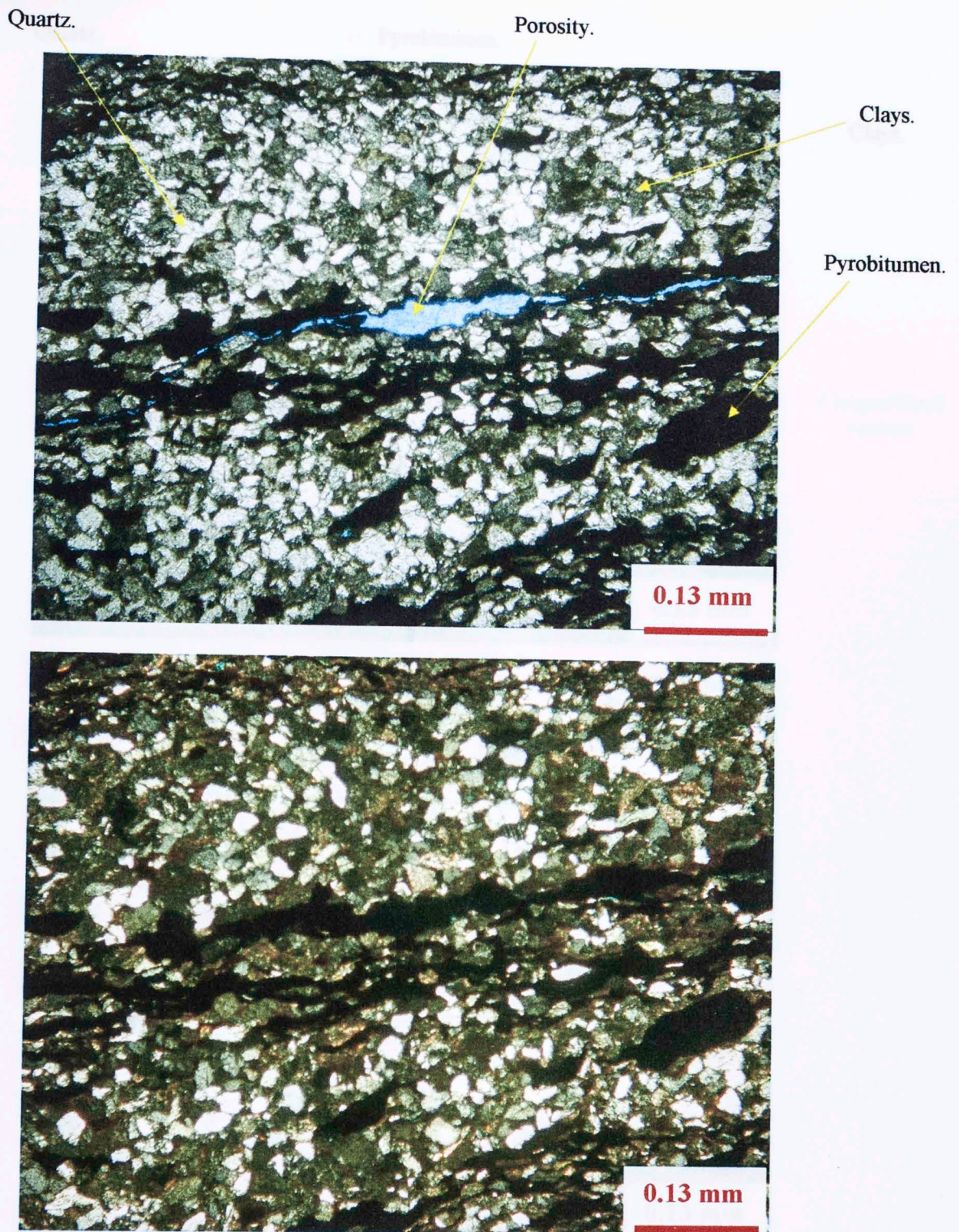


Figure-3.33 Hunt Gillingham #1

*Depth: 14,114.40'*

*Magnification: 40x*

*Plane polarized light (above)*

*Cross polarized light (below)*

Very fine sandstone with significant amount of pyrobitumen, and dissolved migratory pathways.

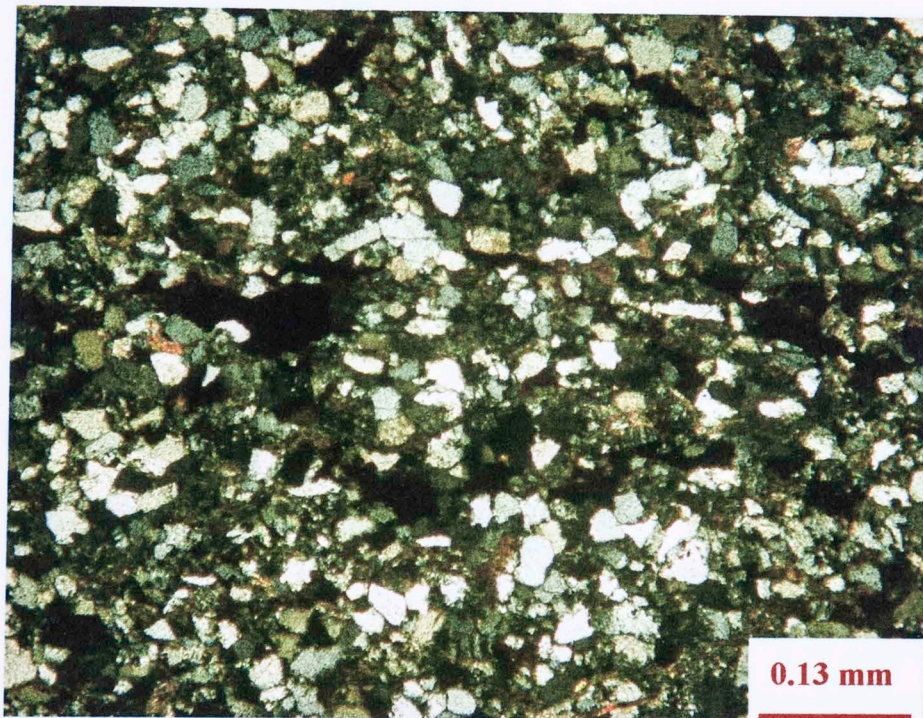
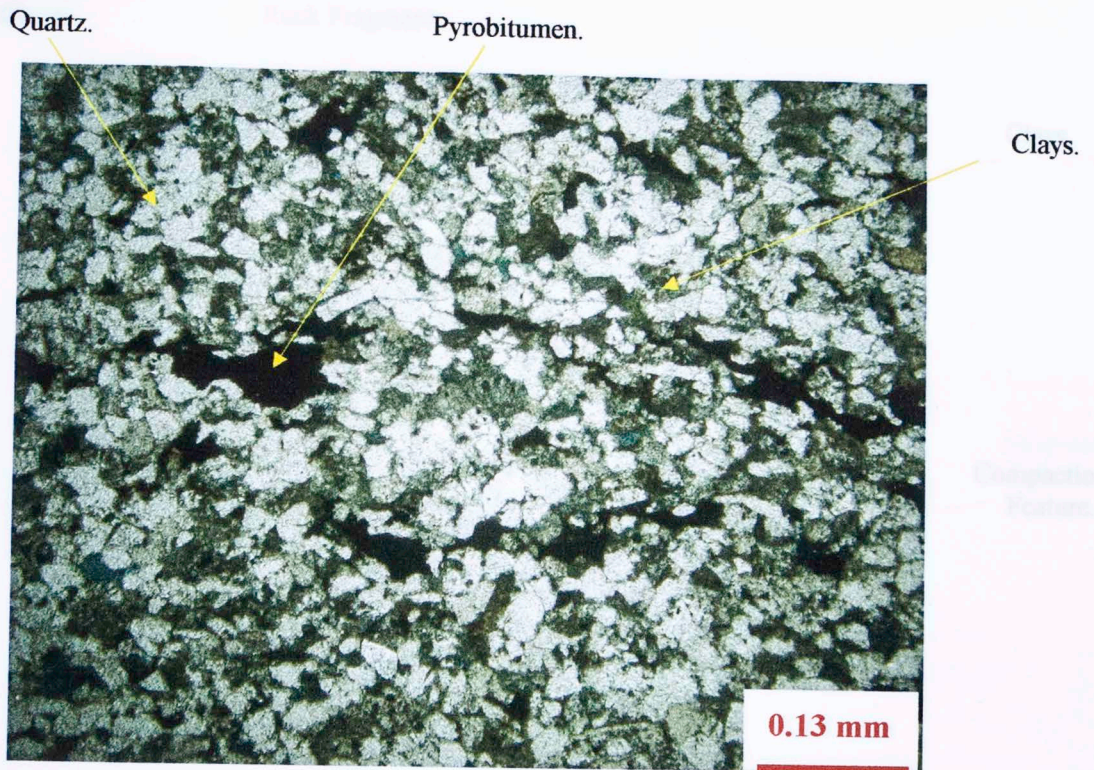


Figure-3.34 Hunt Gillingham #1  
 Depth: 14,112.20'  
 Magnification: 40x  
 Plane polarized light (above)  
 Cross polarized light (below)  
 Very fine sandstone with significant amount of  
 pyrobitumen, and presence of feldspars and  
 muscovite micas.

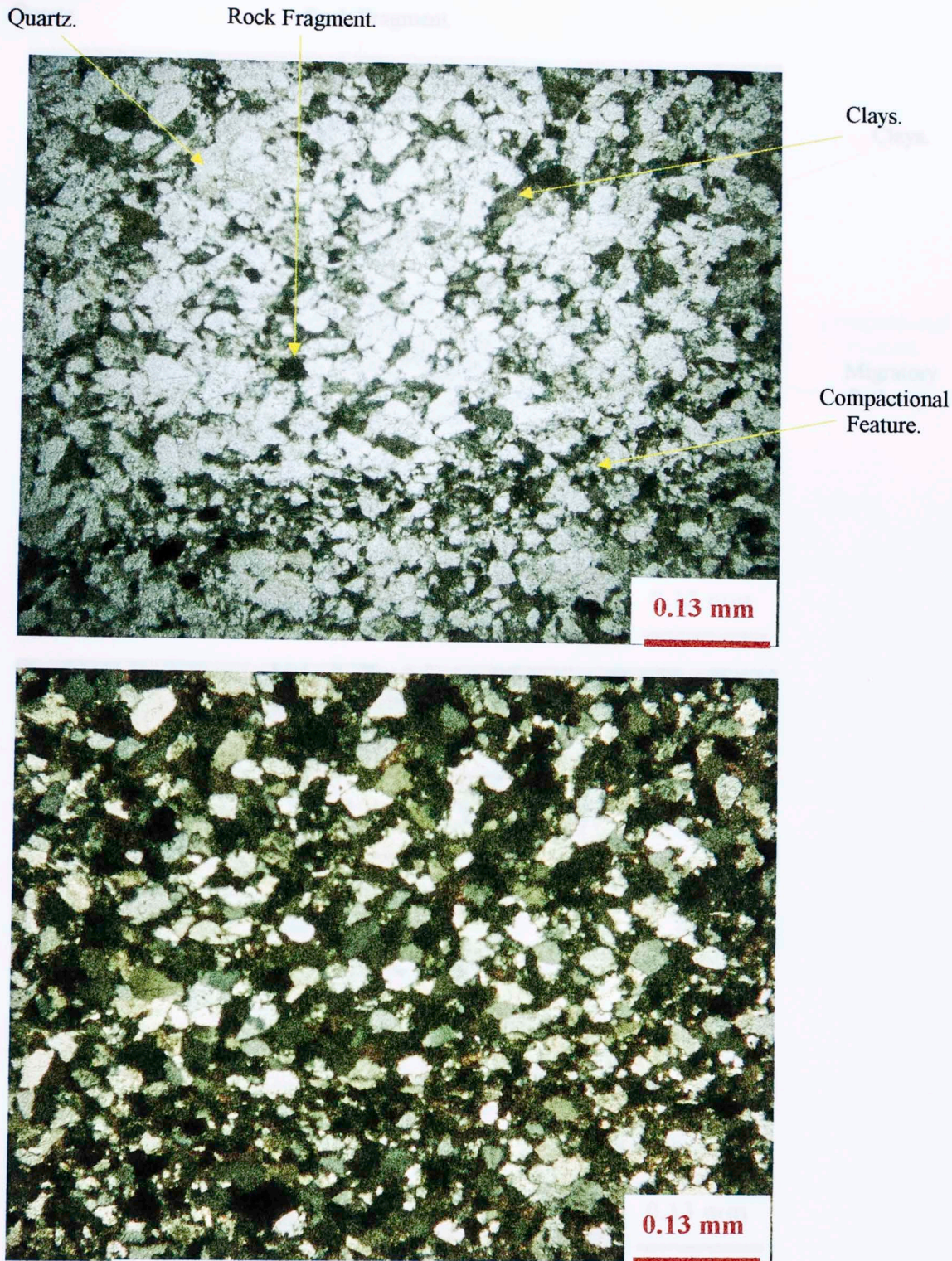


Figure-3.35 Hunt Gillingham #1  
Depth: 14,103.50'  
Magnification: 40x  
Plane polarized light (above)  
Cross polarized light (below)  
Very fine sandstone with apparent compactional  
feature towards the bottom.

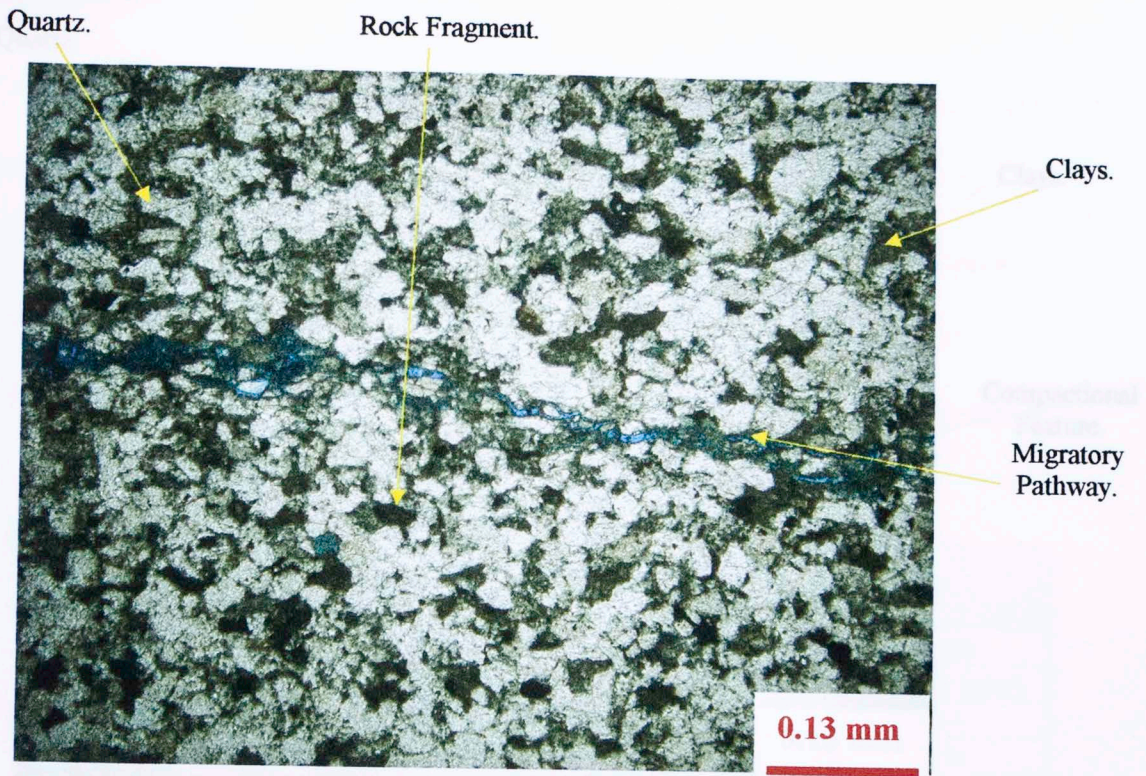
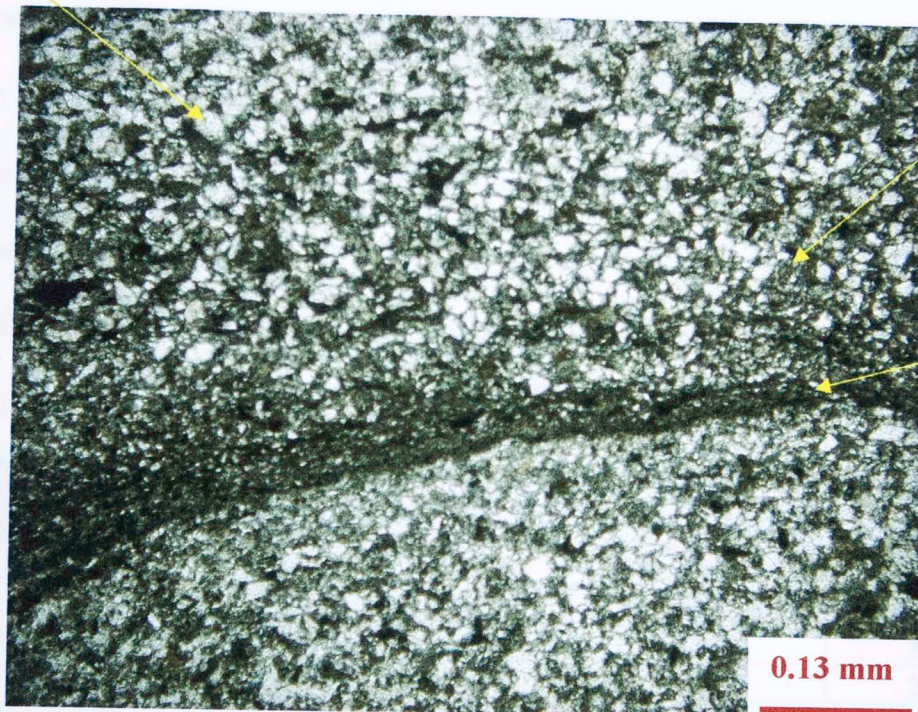


Figure-3.36 Hunt Gillingham #1  
 Depth: 14,096.15'  
 Magnification: 40x  
 Plane polarized light (above)  
 Cross polarized light (below)  
 Very fine sandstone with dissolution creating a migratory pathway.



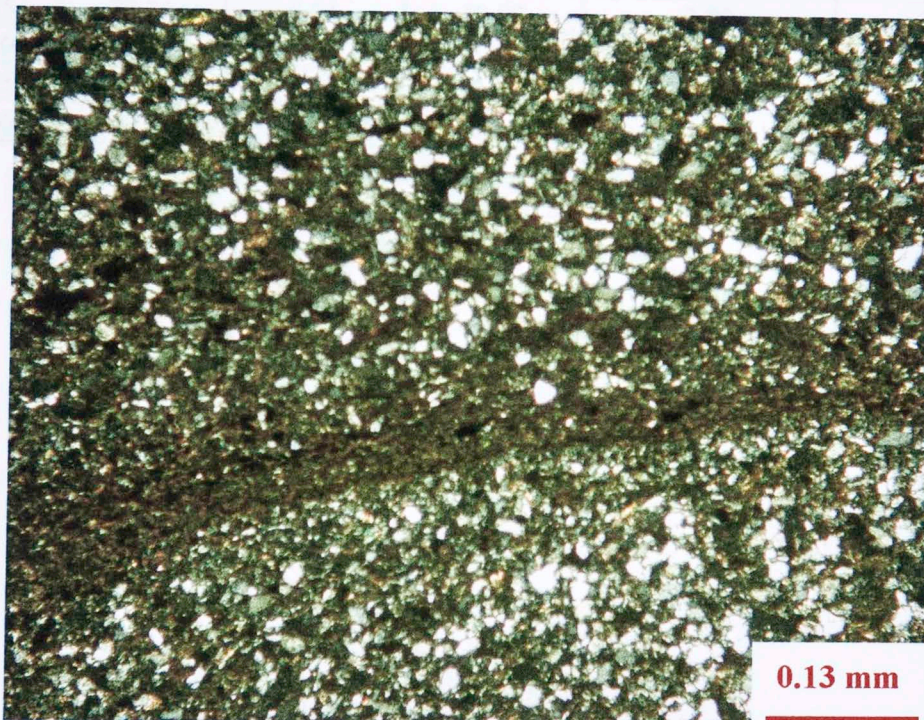
Quartz.



Clays.

Compactional  
Feature.

0.13 mm



0.13 mm

Figure-3.37 Hunt Gillingham #1  
*Depth: 14,089.65'*  
*Magnification: 40x*  
*Plane polarized light (above)*  
*Cross polarized light (below)*  
Very fine sandstone with compacted layer.

The Amoco Smith Unit #1 thin section data are tabulated in Table 3.4. All of the seven thin sections are classified as sub-arkosic arenites according to Folk's (1980) classification scheme. Grain size is fine with moderate sorting. Feldspars and mica minerals are common (Figures 3.40 and 3.42). Quartz, clay minerals and calcite comprise the majority of the cementing minerals present. Going from bottom to top of the core the thin section pictures are shown in Figures 3.37 to 3.43.

<b>Amoco Smith #1 Thin Sections</b>					
<b>Depth</b>	<b>Grain</b>	<b>Cement</b>	<b>Porosity</b>	<b>Hydrocarbons</b>	<b>Grain</b>
<b>(feet)</b>	<b>(%)</b>	<b>(%)</b>	<b>(%)</b>	<b>(%)</b>	<b>Density (g/cc)</b>
13266.30	81.45	6.85	9.20	2.50	2.68
13280.35	82.25	8.96	6.29	2.50	2.70
13295.70	81.50	7.77	8.73	2.00	2.68
13299.25	79.31	6.71	10.98	3.00	2.71
13305.60	84.00	7.54	6.96	1.50	2.69
13307.45	83.00	6.88	8.12	2.00	2.69
13309.00	83.40	8.19	6.91	1.50	2.69

Table 3.4 Depth of thin sections, compositional percentages, and grain densities for Amoco Smith #1.

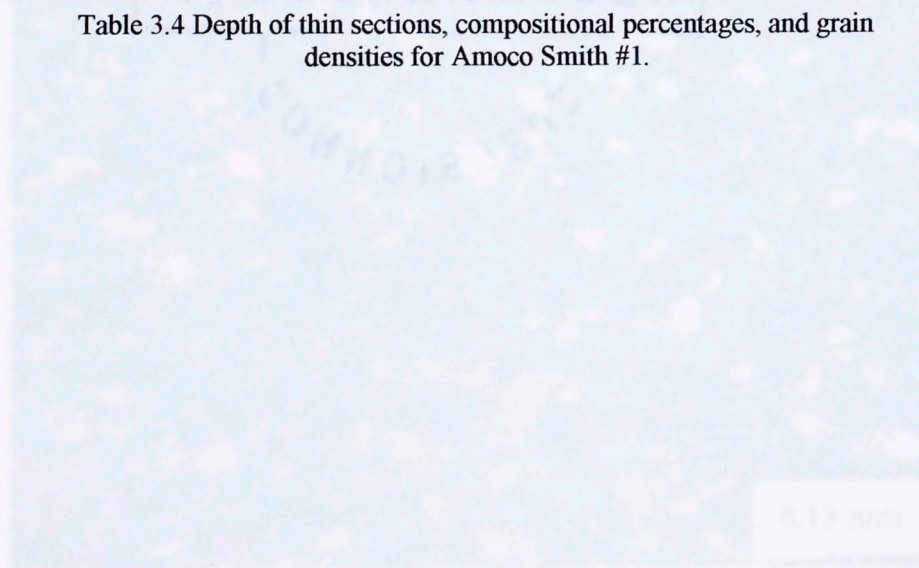


Figure 3.38-Amoco Smith #1  
 Depth: 13,309.00'  
 Magnification: 40x  
 Plane polarized light (above)  
 Cross polarized light (below)  
 Fine grained sandstone with some pyrite

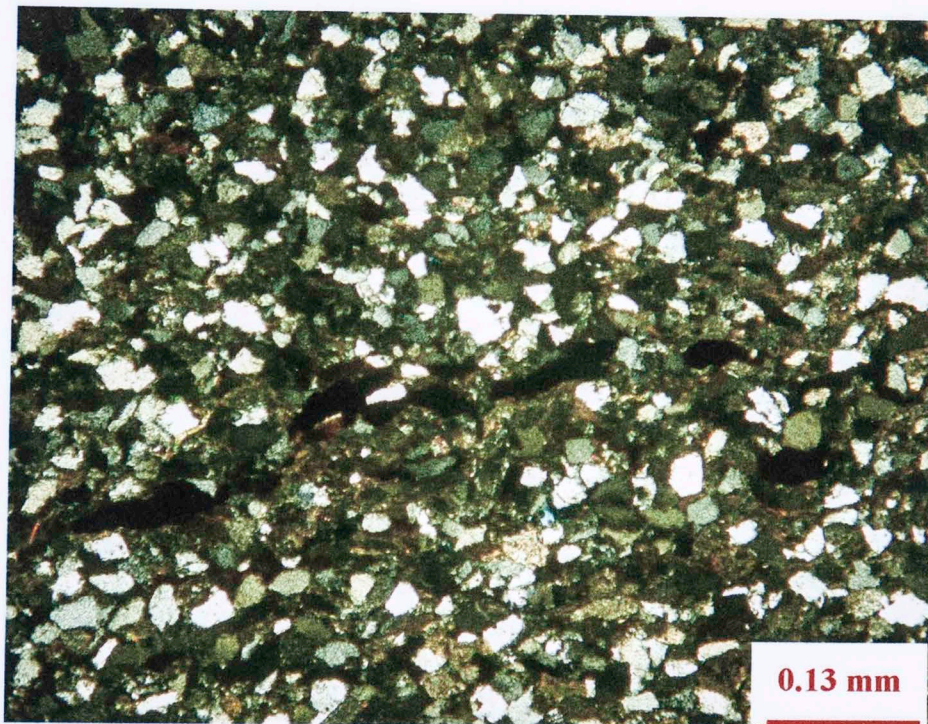
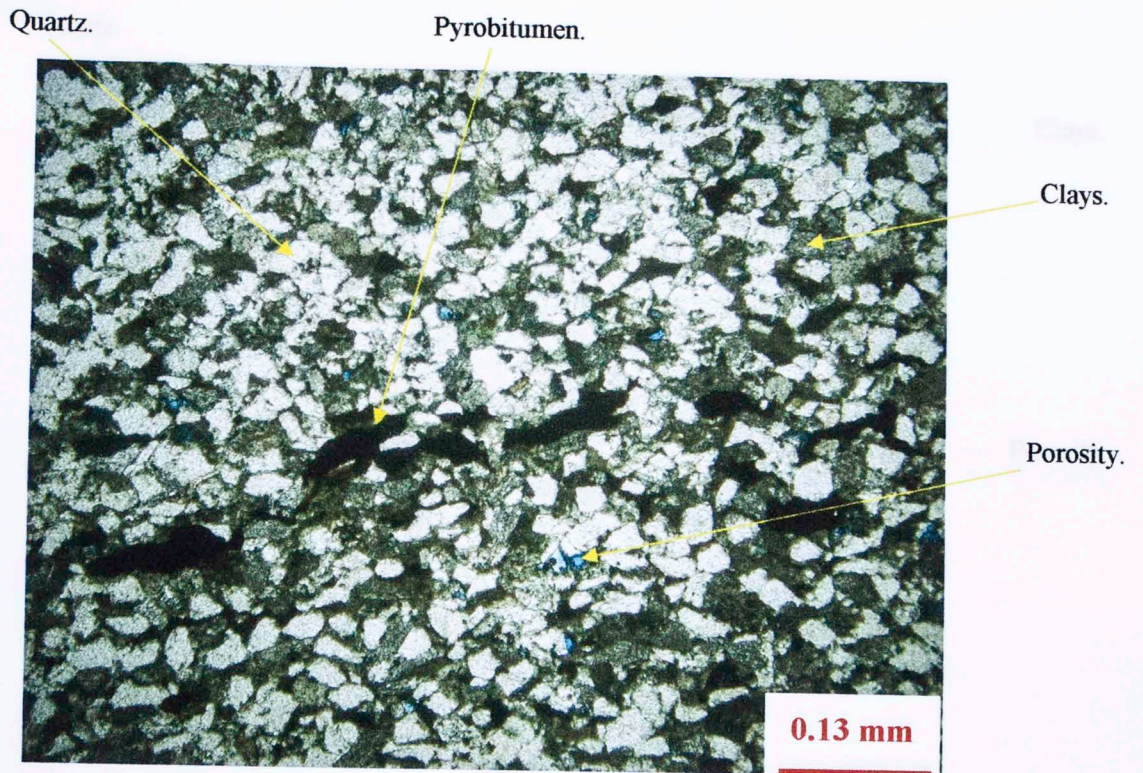


Figure 3.38-Amoco Smith #1  
Depth: 13,309.00'  
Magnification: 40x  
Plane polarized light (above)  
Cross polarized light (below)  
Fine grained sandstone with some pyrobitumen.

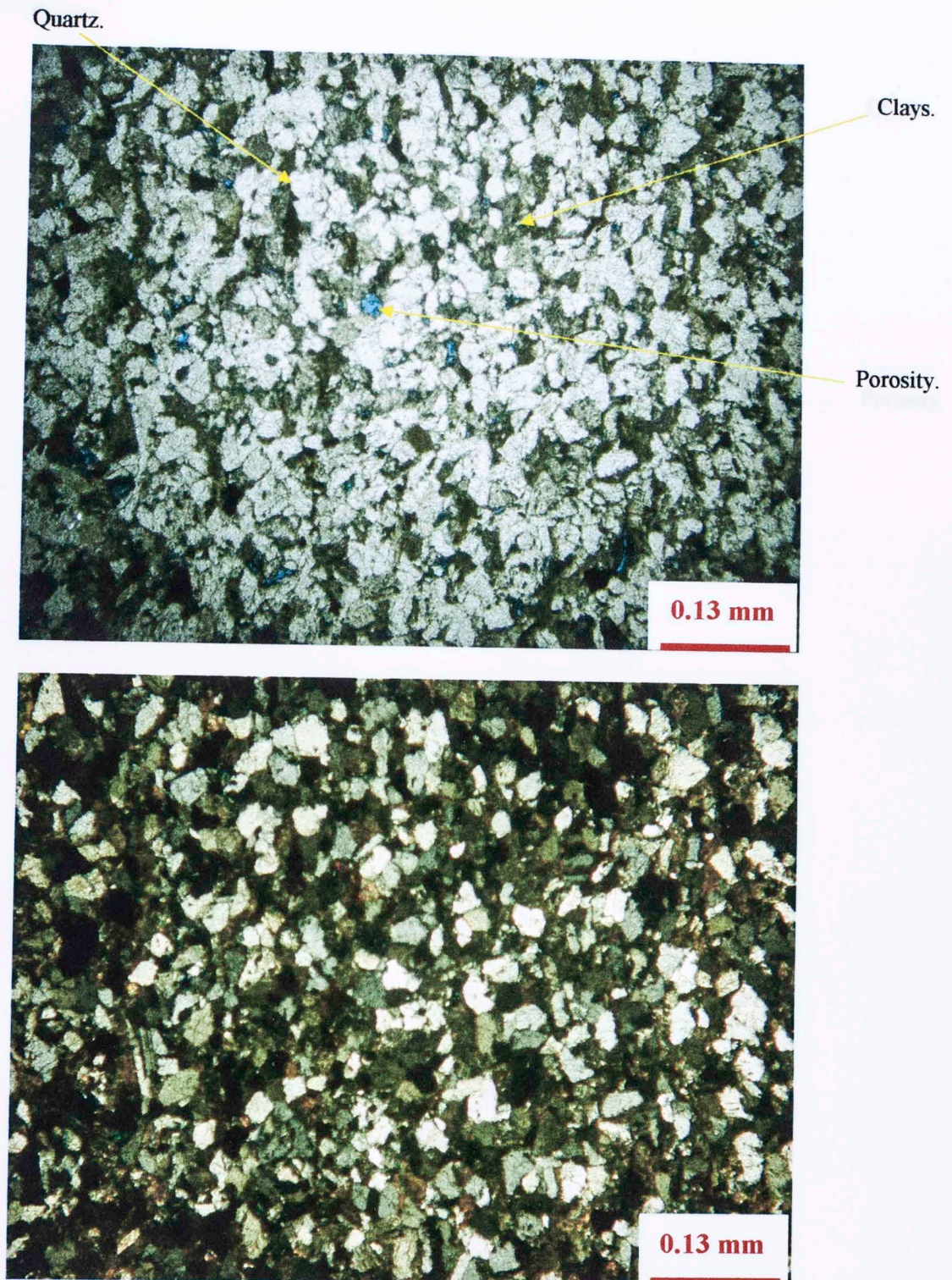
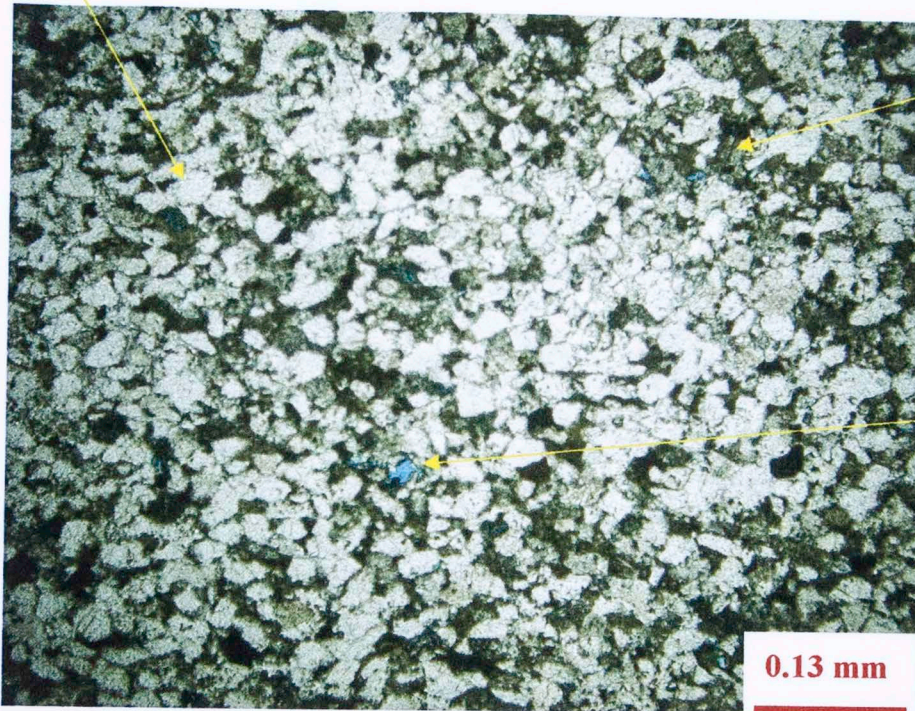


Figure 3.39-Amoco Smith #1  
*Depth: 13,307.45'*  
*Magnification: 40x*  
*Plane polarized light (above)*  
*Cross polarized light (below)*  
Very fine sandstone with high detrital quartz  
content.

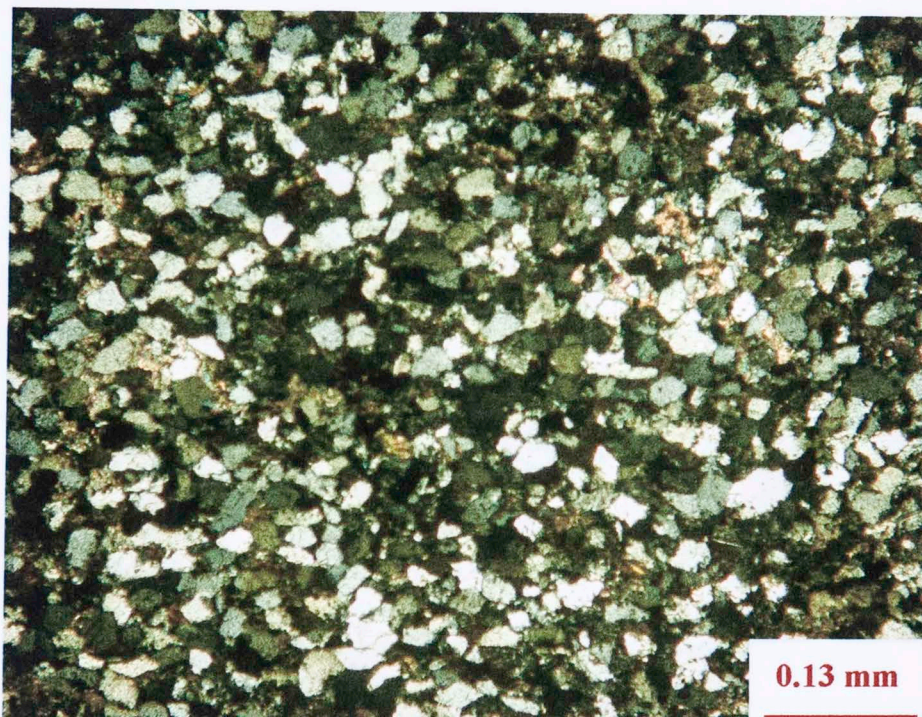
Quartz.



Clays.

Porosity.

0.13 mm



0.13 mm

Figure 3.40-Amoco Smith #1  
*Depth: 13,305.60'*  
*Magnification: 40x*  
*Plane polarized light (above)*  
*Cross polarized light (below)*  
Very fine sandstone with high quartz content.

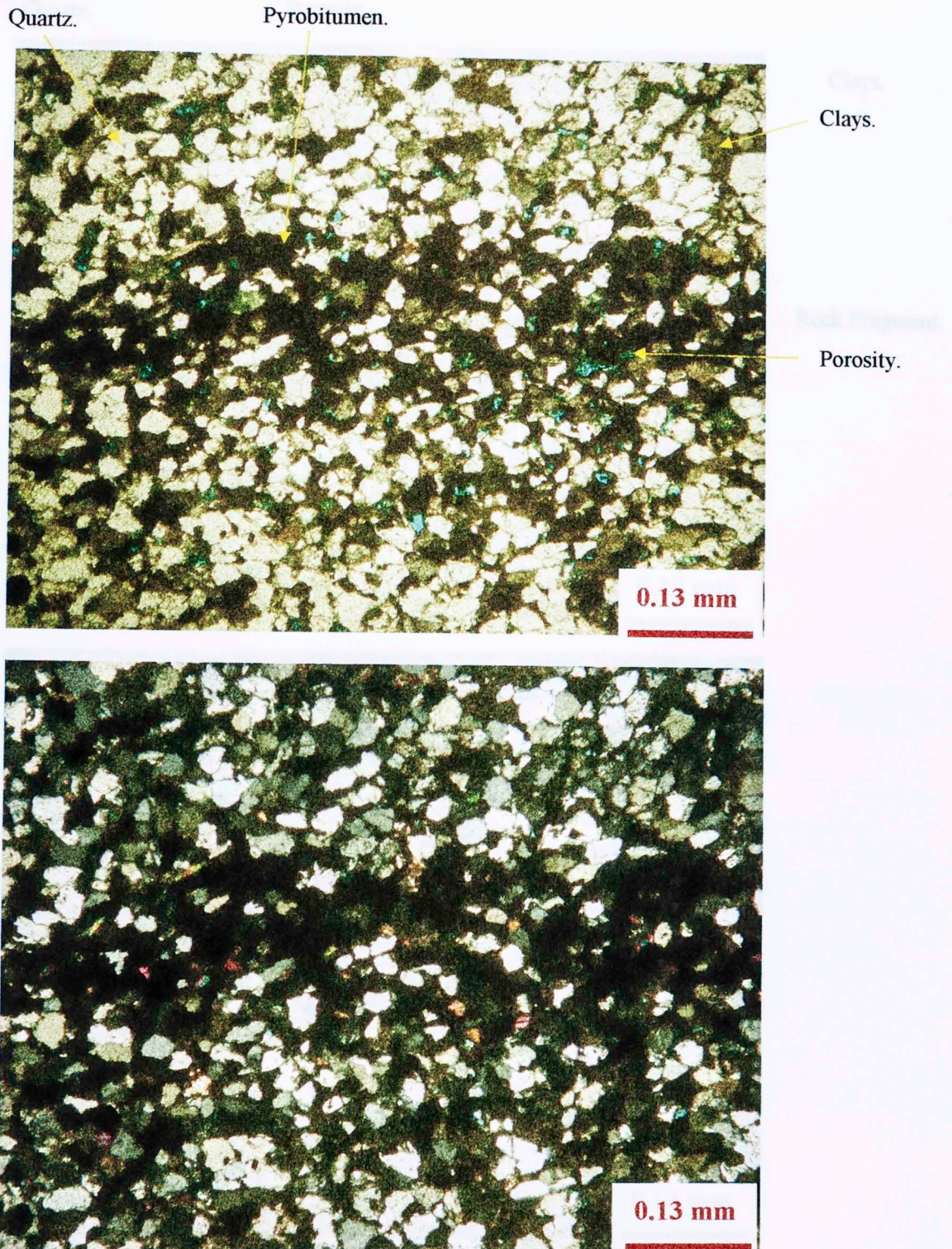


Figure 3.41-Amoco Smith #1  
*Depth: 13,299.25'*  
*Magnification: 40x*  
*Plane polarized light (above)*  
*Cross polarized light (below)*  
Fine sandstone with significant pyrobitumen,  
feldspars and micas.



Figure 3.42-Amoco Smith #1  
*Depth: 13,295.70'*  
*Magnification: 40x*  
*Plane polarized light (above)*  
*Cross polarized light (below)*  
Very fine sandstone with high detrital quartz  
content.

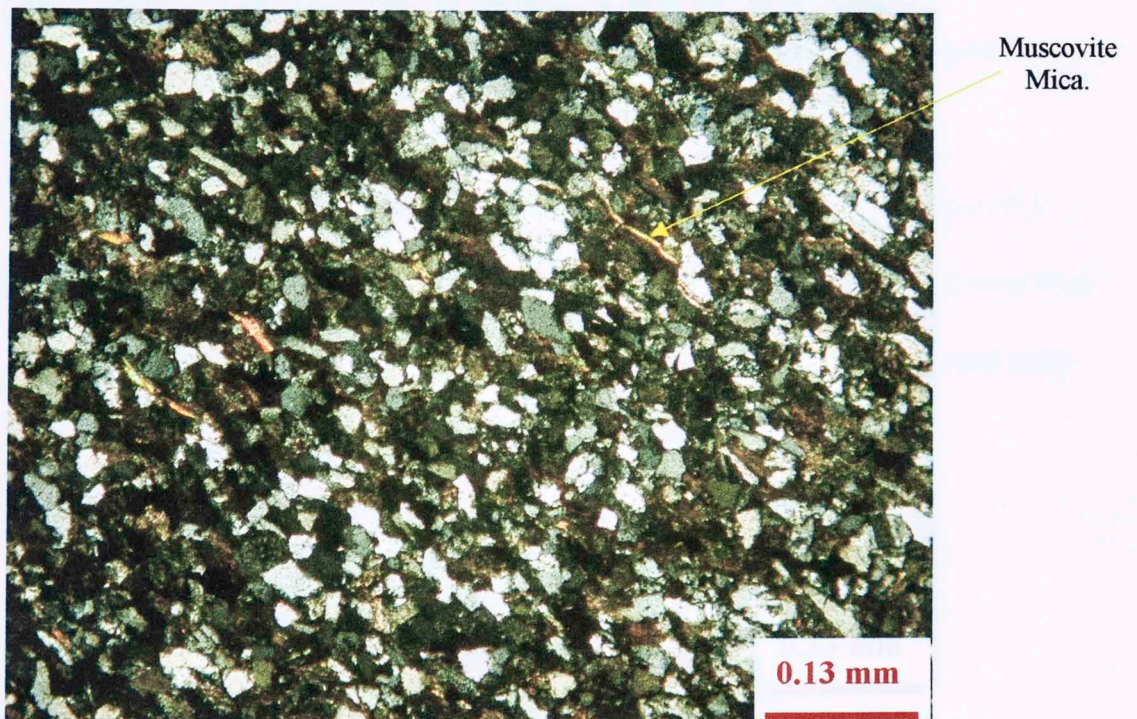
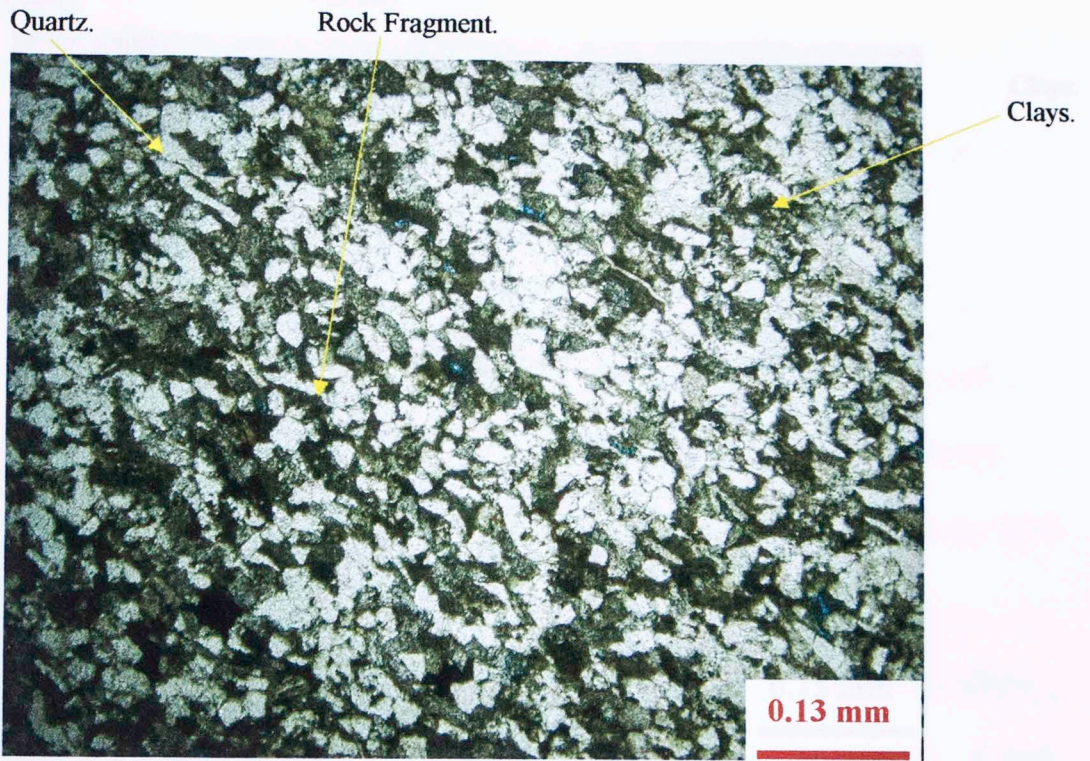


Figure 3.43-Amoco Smith #1  
Depth: 13,280.35'  
Magnification: 40x  
Plane polarized light (above)  
Cross polarized light (below)  
Very fine sandstone with high quartz, feldspar,  
and mica content.



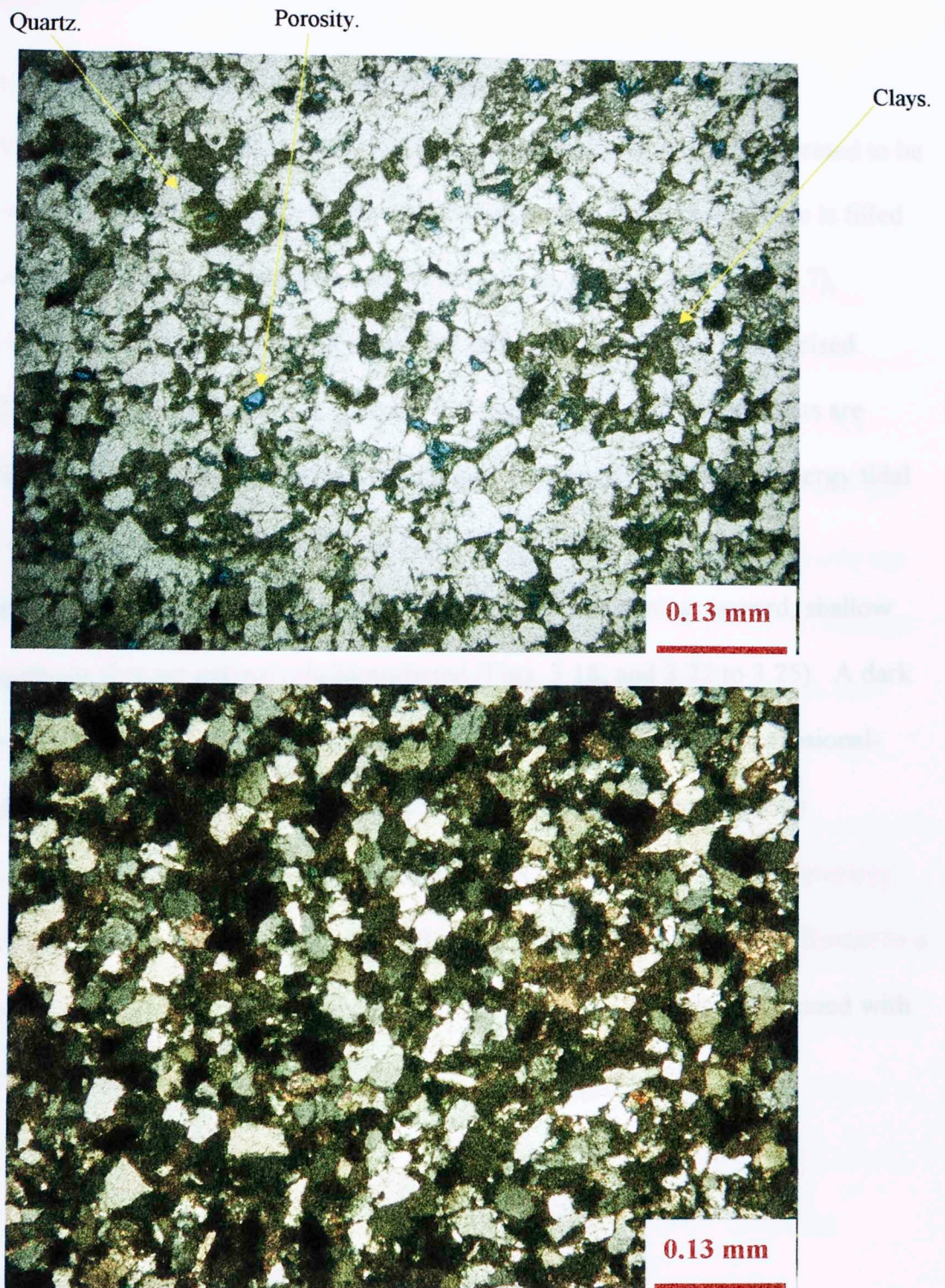


Figure 3.44-Amoco Smith #1  
*Depth: 13,266.30'*  
*Magnification: 40x*  
*Plane polarized light (above)*  
*Cross polarized light (below)*  
Fine sandstone with high detrital quartz content.

#### **d) Depositional Environment Interpretation**

The depositional environment for the Hunt Gillingham #1 core is interpreted to be a shallow marine tidal flat with incised channels. The bottom thirty feet of core is filled with rhythmically-bedded, planar shale and siltstone beds, (Figs. 3.5 through 3.7), deposited in a low energy environment with tidal influence. Overlying this, incised channel fills with erosive bases (Figs. 3.9 and 3.14) containing shale ripup clasts are present (Figs. 3.11 and 3.12). Overlying the channel fill deposits are higher energy tidal mudstone and siltstone beds with wavy and lenticular features.

The Amoco Smith Unit #1 core consists of several coarsening upward, shallow marine sequences that are extensively bioturbated (Figs. 3.18, and 3.22 to 3.25). A dark shale layer overlies these sequences, (Fig. 3.26). Overlying this shale is an erosional-based sandstone with shale clasts (Fig. 3.29). These strata are interpreted to be transgressive shoreface bars with a condensed shale section on top. The transgressive shales have been eroded by an incised channel which may have transported sediment to a deeper marine environment. The proposed depositional model is further examined with log signatures in the following chapter.

#### **b) Gamma Ray**

Gamma ray log measures the rock's emitted natural gamma radiation. In sedimentary rocks the natural gamma radiation emits from three main radioactive elements, potassium, uranium, and thorium. Radioactive elements tend to concentrate in clay minerals such as illite, and in organic matter, both of which are concentrated in

## CHAPTER 4

### WELL LOGS

#### a) General

In the study area, three hundred and forty eight wells penetrate the top of the Lower Red Fork sandstone and two hundred and twenty four wells penetrate the base of the Lower Red Fork sandstone. Ninety one wells produce from the Lower Red Fork sandstone in the study area. The tops and bases of the Lower Red Fork sandstone were picked for all the wells within the area, when present. In order to be consistent with the correlations, the Inola Limestone and the Skinner sandstone were also picked to bracket the Lower Red Fork sandstone. These latter two picks made it easier to correlate the Lower Red Fork sandstone in wells with long distances between them.

The type log (Plate I) shows the formations that were picked, when present, above and below the Lower Red Fork sandstone. The ascending stratigraphic order is the Novi limestone, Inola Limestone, Lower Red Fork sandstone, Middle Red Fork sandstone, Upper Red Fork sandstone, and Skinner sandstone. The tops and bases were all picked on small scale resistivity logs based on conductivity curve correlation. The conductivity, which is the inverse of resistivity, was particularly helpful in picking the tops and bases. The following logs are described below: gamma ray, resistivity, and porosity logs.

#### b) Gamma Ray

Gamma ray log measures the rock's emitted natural gamma radiation. In sedimentary rocks the natural gamma radiation emits from three main radioactive elements: potassium, uranium, and thorium. Radioactive elements tend to concentrate in clay minerals such as illite, and in organic matter, both of which are concentrated in

shales. Quartz sandstones tend to have very low levels of radioactivity, whereas shales tend to be very radioactive. The gamma ray tool measures this radioactivity on a continuous log. The standard gamma ray log scale is from zero to one hundred and fifty API units. The more radioactive a formation is, the closer its values will be to one hundred and fifty API units value or higher and the reverse is true for less radioactive rocks. In this study, a cut off of seventy five API units was used as the maximum API value to define sandstone intervals.

### c) Resistivity

Resistivity log measures the rock's resistivity as an electric current is transmitted through it. The rock's resistivity is dependent on the pore spaces, type of fluid content, mineralogy, cementation, and the rock's composition. If a rock has a very low porosity value and is tight, the resistivity of the rock will be high. If a rock has brine, resistivity will be low as brine is a great conductor of electricity. If a rock contains fresh water, its resistivity will be high as fresh water is not a good conductor. If hydrocarbons are present, the rock's resistivity will be high since hydrocarbons are not very good conductors. Resistivity log readings must take into account all these factors. The Lower Red Fork sandstones average resistivity value over the clean, productive, and porous sandstones is 90 ohms.

### d) Porosity

Porosity logs measure the amount of pore space available within the rock. This is basically a percentage ratio between the amount of void space and the bulk volume of the rock. Three widely used logging tools that yield porosity information are the bulk density log, neutron/density log, and sonic log. The bulk density and neutron/density

logs are the main logs used for obtaining porosity information in the thesis area. Bulk density ( $\rho_b$ ) logging tool measures the density of the formation by the following process. Since formation density cannot be measured directly from the borehole, electron density is utilized by the process of Compton Scattering. The density tool emits gamma rays from a cesium source. Compton Scattering takes place within the formation, and the rays are scattered throughout. Detectors are placed near the source that collect the rays as they reflect to the borehole. The values are then plotted on the log. The bulk density log's scale is from 2.00 to 3.00 grams per centimeters cubed (g/cc).

On the bulk density logs obtained for this study, a limestone density value of 2.71 (g/cc) had been used as zero percent cutoff. A value of 2.57 (g/cc) was used as an eight percent porosity cutoff, and any values less than it would yield higher porosity values on the bulk density log. In the thesis area an eight percent porosity cutoff defines porous sandstone. These values were then plotted and contoured to yield a sandstone porosity map. The reasons for choosing limestone's matrix density are described below.

Grain density measurements were made by Core Lab for Hunt Gillingham #1, and Amoco Smith Unit #1 wells. Fifteen core plug samples were measured for Hunt Gillingham #1, (Table 4.1), and eleven core plug samples were measured for Amoco Smith #1, (Table 4.2). The average grain density for Hunt Gillingham #1 was 2.70 (g/cc), and 2.69 (g/cc) for Amoco Smith #1. The average grain density values are closer to a limestone grain density (2.71 g/cc), than to a sandstone grain density (2.65 g/cc).

9	1176.00	2.68
10	1176.25	2.69
11	1176.50	2.69
Sum of eleven Grain Densities		29.57
Average Grain Density		2.69

Table 4.2 Grain density values for eleven core plugs. The depths at which the samples were used are shown.

<b>Hunt Gillingham #1 Grain Density Values</b>		
<b>Sample #</b>	<b>Depth (feet)</b>	<b>Grain Density (g/cc)</b>
1	14089.65	2.71
2	14090.55	2.72
3	14091.65	2.73
4	14096.15	2.68
5	14103.50	2.67
6	14108.40	2.70
7	14108.55	2.62
8	14112.20	2.69
9	14114.40	2.69
10	14115.40	2.68
11	14117.00	2.69
12	14132.75	2.74
13	14133.15	2.71
14	14143.45	2.73
15	14146.90	2.72
Sum of fifteen Grain Densities		40.49
Average Grain Density		<b>2.70</b>

Table 4.1 Grain density values for fifteen core plugs. The depths at which the samples were taken are shown.

<b>Amoco Smith #1 Grain Density Values</b>		
<b>Sample #</b>	<b>Depth (feet)</b>	<b>Grain Density (g/cc)</b>
1	13262.40	2.69
2	13266.30	2.68
3	13275.10	2.69
4	13280.35	2.70
5	13286.15	2.69
6	13295.70	2.68
7	13299.25	2.71
8	13305.60	2.69
9	13306.10	2.68
10	13307.45	2.69
11	13309.00	2.69
Sum of eleven Grain Densities		29.57
Average Grain Density		<b>2.69</b>

Table 4.2 Grain density values for eleven core plugs. The depths at which the samples were taken are shown.

In the Mid-Ccontinent, limestone matrix has been the historical standard as matrix density. A closer look at the bulk density log revealed that the Lower Red Fork sandstone is closer to limey sandstone density rather than a clean sandstone. Plate VI shows three logs for Amoco Smith #1, from left to right: resistivity, neutron/density, and bulk density. The neutron/density logs show an eight percent porosity cutoff with a limestone as matrix density. On the bulk density log three eight percent porosity cutoffs are drawn for different matrix densities. The red line assumes limestone matrix density (2.71 g/cc). The purple line assumes sandstone matrix density (2.65 g/cc). The light blue line assumes matrix density value of (2.69 g/cc), which is the average grain density for both of the cored wells. As can be seen, the matrix density value of 2.69 is closer to the limestone than sandstone. This justified limestone for the matrix density in this thesis, especially since the majority of the logs used limestone matrix density.

The thickness of porosity sandstone can change significantly depending on which matrix density is used. In Plate VI, limestone (2.71 g/cc) and the average of the cored wells (2.69 g/cc) at eight percent yield sixty six feet of porosity sandstone. The sandstone matrix density (2.65 g/cc) at eight percent yields sixty one feet of porosity sandstone. That's an eight percent difference between the two calculations. Using the limestone matrix density instead of sandstone matrix density in a sandstone reservoir may overestimate the footage of porosity sandstone. Errors in estimation of footage of porosity would lead to inaccurate volumetric calculations and reserve estimates. However this well's measured matrix density at eight percent yielded the same amount of porosity sandstone as limestone matrix density at eight percent, which may not be the case for other sandstone reservoirs.

In the Mid-Continent, limestone matrix has been the historical standard as matrix density for the density logs. This needs to be corrected as a majority of the reservoirs in the Mid –Continent are clean sandstone reservoirs. The Lower Red Fork sandstone in this study area may be an exception since the measured grain density values are closer to a limestone grain density. In other reservoirs, the grain density may not mimic this thesis, which may lead to erroneous porosity cutoffs, and maps.

Majority of the porosity values were obtained from the compensated density neutron logs in the study area. The majority of the wells that were studied have this log available. When they were not available, the bulk density log was utilized with the above mentioned procedure. The density curve used on this log is the same one utilized for the bulk density curve. However there are some assumptions made with this log. The density curve in the neutron/density log assumes that the matrix is composed of 100% rock (i.e. 0% porosity). The matrix density that is assumed is set as the zero percent porosity marker. The log range for the neutron/density log is from negative ten to thirty percent porosity. The neutron/density log header usually highlights what density was assumed as the matrix density. In the Mid-Continent limestone is generally chosen as the matrix density.

The neutron log also assumes limestone matrix, and no shale or gas content. The compensated neutron tool emits neutrons from the logging tool into the formation and records the response of hydrogen atoms on detectors. It is very sensitive to shale because water molecules are incorporated into the crystal lattice of most clays. Therefore the measured porosity is higher for both shale and clay-rich sandstones than for clean sandstones. The tool is also a great gas detector as gas contains fewer hydrogen atoms.



The density log reading decreases and the neutron log reading increases causing a gas effect or “cross over,” where the neutron curve values are greater than the density curve values. In this thesis an eight percent cutoff was utilized for generating porosity sandstone maps.

#### e) Log signatures of the depositional environment

The proposed depositional environment can be visualized with the aid of logs. Figures 4.1 through 4.4 show the Lower Red Fork sandstone with digital gamma ray (GR), resistivity (ILD), and porosity (NPHI and DPHI) curves for the cored wells. On the logs yellow color denotes the cleaner reservoir sands, and the gray denotes the shaly intervals. Hunt Gillingham #1 did not penetrate through the base of the Lower Red Fork Sandstone and did not have any significant porosity. However the well was completed within the following intervals: 14,114 to 14,027 feet. The well only produced 29,634 MCFG, and has been inactive since 1983.

Figure 4.1-Lower Red Fork sandstone with digital gamma ray, resistivity, and porosity curves from Hunt Gillingham #1. Yellow color denotes the cleaner reservoir sands, and the gray denotes the shaly intervals. Hunt Gillingham #1 did not penetrate through the base of the Lower Red Fork sandstone.

Figure 4.2 shows the Lower Red Fork sandstone in greater detail. The interval is highlighted by different arrows representing different depositional packages. The gray arrows signify a tidal flat environment with alternating shales and siltstones, and the fluctuating nature of the gamma ray curve. Overlying the tidal flat facies the red arrow displays the incised channel sandstones. Overlying these sandstones is another sequence of tidal flat and incised channel deposits.

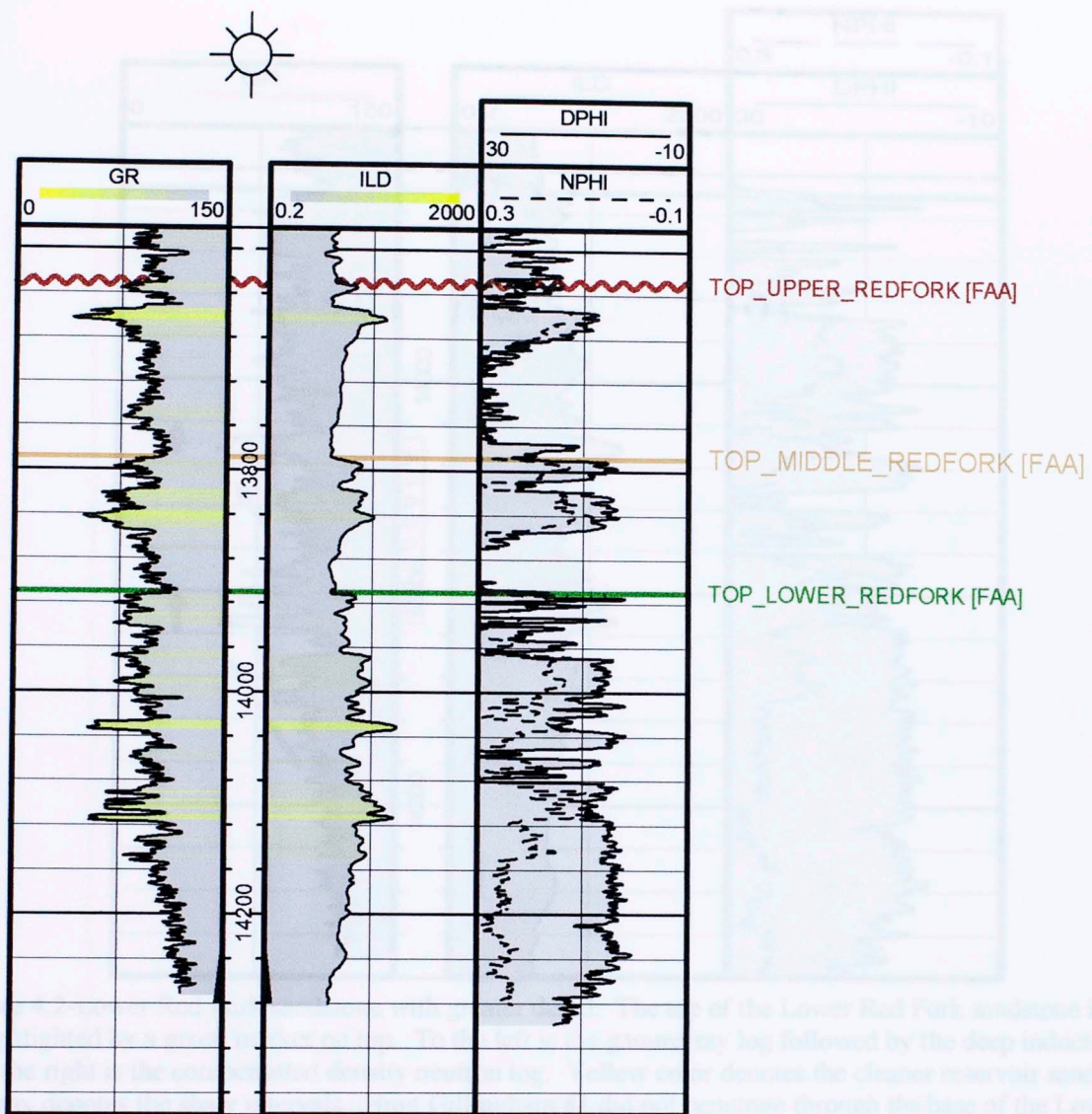


Figure 4.1-Lower Red Fork sandstone with digital gamma ray, resistivity, and neutron/density curves from Hunt Gillingham #1. Yellow color denotes the cleaner reservoir sands, and the gray denotes the shaly intervals. Hunt Gillingham #1 did not penetrate through the base of the Lower Red Fork sandstone.

Figure 4.2 shows the Lower Red Fork sandstone interval in the Amoco Smith #1.

Figure 4.2 shows the Lower Red Fork sandstone in greater detail. The interval is highlighted by different arrows representing different depositional packages. The gray arrows signify a tidal flat environment with alternating shales and siltstones, and the fluctuating nature of the gamma ray curve. Overlying the tidal flat facies the red arrow displays the incised channel sandstones. Overlying these sandstones is another sequence of tidal flat and incised channel deposits.

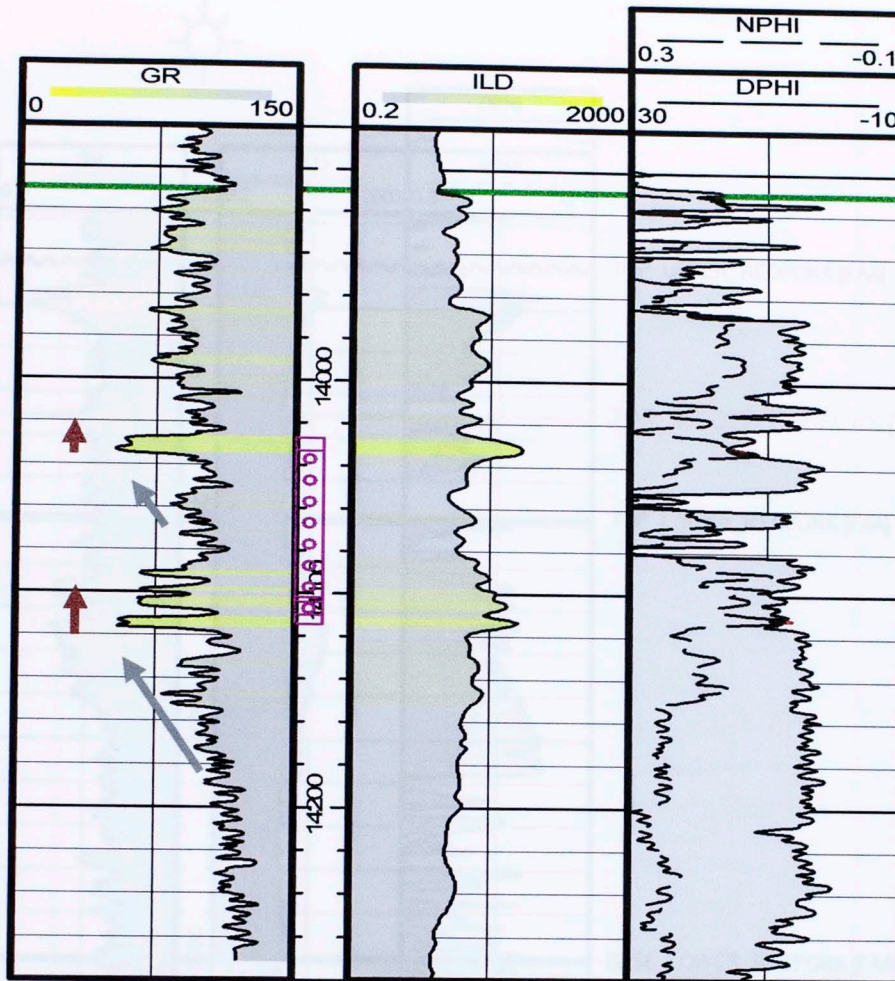


Figure 4.2-Lower Red Fork sandstone with greater detail. The top of the Lower Red Fork sandstone interval is highlighted by a green marker on top. To the left is the gamma ray log followed by the deep induction log. On the right is the compensated density neutron log. Yellow color denotes the cleaner reservoir sands, and the gray denotes the shaly intervals. Hunt Gillingham #1 did not penetrate through the base of the Lower Red Fork sandstone. The perforated interval is highlighted by pink: 14,114 to 14,027 feet. The gray arrows signify an interval that contains, in part, tidal flat environment with alternating shales and siltstones. Overlying the tidal flat facies the red arrow displays the incised channel sandstones.

Figure 4.3 shows the entire Red Fork sandstone interval in the Amoco Smith #1, which is also Type Log I (Plate I) for this thesis. The top of the Upper Red Fork sandstone was utilized as the datum. The entire Red Fork interval in Amoco Smith #1 has significantly more porous sandstone compared to the Hunt Gillingham #1. The well has produced 3.6 BCF of gas, and is still active from the intervals: 13,256 to 13,340 feet.

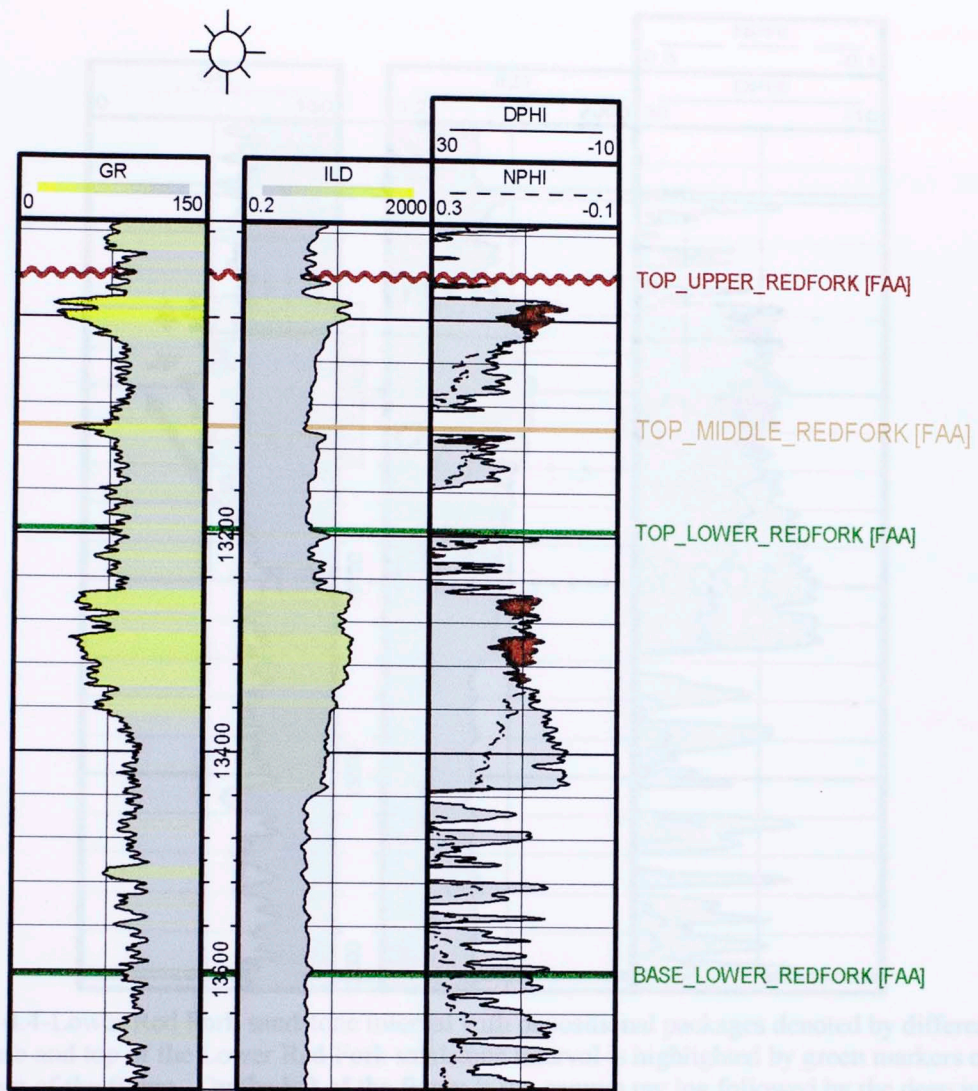


Figure 4.3-Lower Red Fork sandstone with digital gamma ray, resistivity, and neutron/density curves from the type log. Yellow color denotes the cleaner reservoir sands, and the gray denotes the shaly intervals.

Figure 4.4 displays the Amoco Smith #1 well with emphasis on the Lower Red Fork sandstone interval. The interval is highlighted by different arrows representing different depositional packages.

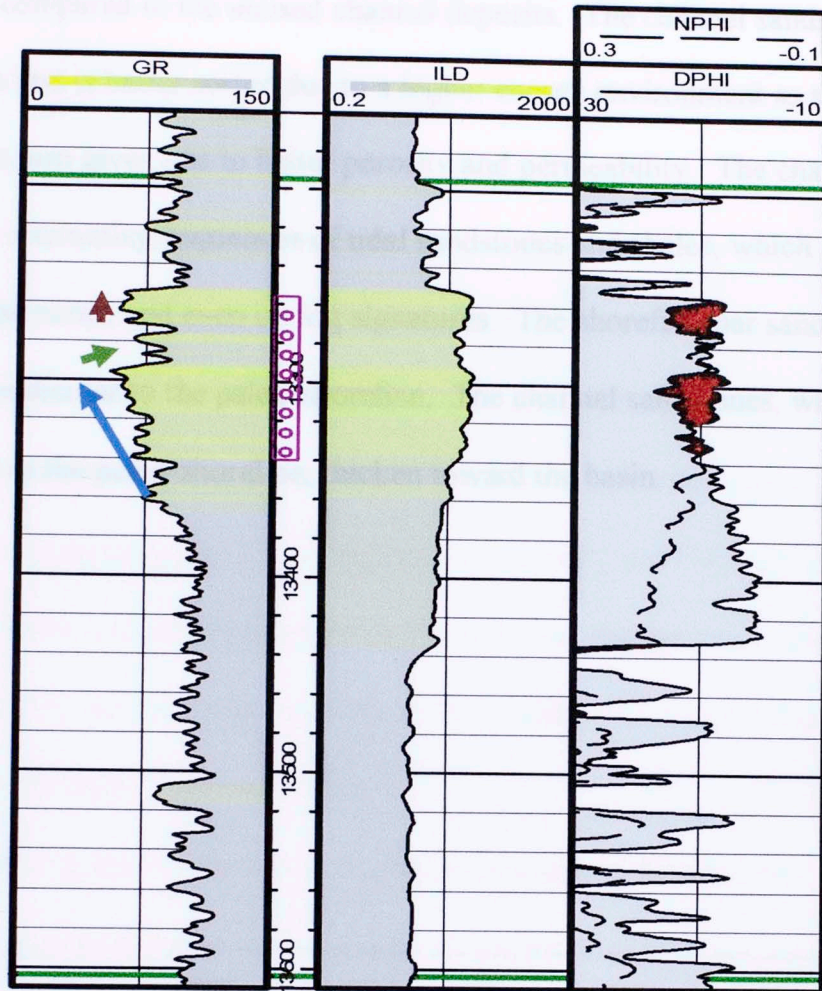


Figure 4.4-Lower Red Fork sandstone interval with depositional packages denoted by different arrows. The base and top of the Lower Red Fork sandstone interval is highlighted by green markers on top and bottom of the figure. On the left of the figure is the gamma ray log followed by the deep induction log. On the right is the compensated density neutron log. The blue arrow denotes shoreface bar sands. Green arrow highlights a subtle transgressive shale. The red arrow shows the incised channel sandstone.

Starting at the bottom of the log there is a thick transgressive marine shale beneath the Lower Red Fork sandstone. The blue arrow denotes coarsening upward prograding shoreface bar sands. There are several packages of these bars overlying one another. The bars are overlain by a subtle transgressive shale, denoted by the green arrow. The red arrow shows the incised channel sandstone that followed regression of the shore line. The channel sandstones display better overall porosity compared to the shoreface bar sandstones. The shoreface bars are deposited in a lower energy

environment compared to the incised channel deposits. The channel sandstone contains coarser grains and is better sorted due to a higher energy environment as seen in the two cores. This in turn gives rise to better porosity and permeability. The channel sandstone is overlain by alternating sequences of tidal sandstones and shales, which are very prevalent in the cores, and even on log signatures. The shoreface bar sandstones thicken and thin perpendicular to the paleo-shoreline. The channel sandstones, which trend perpendicular to the paleo-shoreline, thicken toward the basin.

Plate VII shows the six lines of cross sections. Cross sections A-A', B-B', and C-C' are oriented with the dip of the basin, and are highlighted by the red cross section lines. Cross sections X-X', Y-Y', and Z-Z' are oriented with the strike of the basin, and are highlighted by the blue cross section lines.

The cross sections were based on sequence stratigraphic markers. Figure 5.1 shows a sequence stratigraphic type log with all the markers for the Lower Red Fork sandstone. The large-scale sequence stratigraphic type log is in the back pocket (Plate VIII). The top of the Upper Red Fork sandstone was chosen as the datum for all of the cross sections. The Novi limestone, when present, underlies the Red Fork sandstone.

## CHAPTER 5

### SEQUENCE STRATIGRAPHY AND WELL LOG CROSS SECTIONS

#### a) General

Six cross sections were constructed for this thesis. Twenty nine logs were digitized into LAS files, which were then imported into GeoPlus Petra Software. Three cross sections were made with the dip of the basin as their orientation. The other three cross sections were made with the strike of the basin as their orientation. Plate VII shows the six lines of cross sections. Cross sections A-A', B-B', and C-C' are orientated with the dip of the basin, and are highlighted by the red cross section lines. Cross sections X-X', Y-Y', and Z-Z' are orientated with the strike of the basin, and are highlighted by the blue cross section lines.

The cross sections were based on sequence stratigraphic markers. Figure 5.1 shows a sequence stratigraphic type log with all the markers for the Lower Red Fork sandstone. The large scale sequence stratigraphic type log is in the back pocket (Plate VIII). The top of the Upper Red Fork sandstone was chosen as the datum for all of the cross sections. The Novi limestone, when present, underlies the Red Fork sandstone.

Figure 5.1-Sequence stratigraphic type log. The left and right curved arrows display correlative upward and being upward directions, respectively. Plate VIII displays greater detail.

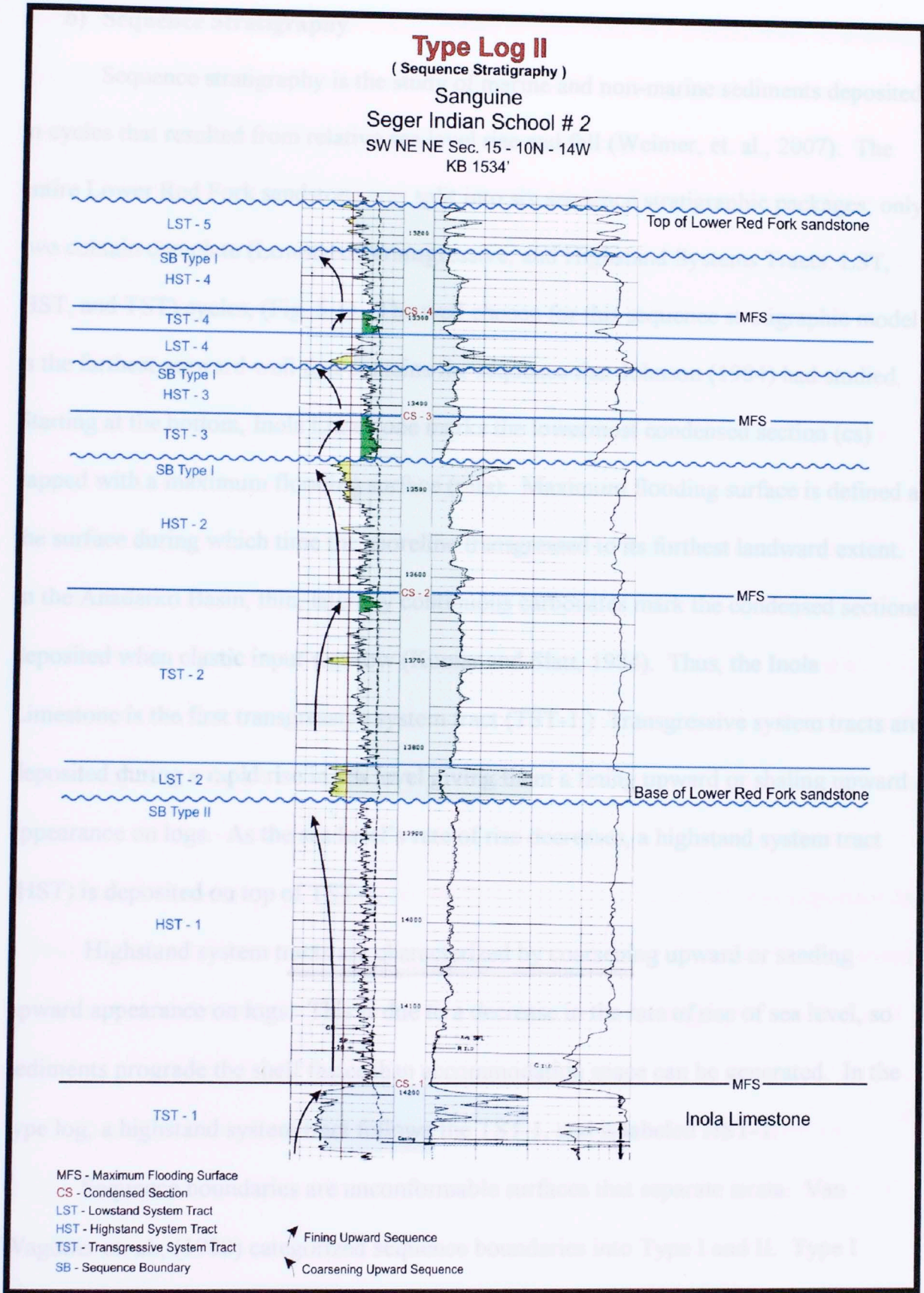


Figure 5.1-Sequence stratigraphic type log. The left and right curved arrows display coarsening upward and fining upward sequences, respectively. Plate VIII displays greater detail.



## b) Sequence Stratigraphy

Sequence stratigraphy is the study of marine and non-marine sediments deposited in cycles that resulted from relative sea level rise and fall (Weimer, et. al., 2007). The entire Lower Red Fork sandstone was split into six sequence stratigraphic packages; only two contain complete (Lowstand, Transgressive, and Highstand Systems Tracts: LST, HST, and TST) cycles, (Fig. 5.1). The well chosen for this sequence stratigraphic model is the farthest seaward well that contains the sequence that Johnson (1984) had studied. Starting at the bottom, Inola Limestone marks the lowermost condensed section (cs) capped with a maximum flooding surface (mfs). Maximum flooding surface is defined as the surface during which time the shoreline transgressed to its furthest landward extent. In the Anadarko Basin, thin, laterally continuous carbonates mark the condensed sections deposited when clastic input was low (Kumar and Slatt, 1984). Thus, the Inola Limestone is the first transgressive system tract (TST-1.) Transgressive system tracts are deposited during a rapid rise in sea level giving them a fining upward or shaling upward appearance on logs. As the sea level's rate of rise decreases, a highstand system tract (HST) is deposited on top of TST-1.

Highstand system tracts are characterized by coarsening upward or sanding upward appearance on logs. This is due to a decrease in the rate of rise of sea level, so sediments prograde the shelf faster than accommodation space can be generated. In the type log, a highstand system tract follows the TST-1, and is labeled HST-1.

Sequence boundaries are unconformable surfaces that separate strata. Van Wagoner et. al., (1988) categorized sequence boundaries into Type I and II. Type I occurs with a significant sea level fall whereas Type II occurs with a more subtle sea

level fall. Seaward movement of the shoreline in both cases is a combination of sediment supply being greater than basinal subsidence (Slatt 2006). (Sequence boundaries are denoted by wavy lines as they are unconformable surfaces.)

In the study area, a Type II sequence boundary (SB Type II) truncated the underlying HST-1. This small lowering of sea level is interpreted throughout the entire area, as the sequence boundary is present in all of the cross sections. A sand body usually ten feet thick in the thesis area was deposited on the sequence boundary (SB). However, beyond the paleo-shelf break this sand body is interpreted to develop into a submarine channel sandstone deposited during a lowstand (LST-2). Following the LST-2, a fining upward sequence (TST-2) was deposited as sea level rapidly rose. The thin sandstone within the TST-2 is interpreted to be a slope channel levee deposit, possibly feeding the channel at HST-1 SB Type II. Following the TST-2 there is a highstand system tract (HST-2) possibly comprised of slope fan deposits. Based on well control these fan deposits are only present in 10N-14W and parts of 10N-13W within the study area. They are part of a sequence that Johnson (1984) studied just north of this study area. Johnson had concluded that the Lower Red Fork sandstone was deposited as submarine canyon fills and submarine fans. These fan sands reached their furthest extent to the south, and thus are not found elsewhere within the study area by the existing well control.

A period of erosion (SB Type I) followed by a sea level rise led to another transgression and deposition of a condensed section (TST-3 in Fig. 5.1). Deposition of the TST was followed by a highstand interval (HST-3) when shoreface bars were deposited within the thesis area. On the type log II (Fig. 5.1) there are no shallow marine

sandstone because only shale was deposited in the deep marine environment. Overlying this is another sequence boundary as lowstand channel sandstone (LST-4) incised into the shoreface bars. A sea level rise followed and another condensed section (TST-4) and highstand (HST-4) strata were deposited. The HST-4 contains shallow marine bars towards the basin due to progradation of the shoreline, as another sequence boundary (SB) formed during a lowstand, after which LST-5 was deposited.

Figure 5.2 highlights the similarities and differences between shallow and deep marine Type Logs I and II, respectively. The wells are hung on top of the Lower Red Fork sandstone. This figure displays the dynamics of reservoir sand deposition in different environments. The shallow marine well is dominated by shoreface bars, whereas the deep marine well is dominated by submarine fans and channel sandstones. Plate IX shows the large scale gamma ray, resistivity, and compensated neutron/density logs from figure 5.2. Figure 5.3 shows the relative location of the two wells with respect to the shelf break.



Figure 5.2 - The similarities and differences between the two type logs incorporated in the study. Type Log I on the right is shallow marine environment example. Type Log II on the left is from a deep marine environment example.

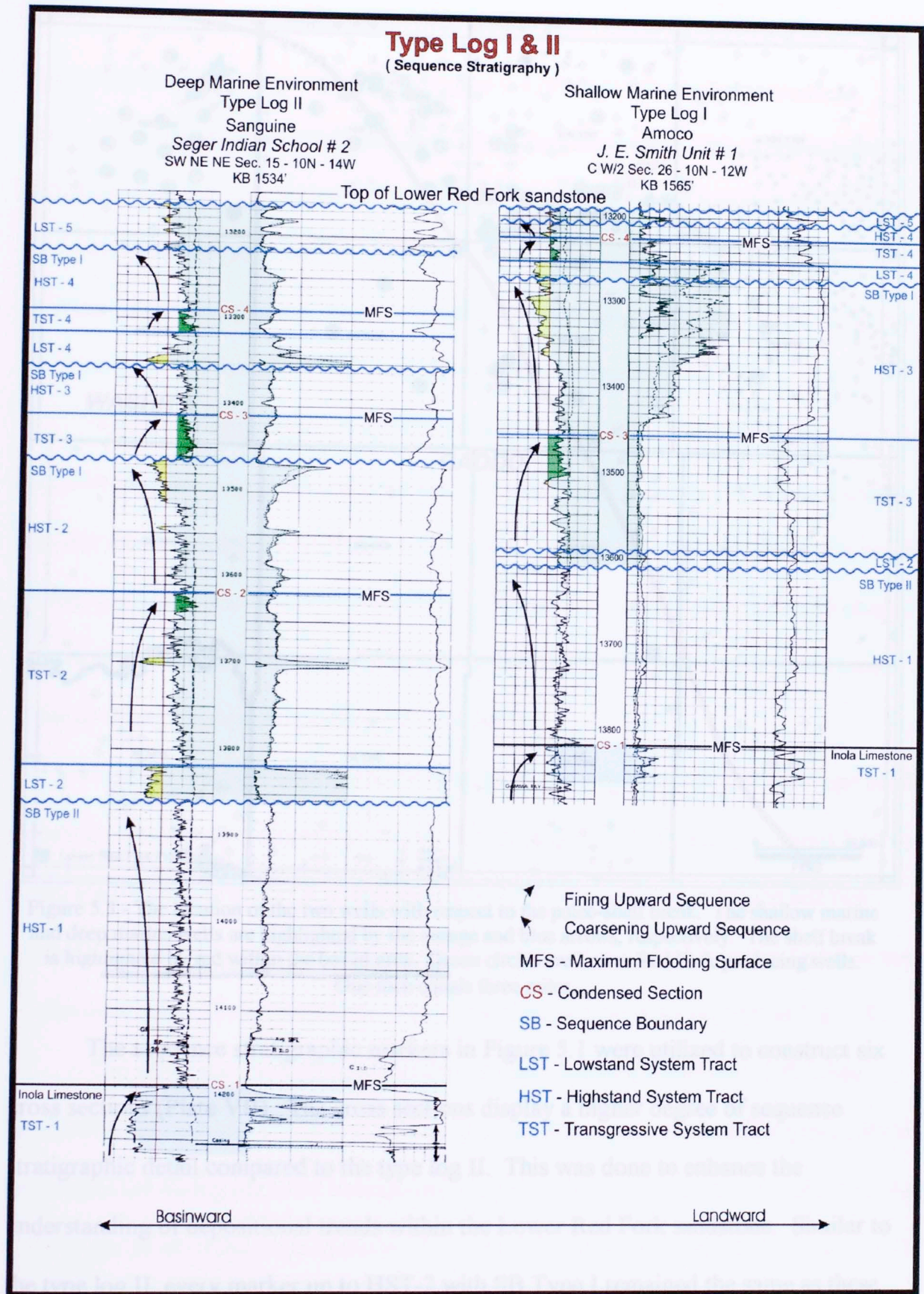


Figure 5.2 –The similarities and differences between the two type logs incorporated in the study. Type Log I on the right is shallow marine environment example. Type Log II on the left is from a deep marine environment example.

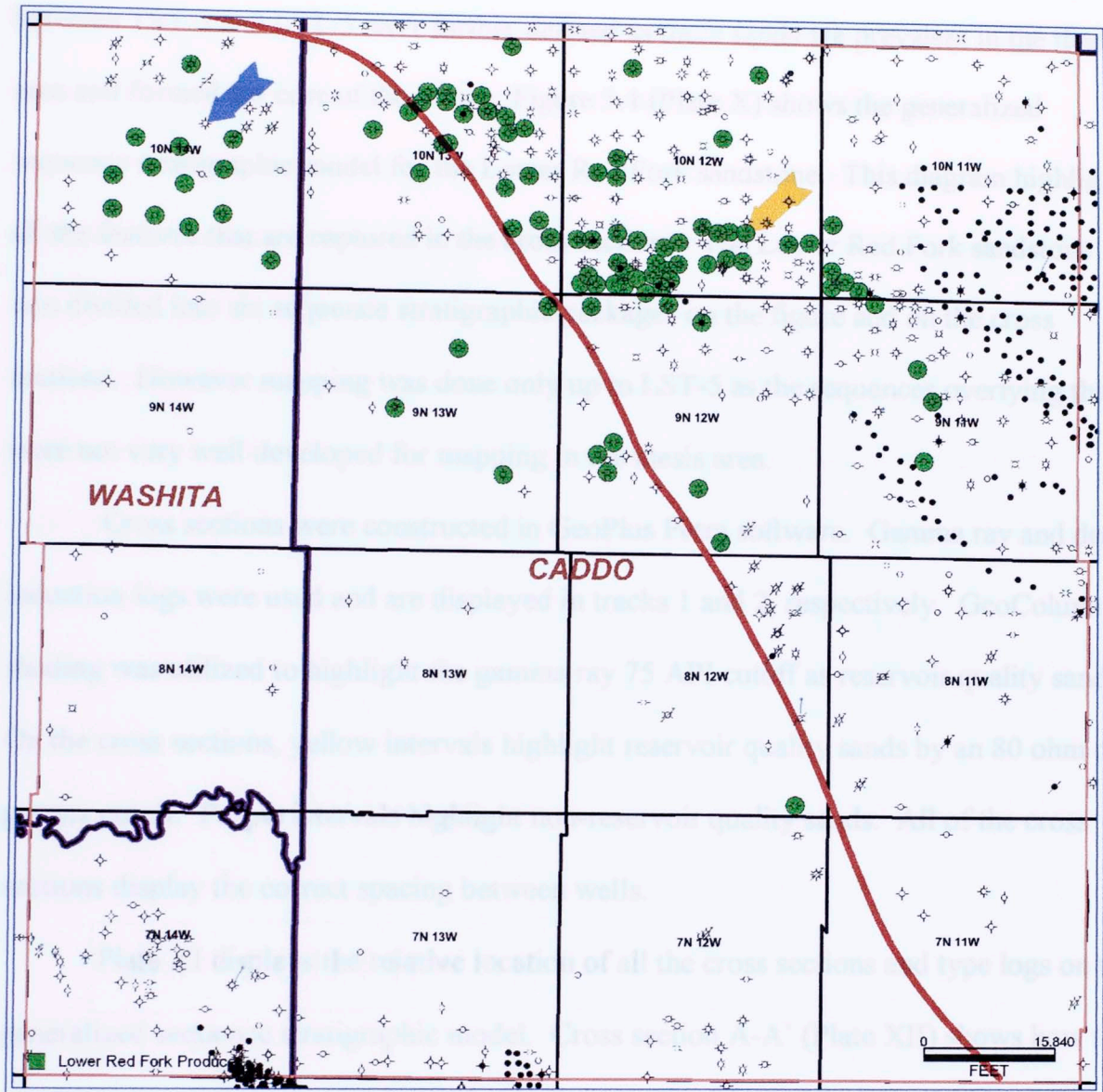


Figure 5.3 - The location of the two wells with respect to the paleo-shelf break. The shallow marine and deep marine wells are highlighted by the orange and blue arrows, respectively. The shelf break is highlighted by red within the boxed area. Green circles are Lower Red Fork producing wells. One inch equals three miles.

The sequence stratigraphic markers in Figure 5.1 were utilized to construct six cross sections (Plate VII). The cross sections display a higher degree of sequence stratigraphic detail compared to the type log II. This was done to enhance the understanding of depositional trends within the Lower Red Fork sandstone. Similar to the type log II, every marker up to HST-2 with SB Type I remained the same as these sandstones were only present in 10N-14W and parts of 10N-13W. Stratigraphic markers

between TST-3 and LST-5 were further defined as these sands are prevalent in the thesis area and formed the core of the thesis. Figure 5.4 (Plate X) shows the generalized sequence stratigraphic model for the Lower Red Fork sandstone. This diagram highlights all the features that are captured in the cross sections. The Lower Red Fork sandstone was divided into six sequence stratigraphic packages on the figure and on the cross sections. However mapping was done only up to LST-5 as the sequences overlying this were not very well developed for mapping in the thesis area.

Cross sections were constructed in GeoPlus Petra software. Gamma ray and deep induction logs were used and are displayed in tracks 1 and 2, respectively. GeoColumn shading was utilized to highlight the gamma ray 75 API cutoff as reservoir quality sands. On the cross sections, yellow intervals highlight reservoir quality sands by an 80 ohm or greater cutoff. Purple intervals highlight non-reservoir quality sands. All of the cross sections display the correct spacing between wells.

Plate XI displays the relative location of all the cross sections and type logs on the generalized sequence stratigraphic model. Cross section A-A' (Plate XII) shows how the strata dip toward the basin (A is landward and A' is seaward) except for the last two wells on the left which display climbing strata due to the Wichita Mountain Uplift in the southwest portion of the thesis area. The climbing strata can also be seen on Fig. 5.4.

This cross section highlights the deeper marine deposits Johnson (1984) had interpreted between the TST-2 and HST-2 SB Type I markers. An overlying thick shale was deposited during sea level transgression, followed by a highstand. This feature is not highlighted in all of the cross sections. Sections B-B' (Plate XIII) and C-C' (Plate XIV) do not have the deeper marine deposits present. It can be concluded from the cross

sections that the entire Lower Red Fork sandstone is a progradational system. This can be better visualized by the generalized sequence stratigraphic model (Fig. 5.4).

Three cross sections with the basin's strike as their orientation are (from landward to seaward) cross sections X-X' (Plate XV), Y-Y' (Plate XVI), and Z-Z' (Plate XVII). The basin is oriented at an oblique angle through the thesis area, thus significant thickening is observed in the left portions of these three cross sections. Cross section Z-Z' (Plate XVII) is the only strike oriented section that shows affects of the Wichita Mountain Uplift. These three cross sections also support the interpretation that the entire Lower Red Fork sandstone is a progradational system, (Fig. 5.4).



Figure 5.4-Generalized sequence stratigraphic model for the Lower Red Fork sandstone. Starting at the top of the sandstone body, the model shows general progradation of the entire Lower Red Fork sandstone towards the progradational systems tract.

# Generalized Sequence Stratigraphic Model for the Lower Red Fork Sandstone.

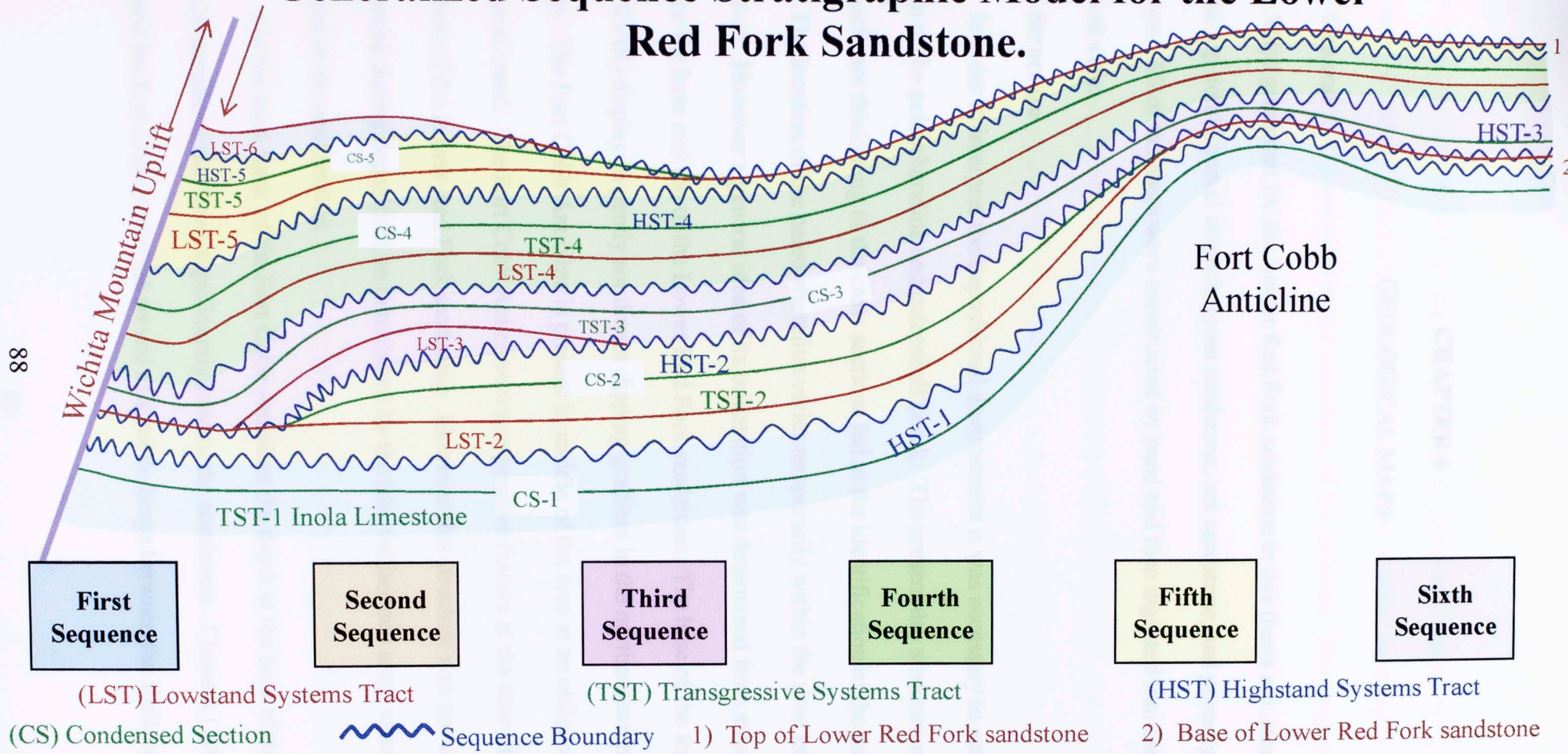


Figure 5.4-Generalized sequence stratigraphic model for the Lower Red Fork sandstone. Starting at the bottom to top six sea level cycles are present. The model shows general progradation of the entire Lower Red Fork sandstone towards the deeper basin up to the Wichita Mountain Uplift.



## CHAPTER 6

### GEOLOGICAL MAPS

#### a) General

Maps generated for the Lower Red Fork sandstone in this thesis are: structure at base and top, total interval isopach, gross sandstone, net sandstone, and porosity sandstone. All of the maps were constructed by hand and then digitized into GeoPlus Petra Software.

#### b) Structure

In order to interpret the depositional environment it was necessary to estimate the location of the paleoshoreline and paleoshelf break. The present day structure of the area and significant thickening in the cross sections led to the identification of the paleoshelf break. The location of the paleo-shoreline varies temporarily within the time interval of deposition. However a general idea of its orientation was determined from structure maps for the base and top of the Lower Red Fork sandstone. The base of the formation (Plate XVIII) displays a gently southwest dipping gradient in the northeastern portion of the map. The Fort Cobb Anticline is present in middle of the area at an oblique angle to the general trend. The Fort Cobb Anticline was a positive feature at the time of deposition of the Lower Red Fork sandstone. However this structure was not very pronounced during deposition, as determined by the interval isopach map, which is discussed in the next section.

On the west flank of the Fort Cobb Anticline the depth at the base of the Lower Red Fork sandstone increases significantly toward the southwest. Clement (1991) suggested the Fort Cobb Anticline served as a subtle hinge between the shallower shelf

and the deeper basinal deposits at the time of Red Fork sandstone deposition. The significant thickening of the Lower Red Fork sandstone west of the flank led to the interpretation of a shelf break along the west flank of the anticline. The cored well in 26-10N-12W, which is on the east flank of the high, contains shoreface bar – shallow marine sandstones. The proposed shelf break complemented the depositional and structure model quite well, with a gentle gradient on the shelf, allowing deposition of shallow marine shoreface deposits. On the west side of the Fort Cobb Anticline the dip is steeper, indicating a slope or basinal environment.

Plate XIX is the structure map at the top of the Lower Red Fork sandstone. The greater number of wells that penetrated the top of the Lower Red Fork sandstone allowed for more control points for this map. The Fort Cobb Anticline is more pronounced at the top rather than at the base structure map due to the variation in control points. Both horizons deepen towards the west and southwest up to the Wichita Mountain Uplift. The Uplift is highlighted on both maps in the southwest region with reverse fault symbols. The depositional package between the top and base of the Lower Red Fork sandstone was defined as the interval isopach.

### **c) Interval Isopach**

The 'total thickness' or interval isopach map of the Lower Red Fork sandstone was generated as Plate XX. Starting at the northeastern portion of the map there is a slight thickening up to the Fort Cobb Anticline. A slight thinning over parts of the Fort Cobb Anticline led to the conclusion that the anticline was a very subtle structural feature at the time of deposition. On the west flank of the anticline there is significant thickening within the interval isopach. This further indicates the location of the shelf break. The

Fort Cobb Anticline served as a hinge between the shallower and deeper depositional environments. Basinward of this shelf break, the interval thickens to more than eight hundred feet towards the west and southwest, up to the Wichita Mountain Front.

A net sandstone map was generated using gamma ray values of 75 API or less as a sandstone cutoff (Plate XXI.) The map shows northwest-southeast trending shallow marine shoreface bars. Toward the shelf break and slope the sandstones thicken and form slope fans. However, there are several trends within the total net sandstone map, including the northwest-southeast trending marine shoreface bars and the northeast-southwest trending slope fans. Sequence stratigraphic markers were used to partition the Lower Red Fork sandstone, as described below.

The first set of maps is from the second sequence, HST-2. Two maps were generated for this sequence: 1) gross interval map and 2) net sandstone map. This sequence was interpreted to be a submarine fan deposit, which Johnson (1984) had documented. Plate XXII shows the gross sandstone map for this sequence. The gross interval map is similar to the interval isopach as it incorporates the sandstones and shales within that interval, but it is defined for a single package or part of one sea level cycle. Plate XXIII displays the net sandstone map. Another map that could have been plotted is the porosity sand map, which is defined as net sandstones that have an eight percent or higher porosity cutoff on porosity logs. This sequence did not contain greater than eight percent porosity within the thesis area. Many wells had porosities only within a three to five percent range, so a porosity sand map was not constructed.

The second set of maps is from the third sequence, HST-3. HST-3 with SB Type I contains the shallow marine shoreface bars. Gross sandstone map for this sequence is

shown in Plate XXIV. Net sandstone map for this sequence is in Plate XXV. Porosity sandstone map of this sequence is in Plate XXVI.

Overlying this is the fourth sequence; lowstand (LST-4) incised channel sandstones are present. Gross sandstone map for this sequence is shown in Plate XXVII. Net sandstone map for this sequence is in Plate XXVIII. Porosity sandstone map of this sequence is in Plate XXIX. The next set of maps within the fourth sequence is from the highstand sequence (HST-4) where shallow marine shoreface sand bars are present. Plate XXX is a gross sandstone map for this highstand. These bars are present farther towards the basin than the older bar sands because of progradation of the shoreline.

Overlying this is the fifth sequence; lowstand (LST-5) incised channel sandstones are present (Plate XXXI). For this second bar/channel sequence only gross sandstone map was generated. Net and porosity sandstone maps were not constructed as the sandstones are more developed towards the deeper parts of the basin. Further towards the basin additional sequences develop up to LST-6, but mapping only covered up to LST-5. Partitioning the Lower Red Fork sandstone into sequence stratigraphic packages produced more meaningful and applicable maps.

## CHAPTER 7

### DISCUSSION

#### a) General

The purpose of the thesis was to determine the depositional environment and sequence stratigraphy of the Lower Red Fork sandstone in order to efficiently explore and develop this sandstone reservoir. This was achieved through analysis of well logs, cores, core plugs, and thin sections. The depositional environment of the cored interval is interpreted to be shallow marine/tidal flat deposits from well logs and detailed core description. Sequence stratigraphy was utilized to enhance understanding of depositional trends and history and also provided markers to construct cross sections and to subdivide the Lower Red Fork sandstone for mapping.

#### b) Uncertainties In Interpretation

Uncertainties in interpreting depositional environments and their sequence stratigraphy are inevitable when integrating: well logs, cores, core plugs, and thin section petrography. Some tools that could reduce the uncertainty include: biostratigraphy, seismic, formation micro-image logs, and dipmeter logs.

#### c) Future Studies

Within the area of study there is a great potential for Red Fork sandstone exploration and development. This study covered the Lower Red Fork sandstone. Both the Middle and Upper Red Fork intervals have additional potential within the thesis area. Currently there is not any significant production from the Middle Red Fork. However, there is potential for Middle Red Fork plays toward the southwest, into deeper parts of the Anadarko Basin. This was deduced by observing the nature of the entire Red Fork

sandstone interval. From brief regional work, it was observed that the entire Red Fork sandstone progrades basinward. Thus, the Lower Red Fork sandstone model developed in this thesis can be applied to younger Red Fork sandstones. Historically the Upper Red Fork sandstone has been a great reservoir, such as in the Clinton-Weatherford Trend through Blaine, Custer, and Roger Mills. The depositional trend for the Upper Red Fork sandstone in this area was interpreted by Clement (1991) to be incised valley fills. These incised valley fills eventually develop into fluvial-deltaic complexes and further towards the basin develop into deep water turbidite deposits (Puckette, et al., 2002). This trend is in close proximity to the area studied in this thesis. Further basinward there is potential for Upper Red Fork sandstone.

## CHAPTER 8

### CONCLUSIONS

A subsurface study of the Lower Red Fork sandstone was accomplished with the following procedures: correlation of logs from three hundred and forty eight wells, analysis of two cores within the area, including core plug reservoir quality and thin section petrography. Routine sequence stratigraphy concepts were applied for constructing cross sections and maps. The principle conclusions of the study are the following:

1. Three types of Lower Red Fork sandstone deposits are present in the thesis area: deep marine submarine fan complex, shallow marine shoreface bars, and incised channels. The deep marine submarine fan sands are limited to the northwestern portions of the study area in 10N-13W and 10N-14W. After these lowstand sandstones were deposited, sea level rose and transgressive shallow marine shoreface bars were deposited. During the next sea level fall incision of the channels into bars occurred. Another rise and fall of the sea level occurred, depositing marine bars and incised channels further towards the basin.
2. The Lower Red Fork sandstone has two distinct log patterns; a coarsening upward and a blocky pattern. The coarsening upward pattern is interpreted to be shallow marine shoreface bars. The blocky pattern is interpreted to be incised channel deposits. The incised channel sandstones thicken and incise into the older shoreface bars leading to complex facies distributions and cross-cutting trends.
3. The structure map at the base of the Lower Red Fork sandstone (Plate XV) reveals the present day structure. Steeper dips basinward of the Fort Cobb

- Anticline are interpreted to be a paleoshelf break with marine shoreface bars landward of this break.
4. An interval isopach map (Plate XVII) of the entire Lower Red Fork sandstone interval indicates thickening toward the west and southwest regions of the study area.
  5. The hydrocarbon trapping mechanism for the Lower Red Fork sandstone is mainly stratigraphic pinchouts.
  6. Porosity determinations of sandstones from density logs needs to be corrected from limestone to sandstone matrix density.
  7. Lower Red Fork sandstone is a sub-arkosic arenite.
  8. The presence of authigenic quartz and clay has reduced the porosity and permeability. Primary porosity was reduced by compaction and pore filling cements. Secondary porosity was developed from dissolution of clays and rock fragments.
  9. The sediment source for the Lower Red Fork sandstone seems to be from the north and northeast. An additional source of sediment transport from the southwest over the uplift is also possible.
  10. The Lower Red Fork sandstone has great potential for exploration and development since these sandstone deposits comprise different facies, each having unique distribution pattern.
  11. Partitioning the Lower Red Fork sandstone into sequence stratigraphic packages produced more meaningful and applicable maps.



12. The entire Red Fork sandstone is part of a progradational sequence. The Lower Red Fork sandstone model has exploration and development applications for the Middle and Upper Red Fork sandstones.

- Adkins, C. J. Jr., 1982. Distribution of subsurface gas facies of the Upper Red Fork sandstone in the Anadarko Basin, Western Oklahoma. Oklahoma State University unpublished M.S. thesis, 175 p.
- Adkins, C. J. Jr., 1997. Partial-Depleted Debris (PDD) Oil Reservoirs in Oklahoma: The Red Fork Play. Oklahoma Geological Survey, Special Publication 97-1, 90 p.
- Beal, C. H., 1956. A subsurface study of the Lower Pennsylvanian sediments of northern Grady and Caddo Counties, Oklahoma. Shale Shaker, v. 6, p. 7-26.
- Boyer, W. A., 1991. East Clinton Field, U.S.A.: Anadarko Basin, Oklahoma. AAPG Bulletin of Petroleum Geology, Atlas of Oil and Gas Fields, v. A-06, p. 207-267.
- Boyer, W. A., 1969. Cherokee Group, east flank of the Nemaha Ridge, north-central Oklahoma: Pt. 1, Shale Shaker, v. 19, no. 8, p. 134-146; Pt. 2 Shale Shaker, v. 19, no. 9, p. 150-161.
- Boyer, W. A., 1959. Facies changes in Pennsylvanian rocks along south flank of Williams Mountains. AAPG, Petroleum Geology of Southern Oklahoma, v. 2, p. 142-155.
- Boyer, W. A., 1957. Major structural and stratigraphic features of the Anadarko basin, in Petroleum and Stratigraphy of the Mid-Continent (Hume, N. J., editor). Tulsa Geological Society, p. 97-113.
- Boyer, W. A., Johnson, K. S., et al, 1979. Oklahoma: in the Mississippian and Pennsylvanian (paleozoic) systems in the United States (Anonymous) U.S. Geol. Surv. Prof. Pap., no. 1110 M-DD, p. R1-R35.
- Boyer, W. A., 1985. Depositional environments, reservoir trends, and diagenesis of the Red Fork sandstones in portions of Blaine, Caddo, and Custer Counties, Oklahoma. Oklahoma City Geological Society, Shale Shaker Digest, v. 11, p. 106-117.
- Boyer, W. A., 1986. Depositional environments, reservoir trends, and diagenesis of the Red Fork sandstones in portions of Blaine, Caddo, and Custer Counties, Oklahoma. Oklahoma State University unpublished M.S. thesis, 132 p.
- Boyer, W. A., et al, 1983. Subsurface Pale and Neogene Facies of Teahawa

## REFERENCES

- Adler, E. J., 1971, Anadarko Basin and Central Oklahoma area: in Figure Petroleum Provinces of the United States; their Geology and Potential, v. 2, AAPG Mem., no. 15, p. 1061-1070.
- Anderson, C. J. Jr., 1992 Distribution of submarine fan facies of the Upper Red Fork interval in the Anadarko Basin, Western Oklahoma: Oklahoma State University unpublished M.S. thesis, 275 p.
- Andrews, R. D., 1997, Fluvial-Dominated Deltaic (FFD) Oil Reservoirs in Oklahoma: The Red Fork Play: Oklahoma Geological Survey, Special Publication 97-1, 90 p.
- Boeckman, C. H., 1956, A subsurface study of the Lower Pennsylvanian sediments of northern Grady and Caddo Counties, Oklahoma: Shale Shaker, v. 6, p. 7-26.
- Clement, W. A., 1991, East Clinton Field, U.S.A.: Anadarko Basin, Oklahoma: AAPG Treatise of Petroleum Geology, Atlas of Oil and Gas Fields, v. A-06, p. 207-267.
- Cole, J. G., 1969, Cherokee Group, east flank of the Nemaha Ridge, north-central Oklahoma: Pt. 1, Shale Shaker, v. 19, no. 8, p. 134-146; Pt. 2 Shale Shaker, v. 19, no. 9, p. 150-161.
- Edwards, A. R., 1959, Facies changes in Pennsylvanian rocks along north flank of Wichita Mountains: AAPG, Petroleum Geology of Southern Oklahoma, v. 2, p. 142-155.
- Evan, J. L., 1979, Major structural and stratigraphic features of the Anadarko basin, *in* Pennsylvanian Sandstones of the Mid-Continent (Hyne, N. J., editor), Tulsa Geological Society, p. 97-113.
- Fay, R. O., Friedman, S. A., Johnson, K. S., et al, 1979, Oklahoma: in the Mississippian and Pennsylvanian (carboniferous) systems in the United States (Anonymous) U. S. Geol. Surv, Prof. Pap., no. 1110 M-DD, p. R1-R35.
- Johnson, C. L., 1984, Depositional environments, reservoir trends, and diagenesis of the Red Fork sandstones in portions of Blaine, Caddo, and Custer Counties, Oklahoma: Oklahoma City Geological Society, Shale Shaker Digest, v. 11, p. 159-175.
- Johnson, C. L., 1984, Depositional environments, reservoir trends, and diagenesis of the Red Fork sandstones in portions of Blaine, Caddo, and Custer Counties, Oklahoma: Oklahoma State University unpublished M.S. thesis, 122 p.
- Kumar, N.; Slatt, T. M., 1984, Submarine-Fan and Slope Facies of Tonkawa

- (Missourian-Virgilian) Sandstone in Deep Anadarko Basin: AAPG, v. 68, p. 1839-1856.
- Levine, S. D., 1984, Provenance and Diagenesis of the Cherokee Sandstones, Deep Anadarko Basin, Western Oklahoma: Shale Shaker, v. 34, no. 10, p. 120-144.
- Moore, G. E., 1979, Pennsylvanian Paleogeography of the Southern Mid-Continent: in Pennsylvanian Sandstones of the Mid-Continent (Hyne, N. J. editor), Tulsa Geological Society, p. 213.
- Puckette, J. O, Anderson, C.,; and Al-Shaieb, Z., 2000, The deep-marine Red Fork Sandstone: a submarine-fan complex, *in* Johnson, K. S. (ed.), Marine clastics in the southern Midcontinent, 1997 symposium: Oklahoma Geological Survey Circular 103, p. 177-184.
- Schneider, R. E.; and Clement, W. A., 1986, The East Clinton gas field, Custer County, Oklahoma: a seismic-stratigraphic case history: Oklahoma Geological Survey, Shale Shaker Digest, v. 12, p. 63-67.
- Slatt, R. M., 2006, Stratigraphic reservoir characterization for petroleum geologists, geophysicists, and engineers: Handbook of Petroleum Exploration and Production, v. 6, p.391.
- Swanson, D. C., 1967, Some major factors controlling the accumulation of hydrocarbons in the Anadarko Basin: Shale Shaker, v. 17, p. 106-114.
- Udayashankar, K. V., 1985, Depositional environment, petrology and diagenesis of the Red Fork Sandstone in central Dewey County, Oklahoma: Oklahoma State University unpublished M.S. thesis, 188 p.
- Van Wagoner, J. C., H. W. Posamentier, R. M. Mitchum, P. R. Vail, J. F. Sarg, T. S. Loutit, and J. Hardenbol, An overview of sequence stratigraphy and key definitions. In C. K. Wilgus, B. S. Hastings, C. G. St. C. Kendall, H. Posamentier, C. A. Ross, and J. C. Van Wagoner (eds.), "Sea-Level Changes-An Integrated Approach." Soc. Econ. Paleo. and Mineral. (SEPM) Spec. Publ. 42, (1988), 39-45.
- Walker, R. G., 1978, Deep-water sandstone facies and ancient submarine fans: models for exploration for stratigraphic traps: American Association of Petroleum Geologists Bulletin, v. 62, p. 932-966.
- Weimer, P.; and Slatt, R. M., 2007, Introduction to the Petroleum Geology of Deepwater Settings: American Association of Petroleum Geologists Studies in Geology, v. 57, p. 57.
- Whiting, P. H., 1982, Depositional environment of Red Fork sandstones, deep Anadarko Basin, western Oklahoma: Oklahoma City Geological Society, Shale Shaker Digest, v. 11, p. 104-119.

Whiting, P. H., 1982, Depositional environment of Red Fork sandstones, deep Anadarko Basin, western Oklahoma: Master's thesis, Texas A&M University, College Station, Texas, 81 p.